AD-A125 746 STUDY OF RESIDUAL STRESSES AND DISTORTION IN STRUCTURAL 1/2
WELDMENTS IN HIGH..(U) MASSACHUSETTS INST OF TECH
CAMBRIDGE DEPT OF OCEAN ENGINEERIN..
UNCLASSIFIED J E AGAPAKIS ET AL. 30 NOV 82 F/G 11/6 NL

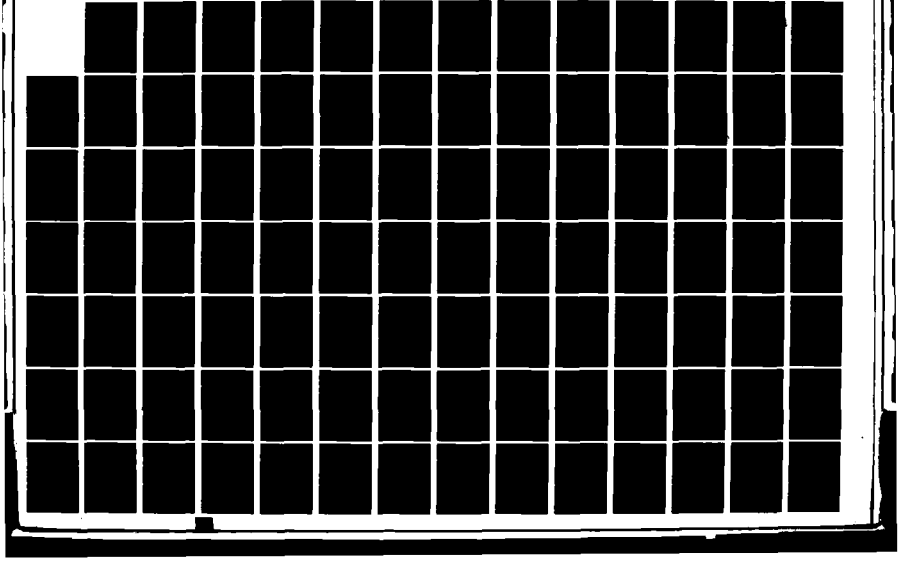

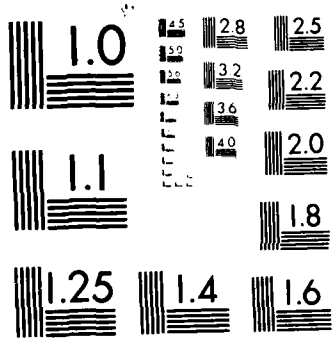

(9)

FINAL REPORT

of

-c-

CONTRACT N00014-75-0469
(M.I.T. OSP #82558)

STUDY OF RESIDUAL STRESSES AND DISTORTION IN STRUCTURAL WELDMENTS IN HIGH-STRENGTH STEELS

by

JOHN E. AGAPAKIS
VASSILIOS J. PAPAZOGLOU
AKIHIKO IMAKITA
KOICHI MASUBUCHI

to

OFFICE OF NAVAL RESEARCH

November 30, 1982

MASSACHUSETTS INSTITUTE OF TECHNOLOGY
CAMBRIDGE, MASSACHUSETTS

MASSACHUSETTS INSTITUTE OF TECHNOLOGY
DEPARTMENT OF OCEAN ENGINEERING
CAMBRIDGE, MASS. 02139

FINAL REPORT

of

Contract N00014-75-C-0469
(M.I.T. OSP #82558)

STUDY OF RESIDUAL STRESSES AND DISTORTION IN STRUCTURAL WELDMENTS IN HIGH-STRENGTH STEELS

to

Office of Naval Research

November 30, 1982

by

John E. Agapakis
Vassilios J. Papazoglou
Akihiko Imakita
Koichi Masubuchi

UNCLASSIFIED

SECURITY CLASSIFICATION OF THIS PAGE *(When Data Entered)*

REPORT DOCUMENTATION PAGE

READ INSTRUCTIONS BEFORE COMPLETING FORM

1. REPORT NUMBER: Final	2. GOVT ACCESSION NO.: AD-A125746
3. RECIPIENT'S CATALOG NUMBER:	
4. TITLE *(and Subtitle)*: STUDY OF RESIDUAL STRESSES AND DISTORTION IN STRUCTURAL WELDMENTS IN HIGH-STRENGTH STEELS	5. TYPE OF REPORT & PERIOD COVERED: Final, December 1, 1977 to May 31, 1982
	6. PERFORMING ORG. REPORT NUMBER:
7. AUTHOR(s): John E. Agapakis, Vassilios J. Papazoglou, Akihiko Imakita and Koichi Masubuchi	8. CONTRACT OR GRANT NUMBER(s): Contract N00014-75-0469 (M.I.T. OSP # 82558)
9. PERFORMING ORGANIZATION NAME AND ADDRESS: Massachusetts Institute of Technology, 77 Massachusetts Ave., Cambridge, Mass. 02139	10. PROGRAM ELEMENT, PROJECT, TASK AREA & WORK UNIT NUMBERS:
11. CONTROLLING OFFICE NAME AND ADDRESS: Department of the Navy, Office of Naval Research, Arlington, Virginia 22217	12. REPORT DATE: November 30, 1982
	13. NUMBER OF PAGES:
14. MONITORING AGENCY NAME & ADDRESS *(if different from Controlling Office)*:	15. SECURITY CLASS. *(of this report)*: Unclassified
	15a. DECLASSIFICATION/DOWNGRADING SCHEDULE:

16. DISTRIBUTION STATEMENT *(of this Report)*

This document has been approved for public release and sale; its distribution is unlimited. Reproduction in whole or in part is permitted by the U.S. Government.

17. DISTRIBUTION STATEMENT *(of the abstract entered in Block 20, if different from Report)*

18. SUPPLEMENTARY NOTES

19. KEY WORDS *(Continue on reverse side if necessary and identify by block number)*

Welding	Numerical Analysis	Stainless Steels
Residual Stresses	Fracture Analysis	Nickel-Bronze Alloys
Distortion	Stress Relief Treatment	
High Strength Steels	Creep Analysis	

20. ABSTRACT *(Continue on reverse side if necessary and identify by block number)*

Work performed on the initial tasks of the project (study of residual stresses and distortion in thick plates, cylindrical shells and bronze weldments is summarized.

Results on the final tasks are detailed. The developed analytical models for the calculation of residual stress relaxation during stress-relief heat treatments are presented. The model predictions are compared with experimental results obtained with edge welded HY-130 and 304 stainless steel

DD FORM 1 JAN 73 1473 EDITION OF 1 NOV 65 IS OBSOLETE

S/N 0102-014-6601

SECURITY CLASSIFICATION OF THIS PAGE *(When Data Entered)*

ABSTRACT (continued)

plates.

Finally, computer programs and manuals developed during this study are presented.

ACKNOWLEDGEMENT

We would like to express our appreciation to Professor Klaus Jurgen Bathe of the Mechanical Engineering Department at M.I.T., for providing ADINA and ADINAT. His interest and help in the modification of the programs are also acknowledged.

The work in this four and a half year research program was performed primarily by graduate students at the Department of Ocean Engineering of M.I.T., under the supervision of Professor Koichi Masubuchi. Specifically, in addition to the authors of this report, the following students worked on this project. In chronological order:

Lipsey, M.D.
Coneybear, G.W.
Mylonas, G.A.
Rogalski, W.J.
Marby, J.P.
Coumis, G.A.
Sousa Sá, P.A.
Conçalves, E.
Suchy, A.F.
McCord, R.S.
Carpentier, K.P.

Many further thanks are due to Antony J. Zona for his assistance in the Welding Lab, to the late Fred Merlis for his help in the experiments, and to Mrs. Muriel Morey for her excellent work in coordinating production of the text and preparing the figures of this report.

Finally, we would like to extend our thanks to Dr. B. A. McDonald of the Office of Naval Research for his guidance and encouragement throughout the program, to P. W. Holzberg and Ivo Fioriti of the D.T.N.S.R.D.C. for providing the TTT and CCT diagrams of HY-130 steel and to Eric Pollack of D.T.N.S.R.D.C. for supplying the necessary HY-130 plates for the experiments.

EXECUTIVE SUMMARY

This is the final report of the O.N.R. sponsored research program entitled "Study of Residual Stresses and Distortion in Structural Weldments in High Strength Steels". All five tasks of this program, which was initiated on December 1, 1977, have been completed as proposed.

Task 1 deals with butt welds in thick HY-130 steel plates. Experimental measurements of temperatures, thermal strains, residual stresses and distortions were performed for a variety of welded specimens during the first three years of the program. Fracture experiments were also performed on simply restrained welded specimens. Analytical studies were conducted, parallel to the experiments, and were completed during the fourth year of the program. Specifically, heat transfer analyses were performed using both a newly developed analytical solution based on a moving finite heat source model, and the multipurpose nonlinear heat transfer finite element computer program ADINAT, which was modified to take into account latent heat effects.

Calculations of the thermal strain, transient stress, and residual stress distributions developed during the multipass GMA welding of thick plates, were also performed using the thermal-elastic-plastic constitutive model of the multipurpose finite element program ADINA. The program was enhanced by incorporating the phase transformation strains developed during the steel allotropic phase changes.

A hybrid crack element was also developed, aimed at facilitating an inexpensive evaluation of the fracture characteristics of weldments in the presence of a residual stress field. Using this element, linear elastic finite element analyses of the fracture experiments were performed. Both the crack opening displacement and the strain energy released during the propagation of a crack in a residual stress field were calculated.

Finally, results from all of the aforementioned analyses were compared with data obtained from experimental measurements. Good correlation was generally observed.

Task 2 deals with girth welds in HY-130 unstiffened cylindrical shells. Temperatures and strains during seam and girth welding of the cylinders were first measured. The axial and circumferential residual stress distributions were then determined and compared with data from other investigators and analytical predictions. Task 2 was completed during the third year of this program.

Task 3, aimed at developing information on weldments in bronze, was carried in its entirety during the fourth year. A literature survey was first conducted to obtain material properties on nickel-aluminum bronze. Experimental studies, consisting of bead-on-plate and edge welds on one quarter inch thick plates, were then performed to determine the resulting temperature, strain, and displacement changes. The experimental results were finally compared with baseline data to study the effects of restraint, block welding, preheating, postheating, and grinding on the final distortion.

In Task 4, the mechanisms and the effectiveness of thermal stress relieving treatments for weldments are studied. A literature survey covering both thermal and mechanical stress relieving treatments was initially performed. Then the M.I.T. one-dimensional program was properly modified to calculate strains and stresses during and after uniform-temperature heat treatments (taking into account stress relaxation due to creep). The analytical predictions were verified by experiments performed on 304 stainless steel plates. Further analysis was performed to evaluate the effectiveness of line heating with a flame. Finally, experiments with HY-130 specimens were conducted during the six-month extension of the program.

Under Task 5, manuals have been prepared for the computer programs related to welding that have been developed or improved during the course of the present research program. This task was also completed during the final six-month extension.

All in all, therefore, the proposed program of research was carried out as originally proposed but with a delay of approximately six months.

This final report, issued at the end of the program extension, covers all five tasks. However, since only a brief summary of the work on the first three tasks is presented here, this report should be considered as a companion to the three technical progress reports previously published.

TABLE OF CONTENTS

1. INTRODUCTION

The objective of this research program, which started on December 1, 1977, is to experimentally and analytically study temperatures, thermal strains, residual stresses and distortion in structural weldments in high-strength steel.

This program includes (1) generation of experimental data, and (2) development of analytical systems. HY-130 is the primary material to be investigated; a limited number of experiments are, however, to be conducted using low-carbon steel specimens. Experiments are to be made using the multipass gas metal arc (GMA) and electron beam (EB) one-pass welding processes.

More specifically,

Materials: HY-130 steel (with some control specimens in low-carbon steel)

Thickness: 1 inch (with some specimens 1/2" thick)

Welding processes: Electron beam (EB) and multipass gas metal arc (GMA) processes

Specimen geometries: The following types of specimens are considered

a. Butt welds in thick plates

   (1) Unrestrained butt welds
   (2) Simple restrained butt welds
   (3) Restrained welds simulating practical weldments

b. Girth welds of cylindrical shells

   (4) Girth welding along the groove of a cylindrical shell
   (5) Girth welding between unstiffened cylindrical shells

The work to be performed has been divided into two main tasks:

Task 1: Research on butt welds in thick plates

Task 2: Research on girth welds in cylindrical shells

The program was initially proposed to cover a three-year period. Table 1.1 illustrates the tasks and phases of this study. The planned progress for each task appears in the original proposal, dated July 1977, where also a more detailed description of each task can be found.

Towards the end of the initial three-year period a proposal, dated November 1980, was sent to O.N.R. requesting a one-year extension of the research program to November 30, 1981. Under this proposal, which was accepted, work on three additional tasks would be done as follows (Table 1.2):

Task 3: Development of information on weldments in bronze

Task 4: Research on thermal stress relieving of weldments

Task 5: Development of improved computer programs

For the most part the program has been carried out as originally proposed. For the completion of the final two tasks, however, a further six-month extension was considered necessary and was requested in a proposal dated October 1981.

Work on all five tasks has been completed by May 31, 1982 and is reported here.

Three progress reports, dated October 10, 1978, August 31, 1979, July 15, 1980 and three technical progress reports, dated November 30, 1979, November 30, 1980 and November 30, 1981 (covering the work performed during the first two, third and fourth years respectively) have already been issued.

This final report, issued at the end of the program extension, covers all five tasks. However, since details on the first three tasks have already been given in the three technical progress reports, only a summary will be presented here. Two recent papers reviewing the work on Task 1 are also included in Appendices A and B. Tasks 4 and 5, which were completed during the six-month extension of the program will be covered in detail in this report. Therefore, this final report should be considered as a companion to the aforementioned three technical progress reports.

TABLE 1.1

TASKS AND PHASES OF THE PROGRAM INITIALLY PROPOSED

	Task 1: Thick Plate	Task 2: Cylindrical Shell
First Year	1.1 Develop details of research plan	2.1 Develop details of research plan
	1.2 Experiments on unrestrained butt welds	2.2 Experiment on girth welding along groove of a cylindrical shell
	1.3 Analysis of data obtained in 1.2	2.3 Analysis of data obtained in 2.2
Second Year	1.4 Develop details of research plan	2.4 Develop details of research plan
	1.5 Measurement of residual stresses in specimens made in 1.2	2.5 Measurement of residual stresses in specimens made in 2.2
	1.6 Experiment on simple restrained butt welds	2.6 Experiment on butt welds between unstiffened cylindrical shells
	1.7 Analysis of data obtained in 1.5 and 1.6	2.7 Analysis of data obtained in in 2.5 and 2.6
Third Year	1.8 Develop details of research plan	2.8 Develop details of research plan
	1.9 Experiment on restrained cracking test specimens	2.9 ---
	1.10 Measurement of strain energy release on specimens made in 1.6 and 1.9	2.10 Measurement of residual stresses in specimens made in 2.6
	1.11 Analysis of data obtained in 1.9 and 1.10	2.11 Analysis of data obtained in 2.10
	Preparation of the Final Report	

↓ Information on residual stresses and strain energy release in specimens used for weld cracking and stress-corrosion cracking

↓ Information on residual stresses and distortion of welded cylindrical shells

TABLE 1.2

TASKS TO BE COMPLETED IN THE 18-MONTH EXTENSION

Task 3: Bronze Weldments
3.1 Literature Review 3.2 Generation of Experimental Information
Task 4: Thermal Stress Relieving
4.0 Literature Review 4.1 Initial Analysis and Verification Tests (304 Stainless Steel) 4.2 Further Analysis and Experiments (HY-130 Steel)
Task 5: Improved Computer Programs
5.1 Development of Improved Manuals of Independent Welding Programs 5.2 Development of Manuals of Programs which are Compatible with the ADINA Program

2. WORK ACCOMPLISHED ON THE FIRST THREE TASKS

2.1 Work Accomplished on Task 1 - Thick Plates

2.1.1 General Status

The objective of Task 1 of this research program is to experimentally and analytically study temperatures, thermal strains, residual stresses and distortion in thick butt welded high strength steel (specifically HY-130) plates. All eleven steps (see Table 1.1) of this task have been completed successfully as originally planned.

Most of the experimental work has been completed during the first three years of the research program. Details of the experimental procedures and the obtained results can be found in the first two technical progress reports to O.N.R. However, the final two steps of Task 1 were completed during the fourth year, and were covered in the third technical progress report.

The analysis of the experimental data and the development of computer programs was also completed during the fourth year. Again, details are provided in the third technical progress report. In what follows, the work performed on Task 1 is briefly summarized. A comprehensive overview is also provided in the paper:

Papazoglou, V.J., Masubuchi, K., Gonçalves, E., and Imakita, A., "Residual Stresses Due to Welding: Computer-Aided Analysis of their Formation and Consequences", presented at the SNAME 1982 Annual Meeting, New York, N.Y., November 18-20, 1982,

which is included in Appendix B of this report.

2.1.2 Experimental Program

The following number of experiments, classified according to types of measurements taken, specimen configuration, and welding process used, were performed during the first four years of this research project (December 1, 1977 to November 30, 1981).

A. Measurement of temperature and thermal strain distributions during welding.

A.1 Unrestrained specimens

A.1.1 Gas Metal Arc Welding

(a) One 24" x 24" x 1" SAE 1020 specimen

(b) Four 24" x 24" x 1" HY-130 specimens

A.1.2 Electron Beam Welding

(a) Two 24" x 24" x 1" SAE 1020 specimens

(b) Two 24" x 24" x 1" HY-130 specimens

(c) One 24 5/16" x 26" x 1" HY-130 specimen

A.2 Clamped specimens

A.2.1 Laser Beam Welding

(a) Two 11" x 14 3/4" x 1" HY-130 specimens

A.3 Simply restrained specimens[1]

A.3.1 Gas Metal Arc Welding

(a) Two 30" x 30" x 1/2" SAE 1020 specimens

(b) Two 30" x 30" x 1" SAE 1020 specimens

(c) Two 30" x 30" x 2" SAE 1020 specimens

(d) Two 30" x 30" x 7/8" HY-130 specimens

(3) One 30" x 30" x 2" HY-130 specimen

A.4 Restrained cracking (window) test specimen

A.4.1 Gas Metal Arc Welding

(a) One 15" x 24" x 2" HY-130 specimen on a 30" x 30" x 3" SAE 1020 base plate

---

[1]These specimens had H-type slits of different dimensions to simulate various degrees of restraint. The degree of restraint was calculated numerically (see Section 2.7.1 of Second Technical Progress Report to O.N.R., November 30, 1980).

B. Measurement of triaxial distribution of residual stresses[2]

B.1 Electron Beam welded specimens

(a) One 24" x 24" x 1" SAE 1020 specimen (see number A.1.2a)

(b) One 24 5/6" x 26" x 1" HY-130 specimen (see number A.1.2c)

B.2 Gas Metal Arc welded specimens

(a) One 18" x 32" x 7/8" HY-130 specimen

(b) One 18" x 32" x 1" HY-130 specimen

C. Measurement of strain energy release during crack propagation

C.1 Simply restrained specimens[3]

C.1.1 Gas metal Arc Welding

(a) One 30" x 30" x 1/2" SAE 1020 specimen

(b) Two 30" x 30" x 1" SAE 1020 specimens

(c) Two 30" x 30" x 2" SAE 1020 specimens

(d) Two 30" x 30" x 7/8" HY-130 specimens

(e) One 30" x 30" x 2" HY-130 specimen

Details of the experimental procedures used and recorded results are provided in the three technical progress reports to the Office of Naval Research.

2.1.3 Heat Transfer Analysis

Efforts to improve the prediction capabilities, of both analytical and numerical solutions of the heat transfer problem during welding, were successfully completed during the first half of the fourth year of this research project, and are summarized in this section. Details on this part

[2] These measurements were performed using the Rosenthal-Norton sectioning technique (see Section 2.6 of First Technical Progress Report to O.N.R., November 30, 1979 for a detailed description of the method).

[3] Same specimens as in A.3.1.

of the research program can be found in the third technical progress report to O.N.R. and the following thesis:

Papazoglou, V.J., "Analytical Techniques for Determining Temperatures, Thermal Strains, and Residual Stresses During Welding", Ph.D. Thesis, M.I.T., May 1981.

Closed-form analytical solutions of the problem of heat transfer during welding, though not as accurate as the numerical ones, are very useful. They provide for the establishment of the general laws that govern the phenomenon, thus facilitating a better understanding of it. Moreover, they allow for a series of parametric analyses that help one understand the relative importance of the various parameters.

Based on these considerations, efforts were undertaken during the course of this investigation towards devising new or improving already existing analytical solutions, with the aim of obtaining more accurate predictions.

Specifically, a new three-dimensional finite heat source model for solving the governing partial differential equation of heat transfer was initially developed, taking into account the temperature dependence of the material properties and the surface heat losses. A parametric investigation of the effects of the variation of various model parameters was then performed. Results were finally compared with other closed form solutions and with experiments. Agreement was generally good for the case of thin plates.

In addition to the above work, the conventional point heat source closed form solution[4] was modified so as to more accurately simulate multipass welding. This modification permitted positioning of the point heat source at the center of each welding pass (at any point through the plate's thickness). Comparison of the results obtained was again performed with experiments and the previously mentioned finite heat source model.

---

[4]Rosenthal, D., "Mathematical Theory of Heat Distribution During Welding and Cutting", Welding Journal, 20 (5), 1941, pp. 220s-234s.

Numerical solutions of the heat transfer problem during welding were also developed in Task 1. Specifically, using the multipurpose finite element program ADINAT,[5] a nonlinear finite element model was devised. The temperature dependence of material properties and the heat losses from the surface were again taken into account. The three-dimensional character of the heat transfer problem was simplified by analyzing only a cross-section of the weldments, located in the mid-length of the weld. Arc initiation and termination effects were neglected and the welding heat source was assumed to move at a constant high speed along a straight line in a planar weld. It should also be noted here that the exact heat transfer mechanism inside the molten metal pool was not modeled. Instead, the thermal conductivity of the molten metal was assumed to be an order of magnitude higher than that of the material in the solidus temperature.

Results of the finite element modeling are presented and compared with experiments in the third technical progress report and in Papazoglou's thesis.

2.1.4 Thermal and Residual Stress Analysis

Using the predicted temperature distributions, one can calculate the transient strains, transient stresses and residual stresses due to welding. The calculation of strains and stresses, however, poses a much more formidable problem than the one encountered in the heat transfer analysis, making the use of numerical techniques a necessity. These difficulties stem from the complicated thermal-elastic-plastic state developed in and around the weld metal during welding.

Two general techniques were followed by the M.I.T. investigators to solve the problem. The first one is based on the rather simple one-

---

[5] Bathe, K.J., "ADINAT-A Finite Element Program for Automatic Dynamic Incremental Nonlinear Analysis of Temperature," AVL Report 82448-5, Mech. Eng. Dept., M.I.T., May 1977 (revised 1981).

dimensional analysis.[6] Results using this analysis were reported in the first two technical progress reports to O.N.R. Some details of this approach are also given in Section 3.3.4 of this report, where the method is extended so as to calculate strains and stresses not only during welding but also during thermal stress relieving. In general, it could be noted that the one-dimensional analysis is best suited for the case of relatively long and thin (less than 1/4" thick) mild steel plates.

The second approach is based on the finite element method, and can handle thick high strength steel sections. A model for taking into account the phase transformation strains during welding of quenched and tempered steels was developed and incorporated into the finite element program ADINA.[7]

Specifically, using the CCT diagram of the material (either known experimentally or derived from the TTT diagram) and the temperature distribution during and after welding, the history of microstructure formation during the cooling states is predicted. The combined transformation and thermal strains are then estimated and incorporated into the modified finite element program ADINA, replacing the conventional thermal strains.

Comparison of the finite element predictions with experimental data yielded a good correlation in general. Further details on this part of the research program are covered in the third technical progress report to O.N.R. and the following thesis:

Papazoglou, V.J., "Analytical Techniques for Determining Temperatures, Thermal Strains, and Residual Stresses During Welding", Ph.D. thesis, M.I.T., May 1981.

An overview is also given in both Appendices A and B of this report.

---

[6] Papazoglou, V.J., "Computer Programs for the One-dimensional Analysis of Thermal Stresses and Thermal Movement during Welding", Manual # 2 of Report under Contract N00014-75-C-0469 to O,N.R., M.I.T., 1977.

[7] Bathe, K.J., "ADINA-A Finite Element Program for Automatic Dynamic Incremental Nonlinear Analysis", AVL Report 82448-1, Mech. Eng. Dept., M.I.T., September 1975 (revised December 1978).

2.1.5 Fracture Analysis

Efforts to analyze the fracture experiments performed in Task 1.10 were completed successfully during the first half of the fourth year of this research program. These efforts consisted of numerically calculating the stress intensity factor and the crack opening displacement using the finite element method and based on a newly developed hybrid crack element.

Specifically, a circular blade saw cut was used in the experiments to simulate a propagating crack in the weld metal of the H-type slit specimens. Crack opening displacement (C.O.D.) and surface strains were measured and used by an iterative finite element code in order to estimate the transverse residual stress distribution through the thickness, and the elastic strain energy released during each notch size increment.

After the residual stress distribution (through the thickness) was obtained, the stress intensity factor was calculated by another finite element code. This last program automatically considers the increasing size of the crack. A special hybrid crack element was developed, in order to account for the crack tip singularity and the stress distribution applied on the crack surface. In addition to the stress intensity factors, the crack opening displacement was also calculated by the program and was then compared to the experimentally measured one. Good agreement between the two was observed for the case of small cracks. Both finite element programs that were developed for the fracture analysis were based on the general finite element program FEABL.[8]

Further details on this part of the research program can be found in the third technical progress report and in the following thesis:

Gonçalves, E., "Fracture Analysis of Welded Structures", Ph.D. thesis, M.I.T., May 1981.

A review is also provided in Appendix B of this report.

---

[8]Orringer, O., French, S.E., and Winreich, M., "User's Guide for the Finite Element Analysis (FEABL 2, 4 and 5) and the Element Generation Library (EGL)", Aeroelastic and Structure Research Lab., Department of Aero. and Astro., M.I.T., January 1978.

2.2 Work Accomplished on Task 2 - Cylindrical Shells

2.2.1 General Status

The objective of Task 2 of this research program is to experimentally and analytically study temperatures, thermal strains, residual stresses and distortion in girth welded high strength steel (specifically HY-130) unstiffened cylindrical shells. All steps of this task (see Table 1.1) have been completed as originally planned.

The work on this task has been completed during the first three years of the research program. Details of this work can be found in the first two technical progress reports to O.N.R. In what follows, a brief summary of the work performed is outlined.

2.2.2 Experimental Program

An initial experiment was performed outside M.I.T. on butt welding two unstiffened low carbon steel cylindrical shells. This exploratory experiment was of great value, providing the M.I.T. investigators with experience that was later utilized in a similar experiment conducted at M.I.T. using HY-130 steel cylinders.

The second experiment, performed at the M.I.T. facilities, involved HY-130 cylindrical shells. The shells were formed from 60 in. x 63 in. x 3/4 in. HY-130 flat plates by first bending them to semi-circular cylindrical shells and subsequently seam-welding the two halves together using the GMA welding process. After completion of the seam weld, the 60 in. long, 18 in. OD cylinder was sawed into three equal sections, and preparations of the grooves were made for the joining of two of these sections. Finally, the two cylindrical sections were girth welded together using the GMA welding process.

Temperature changes and transient strains in the axial and circumferential directions were measured at preselected locations during both the seam and girth welding operations, using thermocouples and electric resistance strain gages, respectively. The radial distortion at two points was also continuously measured during the girth welding of the two cylinders.

Finally, using electric resistance strain gages and the strain relaxation technique, the residual stresses on the outer surfaces of the welded cylinders were measured. The axial and tangential stresses, as distributed in both the axial and circumferential directions, were determined and compared with data from other investigators.

2.2.3 Analytical Program

The problem of welding two unstiffened cylindrical shells was analyzed using existing computer programs developed at M.I.T. during the past several years. A program based on the analytical solution for a moving point heat source was used for the heat flow analysis. Then, strains, stresses, and distortion during welding were analyzed using an axisymmetric finite element program.

Good correlation was observed between the numerically and experimentally obtained temperature distributions. However, this was not the case for the strain and stress analysis. It is believed that if adequate funding was available, better results would have been obtained using the modified finite element programs ADINAT and ADINA.

2.3 Work Accomplished on Task 3 - Bronze Weldments

2.3.1 General Status

The objective of Task 3 of the current research project is to experimentally generate information on temperature changes, transient strains and distortion on bronze weldments. In particular, Nickel-Aluminum (Ni-Al) bronze was chosen as the material to be investigated, because of the problems encountered in controlling distortion during the manufacturing of propeller blades using this material. It should be pointed out that this investigation was prompted from the fact that, to the best of our knowledge, no published information is available on the subject.

The work on this Task was initiated and completed during the fourth year of this research program. Details on this work can be found in the third progress report to O.N.R. and the following thesis:

McCord, R.S., "An Investigation of Strain, Distortion, and Heat Flow Distribution During Welding of Nickel-Aluminum Bronze", Ocean Engineer's thesis, M.I.T., June 1981.

In what follows, a brief summary is given of the work performed.

2.3.2 Literature Review and Experimental Program

A literature survey was first conducted to obtain information on the mechanical and physical properties of Ni-Al bronze and their dependence on temperature. This was necessary for the numerical analysis of heat flow and thermal stresses during welding.

Two series of experiments, using a total of eight specimens, were conducted to measure temperature, thermal strain, and distortion changes during the welding of Ni-Al bronze plates. Emphasis was placed on comparing the final distortions of the plates after welding.

The first series of experiments consisted of laying a bead-on-plate weld in two passes. Specimens 1 through 6, all measuring 24 in.x 12 in.x 1/4 in., were welded in this manner, with the heat input being held approximately constant for all specimens. Specimens #1 and #2 were welded in the unrestrained condition so that baseline data could be gathered for comparison purposes with other conditions. Specimen #3 was restrained during both weld passes using C-clamps. Specimen #4 was block welded in four blocks; in each block, measuring 6 in in length, both passes were completed before moving on to the next one. Specimen #5 was welded in the unrestrained condition; it was preheated and postheated using oxyacetylene torches, and finally the weld was ground down at preselected locations. Specimen #6 was welded in the restrained condition.

The second series of experiments consisted of laying, in two passes, a bead on the edge of two specimens, #7 and #8, each measuring 21 3/4 in.x 5 3/4 in.x 1/4 in. Heat input as well as all other parameters were kept constant in both cases.

Temperature, strain, and distortion changes were recorded continuously during the welding of all specimens. Results are reported in the third progress report to O.N.R. and in McCord's thesis.

3. WORK ACCOMPLISHED ON TASK 4 - THERMAL STRESS RELIEVING

3.1 General Status

The objective of Task 4 of this research project is to study the mechanisms and evaluate the effectiveness of thermal stress relieving in weldments. Task 4 consists of the following subtasks (see Table 1.2):

Task 4.1: Initial Analysis and Verification Tests

Task 4.2: Further Analysis and Experiments

Both subtasks are now completed as originally proposed.

An extensive literature survey was initially performed covering thermal, mechanical and vibratory stress relieving treatments. Special attention was given to the applicable military and industrial codes.

An initial analysis of the effectiveness of mechanical and thermal stress relieving treatments was performed for the cases of long, thin plates butt- or edge-welded. The one-dimensional computer program earlier developed at M.I.T. was modified to calculate strains and stresses during and after uniform-temperature heat treatments. Stress relaxation, due to creep at high temperatures, was also included in the analytical model.

Experiments to verify the analytical results were then conducted using 304 stainless steel plates. This was decided since extensive creep data for HY-130 steel could not be located in the literature.

Further analysis was then performed in order to investigate the effectiveness of low-temperature thermal stress relieving treatments. Specifically, the one-dimensional computer program was further modified, so as to calculate the temperature, strain, and stress distributions during and after line heating with a flame.

Finally, verification experiments were conducted using edge-welded HY-130 steel plates. Both uniform and line heating were tested.

A summary of the work performed is presented in the next sections of this chapter. Additional data is in the following theses:

Agapakis, J.E., "Welding of High Strength and Stainless Steels: A Study on Weld Metal Strength and Stress Relieving", S.M. Thesis, M.I.T., May 1982.

Carpentier, K.P., "Thermal Stress Relief of HY-130 Weldments", S.M. thesis, M.I.T., May 1982.

3.2 Literature Survey

It is a well established fact that during the fabrication of welded structures, residual stresses are developed having peak values that reach the yield stress of the material being welded. This fact was confirmed by both analysis and experiments for the case of HY-130 steels in the course of the present research program.

Residual stresses must be a major cause of concern since they usually are detrimental, directly or indirectly, to the integrity and the service behavior of a welded structure. As a consequence, several methods, aimed at reducing residual stresses, have been proposed and are currently in use. These methods include both mechanical and thermal treatments.

In the next few parts of this section, a brief evaluation of the various methods is attempted and some important results are presented. A more complete review is given in the previously mentioned theses.

3.2.1 Thermal Stress Relieving Treatments

Thermal stress relieving basically involves heating of the part to a subcritical temperature, below A_{c_1}[9], holding it at that temperature to ensure uniformity, and slow cooling to room temperature, usually in air, to prevent the reintroduction of stresses. The stress relieving temperatures usually are of the order of 1100°F to 1300°F (590°C to 700°C), where the yield strength has drastically decreased and creep occurs. The welding residual stresses can no longer be supported. Thus the stress distribution will be relatively uniform and at a very low level.

[9] By A_1 we denote the lower critical temperature, where perlite begins to transform into austenite (A_{c_1} is used for heating and A_{r_1} for cooling).

Up to A_{c_1}, the higher the stress-relieving temperature, the more completely the stress is removed.

Full relief of the residual stresses can only be ensured through an annealing treatment. This, however, would be more costly and time consuming and would cause more problems due to the higher temperatures.

Stress relieving is always followed by some dimensional changes. Even warpage and distortion can result when the residual stresses are high enough. Therefore, it may be necessary to straighten the part and sometimes to stress relieve again to reduce the straightening stresses.

Stress relief heat treatment can be applied either to the structure as a whole, or to specific portions of it if the size is prohibitively large. In the former case, electric and fossil-fired furnaces are generally used, whereas the localized heat treatment is effected by means of electric resistance, induction, gas flame, and exothermic heating techniques.

For local stress relieving heat treatments, it is absolutely necessary to ensure that the temperature distribution during the heat treatment does not induce new thermal stresses which exceed the material yield stress and can lead to the development of new residual stresses on cooling. This imposes strict requirements on the level and uniformity of temperature, on the heating and cooling rates, and on the width of the heating zone. The latter largely determines the existing temperature gradient through the thickness (between the heated and unheated surfaces).

For butt welded plates, it was experimentally proven that satisfactory relief of residual stresses can be expected if uniform heat input is applied over a band-width of twice the length of the weld, as shown in Figure 3.1a.[10] According to British codes, this bandwidth becomes equal to $5\sqrt{Rt}$ for a circumferential girth weld on a cylinder of radius R and thickness t (Figure 3.1b). Different specifications, however, are spelled out in different welding codes.

---

[10] Burdekin, F.M., "Heat Treatment of Welded Structures", The Welding Institute, Abington, England, 2nd edition, 1969.

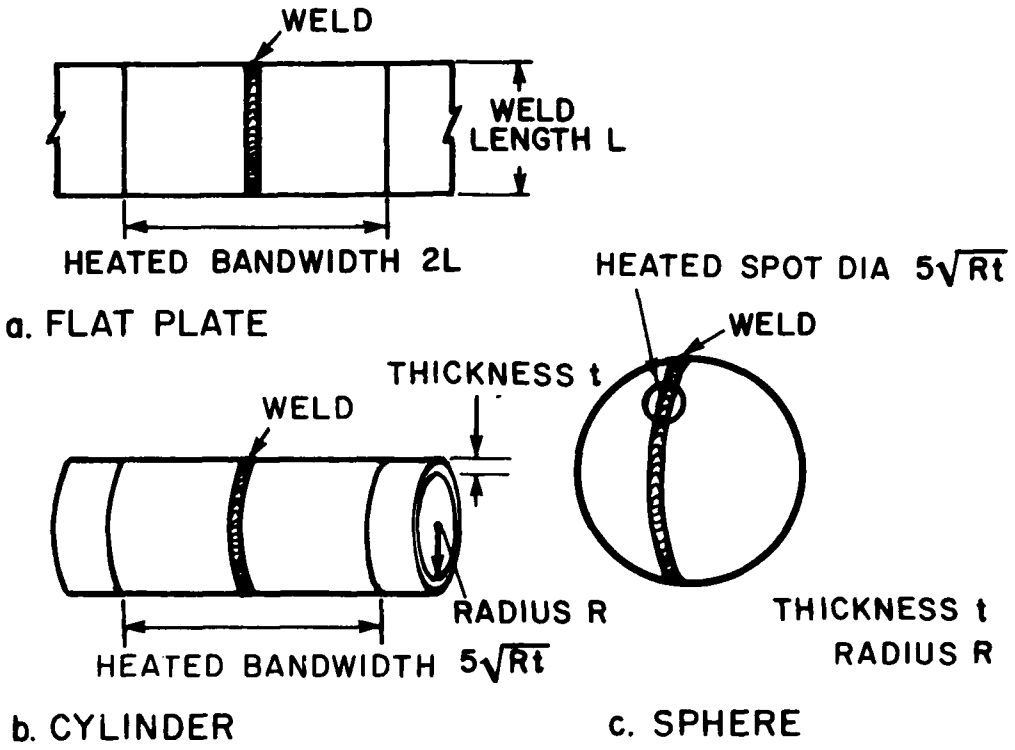

FIGURE 3.1 Band widths for local heat treatments to achieve stress relief in: (a) flat plate situations, (b) circumferential butt joints in cylinders, and (c) butt joints in spheres

Nevertheless, there are generally three main requirements that govern the selection of the heat treating method:

(a) It should be able to produce the required temperature.

(b) The required temperature should be controlled within specified limits (e.g., $\pm$ 10° to 20°F for steels).

(c) It should be possible to achieve a uniform and even heating and cooling rate throughout the heaviest section to be treated.

The last requirement is especially important for the case of joints of complex geometry and variable thickness.

3.2.2 Effects of Thermal Stress Relieving

Stress relieving heat treatments are usually effective in reducing the high residual stresses present in a weldment. However, they also have an effect on the microstructure and the properties of both the base plate and the weld metal since they are carried out at relatively high temperatures. These effects vary with the material under consideration.

During the last decade, the desirability of post weld heat treatments and their effects were extensively investigated by the Working Group on Thermal Stress Relief of the Commission X of the International Institute of Welding. Information from the series of documents[11] that were produced is summarized in this section.

Specifically for non work-hardened base metal of C-Mn and micro-alloyed steels, it was generally concluded that tensile properties are impaired to a significant extent, especially at higher temperatures. Resistance to brittle fracture is affected but not drastically. Temperature is a more important factor than soaking time. For low alloy and creep resistant steels, which are used in a normalized and tempered or a quenched and tempered condition, the effect of stress relieving treatments on the properties will depend on the temperature. The effect will be minimal if the treatment is carried out at a temperature lower than that of initial tempering. Additional tempering will result however, if higher temperature treatment is performed. This is usually beneficial for the resistance to brittle fracture, but detrimental for other properties such as creep resistance, and usually is not recommended by the codes. On the other hand, for the case of work-hardened base material, the heat treatments usually restore the base properties and prevent strain aging, and are therefore beneficial.

---

[11] I.I.W. Working Group on Stress Relief by Heat Treatment, "Final Report: Desirability of Post Weld Heat Treatments in Welded Construction," I.I.W. Document X-913-78, February 1979.

The effect of stress relieving heat treatments on the properties of the heat affected zone (HAZ) will not only depend on the type of steel but also on the microstructural state of the HAZ. Therefore, welding procedure and conditions, heat input, plate thickness and distance to the fusion line are important parameters. For C-Mn steels the heat treatment will in general soften the HAZ structures, except if carbide precipitation occurs. The yield strength of the HAZ will usually be higher than that of the base material after the same treatment. In most cases, heat treatments are also beneficial for resistance to brittle fracture for these steels. For low alloy steels, the main problem is to retain satisfactory toughness in the HAZ. The effect of treatment is usually strongly dependent on the type of steel and the exact metallurgical changes associated with the welding and heat treating tempering.

Although not much work has been done on the effect of heat treatments on the properties of weld metal, it appears that tensile properties diminish considerably on tempering. Again, temperature seems to be more important than the soaking time. As in the base metal, embrittlement can occur and instances of stress relief cracking have been reported.

Stress-relief cracking is defined as "intergranular cracking in the heat affected zone or weld metal that occurs during the exposure of welded assemblies to elevated temperatures produced by post-weld heat treatments or high-temperature service". It has also been referred to in the literature as "post-weld-heat cracking" or "reheat cracking" and in general is caused when some relief of stresses by creep occurs. This form of cracking became a problem with the austenitic stainless steels in the 1950's and with the low-alloy constructional steels in the 1960's. It also occurs in ferritic creep-resisting steels and nickel base alloys and is generally related to precipitation hardening. Non-precipitation hardening materials, such as plain carbon steels and certain nickel alloys, are not susceptible to reheat cracking.

The cracks can be positively identified by metallographic examination due to their characteristic branching intergranular morphology, along the coarse-grain region of the heat-affected zone. Cracking usually occurs at high temperature, when creep ductility is insufficient to

accommodate the strains required for the relief of applied or residual stresses. When residual stresses are high, as in thicker and restrained sections, reheat cracking is most likely to occur.

Extensive investigations of the cracking mechanism and of possible remedies have been undertaken all over the world, and are in detail reviewed by Meitzner[12] and Dhooge, et al.[13] In 1970 I.I.W. established, in Commission X, a Working Group on "Reheat Cracking" to collect and assimilate information on the subject.

2.2.3 Stress Relieving of HY-130 Steels

The very high residual stresses that develop during welding of HY-130 steels make stress relief treatments very attractive. Substantial reduction of stresses was shown to occur in both the base and weld metal at temperatures between 950°F (510°C) and 1050°F (566°C).[14] However, a severe degradation of notch toughness may also occur at these temperatures. This embrittlement, which is phenomenologically similar to temper embrittlement, is believed to be influenced by the soaking temperature, the time at temperature, the cooling rates, the plastic strain, the exact alloy composition and prior heat treatment.

Extensive investigation on the subject was performed by the U.S. Steel Corporation and the U.S. Navy (N.S.R.D.C. Materials Laboratory). Results by Rosenstein[15] indicated that stress relief cycles are cumulative in nature,

---

[12] Meitzner, C.F., "Stress Relief Cracking in Steel Weldments", An Interpretive Report, Welding Research Council, Bulletin 211.

[13] Dhooge, A., et al.,"A Review of Work Related to Reheat Cracking in Nuclear Reactor Pressure Vessel Steels", International Journal of Pressure Vessels and Pipeing No. (6) 1978, pp. 329-409.

[14] N.S.R.D.C. reports on "Stress Relief Embrittlement of AX-140 and E-11018 Weld Metals", and "Stress Relief Characteristics of a 5% Ni Weld Metal", obtained after private communication, October 1981.

[15] Rosenstein, A.H., "Phenomenological Investigations of Stress Relief Embrittlement, Welding Journal, March 1970, pp. 122s-131s.

by comparing the tensile and Charpy properties resulting from consequent heat treatments of short duration and one single treatment of long duration, both having the same soaking times.

Furthermore, it was observed that the degradation of notch toughness was maximum when stress relieving at 950°F (510°C) and minimum when at 1050°F (566°C). However, investigations of the effects of stress relieving on the weld metal have shown that the higher temperatures may substantially reduce the yield and tensile strength of the weld metal, and thus may cause undermatching. Therefore, the most practical temperature range for effective stress relieving of HY-130 weldments is between 1000°F (538°C) and 1025°F (552°C).

Additionally, it was established that the degradation of toughness at 950°F (510°C) occurs during both soaking and cooling. The isothermal degradation was shown to be directly dependent upon time at temperature. The degradation during cooling, on the other hand, is inversely related to the cooling rate and does not depend on the soaking time. Therefore, cooling embrittlement constitutes the major portion of degradation after short times at temperature and only a minor one after long soaking periods.

It was also shown that stress relief at the tempering temperature of 1050°F (566°C) results in softening at temperature (accompanied by increased toughness) and embrittlement on cooling. Therefore, the resulting properties will depend both on the cooling rate and the soaking time. Furthermore, it should be mentioned that the toughness degradation due to stress-relief can in general be recovered by retempering to a lower strength level.

3.2.4 Alternative Methods of Stress Relieving

When the metallurgical effects of thermal treatments are undesirable, it is possible to achieve stress relief by mechanical means.

One such method is the well-known overstressing above yield. In general, loading the welded structure to a level higher than its intended service loading will reduce the effect of the existing residual stresses on its service performance. Additionally, a first overloading succeeds

in producing compressive residual stresses around any undetected defects, resulting in what are believed to be beneficial effects on the fatigue characteristics of the weldment. The mechanical treatment, however, does not produce any improvement in the fracture toughness of the HAZ as opposed to the thermal treatments.

An alternative to overstressing is the vibratory stress relief (VSR) treatment. Experimental work on this method started in the 1930's and initially gave rise to very optimistic predictions. During the last decade both experimental and analytical work was intensified in an effort to investigate the mechanisms and effectiveness of the VSR. Although this technique is currently used in the industry with some success, there still remains much to be learned about its mechanism, or even if it actually does relieve stresses as claimed. Nevertheless, the energy savings accrued, in comparison to thermal stress relief treatments, is a sufficient enough reason to exploit its use.

The impact from explosive contact charges was also shown to be capable to redistribute (rather than to relieve) welding residual stresses. Important parameters in such a treatment are the intensity and distribution of the explosive load.

For the purposes of this study, however, no further consideration was given to mechanical or explosive stress relieving techniques. Instead, the method of thermal stress relief treatment was examined both analytically and experimentally.

The metallurgical aspects of thermal stress relieving were also considered to be outside the scope of this investigation. In what follows only the effectiveness of thermal stress relieving treatments in terms of the attained reduction of residual stresses, is examined.

3.3 Analysis of Residual Stress Relaxation Due to Heat Treatments

Residual stress changes can arise during all three stages of a heat treatment, Specifically, referring to Figure 3.2 during the heating part of the process, residual stresses decrease due to the temperature dependence of the mechanical properties, mainly through a reduction of the

yield strength with temperature. During the holding (or soaking) period, the temperature is kept constant and residual stresses are reduced due to creep. Experimental evidence suggests that the major portion of this stress reduction occurs in the first part of this stage.[16] Finally, during the cool-down period, residual stresses increase due to the temperature dependence of the mechanical properties, but hopefully (when the treatment is successful) not to their initial levels.

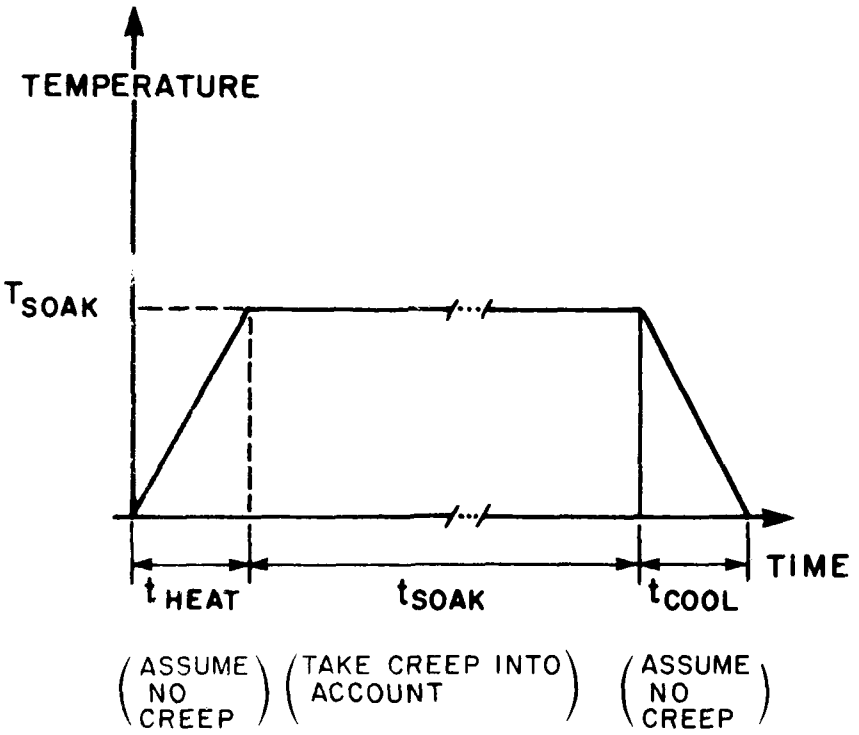

FIGURE 3.2 Stress relieving temperature history

[16] N.S.R.D.C. reports, op.cit.

3.3.1 General Considerations

To judge the effectiveness of a stress relief treatment, with regards to the accomplished reduction of residual stresses, it should be necessary to measure the maximum residual stresses before and after the treatment. The difference would be a realistic measure of performance. However, an acceptable alternative to the time-consuming, costly and usually destructive residual stress measurements, would be a proper analytical model. Furthermore, such a model would be very helpful in determining an optimal lower temperature heat treatment, where a properly selected heating pattern would most effectively reduce stresses, while keeping the metallurgical changes minimal.

In that direction, various approaches have been followed in the literature by several investigators. Very simple uniform residual stress distributions are usually assumed for the weld metal, so that the uni-dimensional stress-strain curves can be directly employed. Such analytical results are obtained and experimentally verified by Tanaka.[17] For more complex cases and two- or three-dimensional stress states numerical models have been proposed to handle the thermal-elastic-plastic and creep analysis required. Ueda and Fukuda[18] present a finite element model capable of calculating welding residual stresses and stress relief due to creep. Fujita, et al.,[19] develop a thermo-visco-elastic-plastic model to study the mechanism of stress relief annealing. Finally, Cameron and Pemberton[20]

---

[17] Tanaka, J., "Decrease in Residual Stresses, Change in Mechanical Properties and Cracking Due to Stress Relieving Heat Treatment of HY-80 Steel", Welding in the World, 10 (1/2), 1972.

[18] Ueda, H., and Fukuda, K., "Analysis of Welding Stress Relieving by Annealing Based on Finite Element Method", Trans. of Japan Weld. Res. Inst., 4 (1), 1975.

[19] Fujita, Y., Nomoto, T., Aoyagi, A., "A Study on Stress Relaxation due to Heat Treatment", Dept. of Naval Architecture, University of Tokyo, May 1973, IIW Doc. X-697-73.

[20] Cameron, I.G., and Pemberton, C.S., "A Theoretical Study of Thermal Stress Relief in Thin Shells of Revolution", Intl. J. for Num. Meth. in Eng., 11, 1977, pp. 1423-1437.

present a numerical model of the thermal stress relief in thin shells of revolution.

For the purposes of the current study, it was decided that the analysis of the thermal stress relieving operation be accomplished using the simple one-dimensional computer program, successfully employed in the past at M.I.T. for the prediction of residual stresses in long, thin, butt or edge welded plates.[21] Some modifications had to be made in this program in order to handle the case of thermal stress relieving. These modifications will be dealt with below at the appropriate places.

3.3.2 Description of the One-Dimensional Model - Assumptions

The fundamental assumptions incorporated in this model are:

(a) The plate is infinite and very thin (referring to Figure 3.3 $L \to \infty$ and $H \to 0$).

(b) The welding arc is modeled as a line heat source, and there is no temperature gradient through the thickness of the plate. (Two-dimensional temperature distribution).

(c) Furthermore, the temperature distribution is stationary if viewed from a system moving with the heat source. (Quasi-stationary state).

(d) Stress is non-zero only in the direction parallel to the weld centerline. (One-dimensional stress distribution).

(e) These stresses are a function of the transverse distance from the weld centerline only.

Additional assumptions for the analysis of thermal stress relief treatment were made as follows:

(f) Any arbitrary temperature distribution and history would be input to the modified program. However, in this project only uniform and line heating were analyzed. In the former case, a uniform temperature distribution was assumed over the entire plate, changing with time as in Figure 3.2.

[21] Papazoglou, V.J., "Computer Programs for the One-Dimensional Analysis of Thermal Stresses and Metal Movement during Welding", M.I.T., January 1977.

In the case of line heating, however, the temperature distribution during the treatment was calculated in a way analogous to the temperature distribution during welding.

Two further assumptions were introduced for the case of uniform heating:

(g) Due to the relatively fast heating and cooling rates it was assumed that no creep occurs during the heating and cooling stages of the treatment.

(h) During the holding or soaking period at the stress relieving temperature, residual stresses can only decrease due to creep. In other words, if creep is not included in the model, no change in stresses will take place during this period.

3.3.3 Temperature Distribution

During welding, the non-uniform and changing with time temperature distribution is estimated in the one-dimensional program by the well-known Rosenthal solution. The exact solution for a line heat source moving along a thin and infinite plate (as in Figure 3.3) is:

$$\theta - \theta_o = \frac{Q}{2\pi kH} \cdot e^{-\frac{v}{2\kappa}\xi} \cdot K_o\left(\frac{vr}{2\kappa}\right) \qquad (3.1)$$

where θ is the temperature at point (x, y) at time t, θ_o is the initial temperature, H the plate thickness, k the thermal conductivity, κ the thermal diffusivity ($\kappa = k/\rho c_p$), ρ is the density, c_p the specific heat, Q the total heat input, v the welding speed and Ko(x) is the modified Bessel function of second kind and zero order.

The moving coordinates ξ and r are:

$$\xi = x - vt \qquad (3.2)$$

and

$$r = (\xi^2+y^2)^{1/2} \qquad (3.3)$$

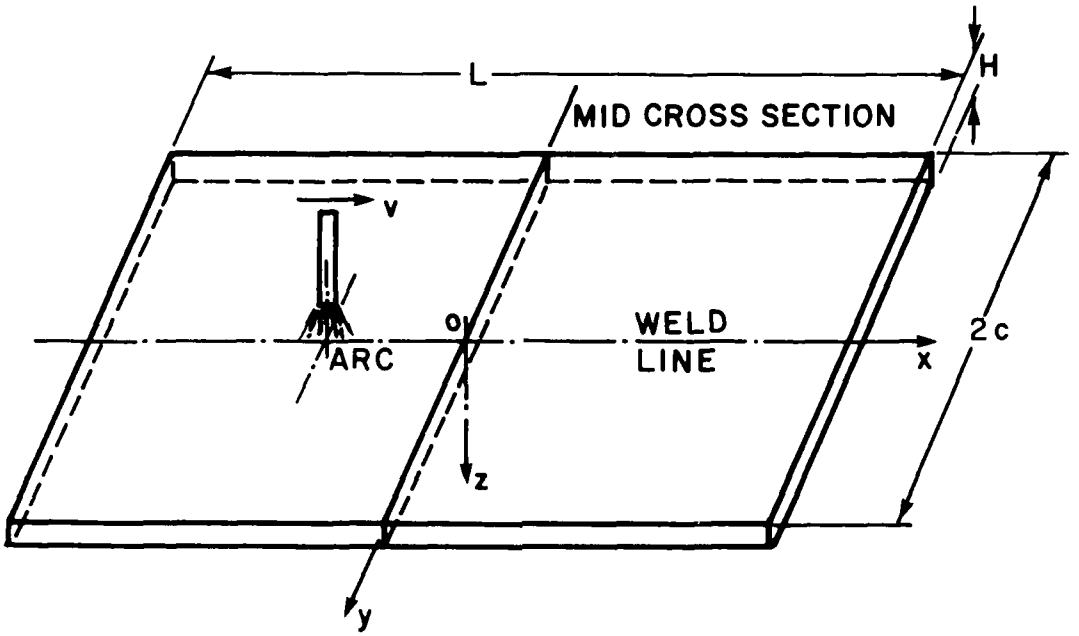

FIGURE 3.3 Weldment configuration (Butt welding of plates)

The total heat input, Q, is

$$Q = V.I.n_a \tag{3.4}$$

where V, I are the arc voltage and current respectively and n_a the arc efficiency.

Finally, it should be noted that Equation (3.1) was also modified to account for heat losses due to ratiation and convection from the surfaces of the plate, becoming:

$$\theta - \theta_o = \frac{Q}{2\pi\lambda h} \cdot e^{-\frac{v}{2\kappa}\xi} \cdot K_o\left(r\sqrt{\left(\frac{v}{2\kappa}\right)^2 + \frac{h}{\lambda T}}\right)$$

where h = average surface heat loss coefficient.

During heat treatment in a furnace the temperature distribution can be assumed to be uniform along the entire plate. For the case of a localized treatment, however, by flame heating for example the temperature distribution can be calculated modifying the solution for a point heat source moving on an semi-infinite body:

$$\theta - \theta_o = \frac{Q}{2\pi k} \cdot e^{-\frac{v}{2\kappa}\xi} \cdot \frac{e^{-\frac{v}{2\kappa}R}}{R} \tag{3.5}$$

where

$$R = (\xi^2 + y^2 + z^2)^{1/2} \tag{3.6}$$

and all the other variables same as in Equation (3.1).

This solution of the governing differential equations satisfies the following boundary conditions:

$$\lim_{R \to 0} \left\{ -2\pi R^2 k \frac{\partial \theta}{\partial R} \right\} = Q \tag{3.7}$$

and also

$$\lim_{R \to \infty} \theta = \theta_o \tag{3.8}$$

Condition (3.7) is the heat equilibrium equation on an infinitely small hemisphere drawn around the point heat source. Condition (3.8) merely states that the temperature must not change at great distances from the source.

In order to more accurately describe the temperature distribution, however, for the case of a finite width and finite thickness plate heated with a traveling heat source, as in Figure 3.4 two more boundary conditions have to be satisfied:

$$\frac{\partial \theta}{\partial z} = 0 \text{ at } z = 0 \text{ and } z=H \tag{3.9}$$

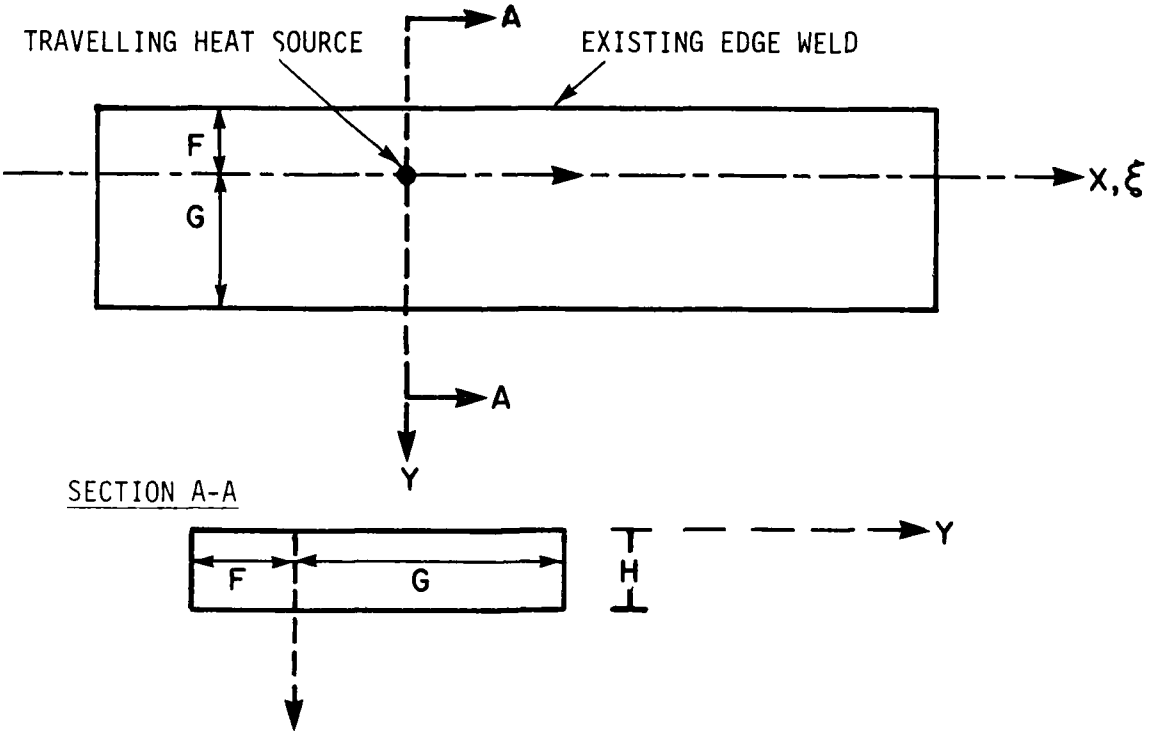

FIGURE 3.4 Geometry of plate undergoing strip heating

$$\frac{\partial \theta}{\partial y} = 0 \text{ at } y = G \text{ and } y = -F \tag{3.10}$$

To satisfy these boundary conditions an infinite number of heat source images with respect to the plate boundaries must be used, as in Figure 3.5. Then the solution becomes:

$$\theta = \theta_o + \frac{Q}{2\pi k} e^{-\lambda v \xi} \left[\frac{e^{-\lambda v R}}{R} + \sum_{n=1}^{\infty} \left[\frac{e^{-\lambda v R_n^T}}{R_n^T} + \frac{e^{-\lambda v R_n^B}}{R_n^B} \right] + \sum_{n=1}^{\infty} \left[\frac{e^{-\lambda v R_m^L}}{R_m^L} + \frac{e^{-\lambda v R_m^R}}{R_m^R} \right] + \sum_{n=1}^{\infty} \sum_{m=1}^{\infty} \left[\frac{e^{-\lambda v R_{nm}^{TL}}}{R_{nm}^{TL}} + \frac{e^{-\lambda v R_{nm}^{TR}}}{R_{nm}^{TR}} + \frac{e^{-\lambda v R_{nm}^{BL}}}{R_{nm}^{BL}} + \frac{e^{-\lambda v R_{nm}^{BR}}}{R_{nm}^{BR}} \right] \right] \tag{3.11}$$

where

$$R_n^T = \sqrt{\xi^2 + y^2 + (2nH-z)^2}$$

$$R_n^B = \sqrt{\xi^2 + y^2 + (2nH+z)^2}$$

$$R_m^L = \sqrt{\xi^2 + (O_m^L - y)^2 + z^2}$$

$$R_m^R = \sqrt{\xi^2 + (O_m^R + y)^2 + z^2} \qquad (3.12)$$

$$O_m^L = O_{m-1}^R + 2G \text{ with } O_1^L = 2G$$

$$O_m^R = O_{m-1}^L + 2F \text{ with } O_1^R = 2F$$

$$R_{nm}^{TL} = \sqrt{\xi^2 + (O_m^L - y)^2 + (2nH + z)^2}$$

$$R_{nm}^{TR} = \sqrt{\xi^2 + (O_m^R + y)^2 + (2nH = z)^2}$$

$$R_{nm}^{BL} = \sqrt{\xi^2 + (O_m^L - y)^2 + (2nH + z)^2}$$

$$R_{nm}^{BR} = \sqrt{\xi^2 + (O_m^R + y)^2 + (2nH - z)^2}$$

A finite number of images was used in the computer implementation of Equation (3.11).

3.3.4 Stress Analysis

To calculate the transient and residual stresses during and after welding and subsequent heat treatments, the method of successive elastic solutions is employed. The procedure, outlined by Mendelson,[22] was first

[22] Mendelson, A, "Plasticity: Theory and Applications", Macmillan Publ. Co., New York, 1968.

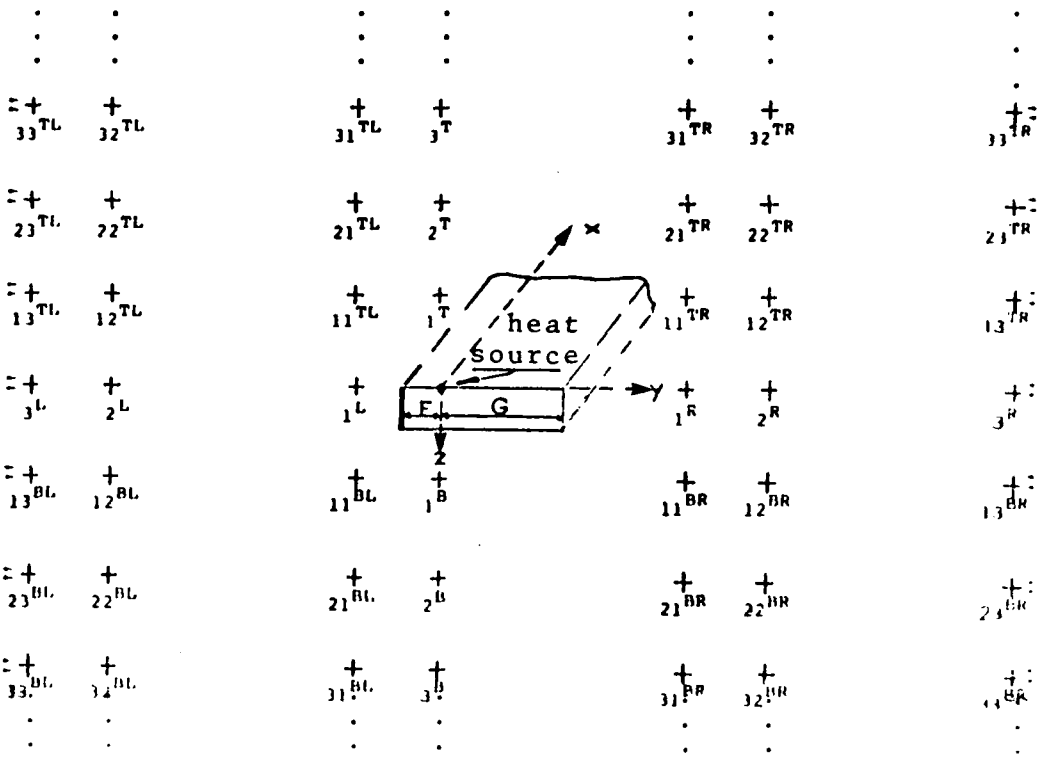

FIGURE 3.5 Arrangement of heat source images for a finite width and thickness plate

used in the solution of welding problems by Tall[23], and later by Masubuchi[24].

To analyze the stress state at the center cross section of the plate (Figure 3.3) due to an arbitrary, and changing with time, temperature distribution, $\theta(y,t)$, it is assumed that at time t, the section is a part of an infinitely long plate subject to the same temperature distribution

[23] Tall, L., "Residual Stresses in Welded Plates, A Theoretical Study", Welding Journal, 43 (1), 1964, pp. 10s-23s.

[24] Masubuchi, K., Simmons, F.B., and Monroe, R.E., "Analysis of Thermal Stresses and Metal Movement During Welding", RSIC-820, Redstone Scientific Information Center, Redstone Arsenal, Alabama, July, 1968.

over its entire length, as in Figure 3.6. This temperature profile will remain the same during the current time increment, Δt.

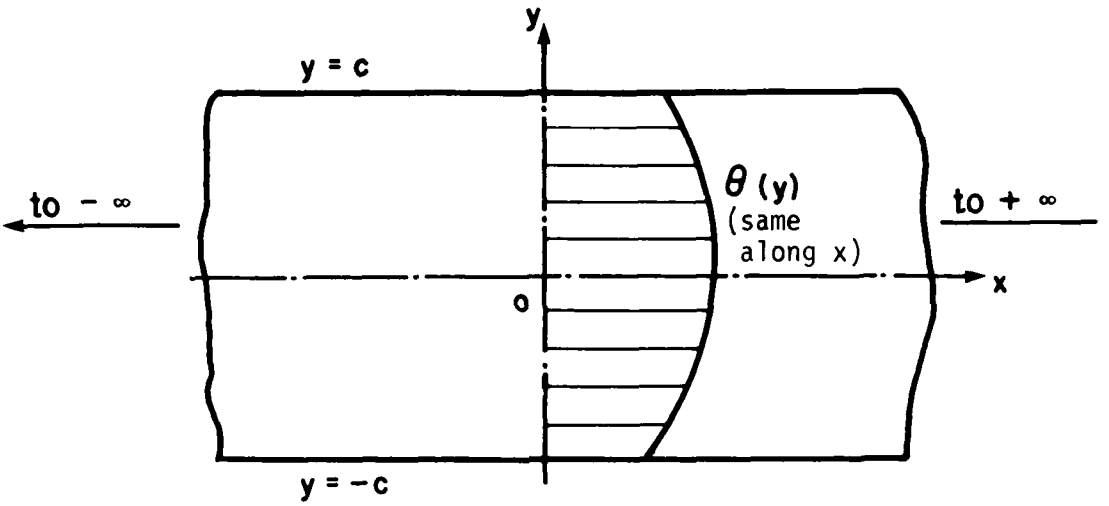

FIGURE 3.6 Thin infinite strip with temperature distribution across the width

The only non-zero stress and strain are assumed to be $\sigma_x = \sigma_x(y)$ and $\varepsilon_x = \varepsilon_x(y)$.

Compatibility equations for one dimension reduce to

$$\frac{d^2\varepsilon_x}{dy^2} = 0 \tag{3.13}$$

or

$$\varepsilon_x = c_1 + c_2 y \tag{3.14}$$

where c_1 and c_2 are constants to be determined. The above equation essentially states that plane sections will always remain plane.

Considering an incremental approach, at the end of a time interval Δt the following will hold along the cross section

$$\varepsilon_x = \frac{\sigma_x}{E} + \alpha \cdot \Delta\theta + \varepsilon_x^{in} + \Delta\varepsilon_x^{in} \tag{3.15}$$

or

$$\sigma_x = E(\varepsilon_x - \alpha\cdot\Delta\theta - \varepsilon_x^{in} - \Delta\varepsilon_x^{in}) \tag{3.16}$$

where

σ_x/E = Elastic part of strain, ε_x^{el}

$\alpha\cdot\Delta\theta$ = Thermal strain, ε_x^{th}

$\Delta\theta = \theta - \theta_o$

ε_x^{in} = Accumulated (during the previous time increments) inelastic strain = $\varepsilon_x^{pl} + \varepsilon_x^{c}$

ε_x^{pl} = Plastic strain

ε_x^{c} = Creep strain

$\Delta\varepsilon_x^{in}$ = Change in inelastic strain during the time increment Δt

From global equilibrium (no external forces and moments acting on the plate)

$$\int_{-c}^{+c} \sigma_x \, dy = 0 \tag{3.17a}$$

$$\int_{-c}^{+c} \sigma_x y \, dy = 0 \tag{3.17b}$$

Substituting Eqs. (3.14) and (3.15) into (3.17), a set of linear equations is obtained for the detemination of the unknown coefficients c_1 and c_2. Solving this system and substituting back into Eq. (3.14), the following expression is obtained for the total strain:

$$\varepsilon_x(y) = (A_1 - yA_2) \int_{-c}^{+c} E(\alpha\cdot\Delta\theta + \varepsilon_x^{in} + \Delta\varepsilon_x^{in}) \, dy$$

$$- (A_2 - yA_3) \int_{-c}^{+c} E(\alpha\cdot\Delta\theta + \varepsilon_x^{in} + \Delta\varepsilon_x^{in}) y \, dy \tag{3.18}$$

where

$$A_1 = \left[\int_{-c}^{+c} Ey^2 dy\right] /B$$

$$A_2 = \left[\int_{-c}^{+c} Eydy\right] /B \qquad (3.19)$$

$$A_3 = \left[\int_{-c}^{+c} Edy\right] /B$$

and

$$B = \left[\int_{-c}^{+c} Edy\right] \cdot \left[\int_{-c}^{+c} Ey^2 dy\right] - \left[\int_{-c}^{+c} Eydy\right]^2$$

Equations (3.16) and (3.19) are not enough to solve the problem. What is still needed is a stress-strain law and a relation between stress and creep strain increments.

To proceed further, the assumption is made that creep will only take place during the soaking stage of the temperature history. Thus, during this period the accumulated plastic strain, ε_x^{pl}, will remain constant. The heating and cooling stages where no creep occurs are treated in exactly the same way as the welding problem.

(A) Specifically during welding when creep is not taken into account:

$$\varepsilon_x^{in}(y) = \varepsilon_x^{pl}(y) \qquad (3.20)$$

At each time step, the total strain is first calculated along the cross section from Eq. (3.18) assuming that no plastic strain exists.

$$\varepsilon_x^{pl}(y) = 0 \qquad (3.21)$$

The mechanical strain, ε^m, then is:

$$\varepsilon_x^m(y) = \varepsilon_x(y) - \varepsilon_x^{th}(y) = \varepsilon_x(y) - \alpha \cdot \Delta\theta(y) \qquad (3.22)$$

Now assuming a bilinear stress-strain law, a first approximation of the plastic strain along the cross section can be obtained, as in Figure 3.7. This value can be used again in Eq. (3.18) to obtain a second

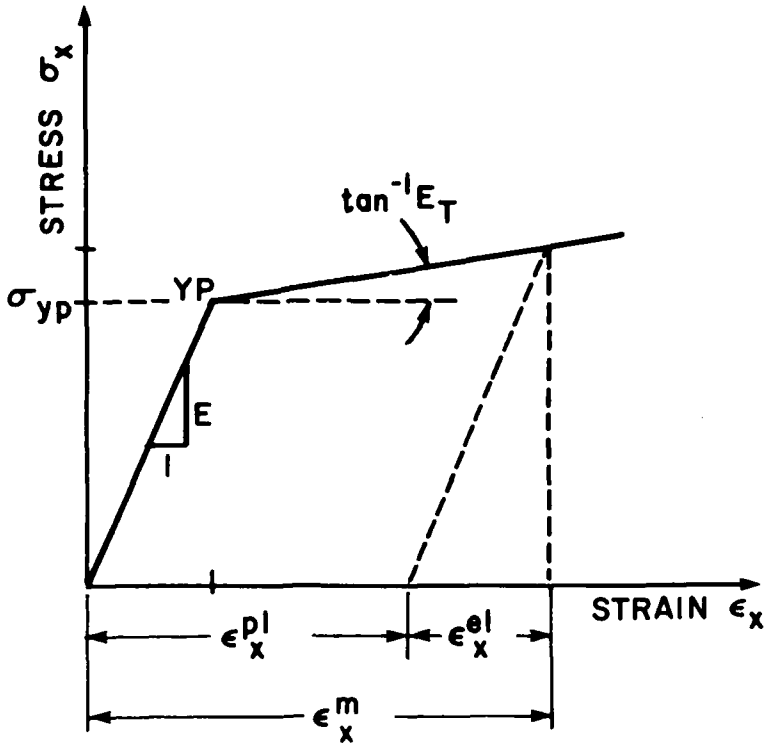

FIGURE 3.7 Bilinear stress strain law used in 1-D model

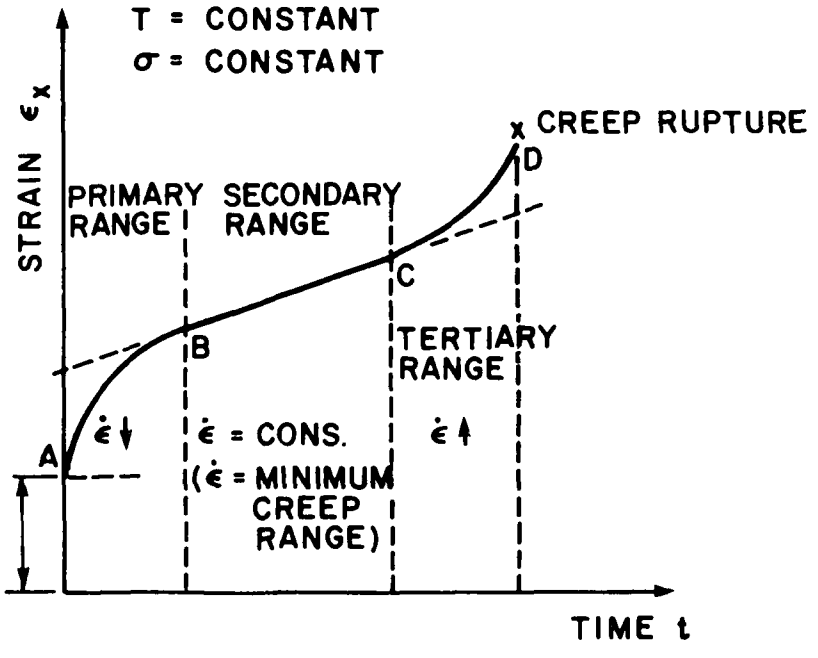

FIGURE 3.8 Uniaxial creep curve

approximation of the total strain and the process can be repeated until convergence is reached.

Further details of this iterative procedure, which can also be applied during the heating and cooling stages of a heat treatment, can be found in the previously mentioned references on the successive elastic solutions method. However, it should be noted that during the calculation of the total strains at each time step, the accumulated plastic strains from previous time steps should be included to account for possible elastic unloading or reverse yielding.

(B) During the holding period, when creep is taken into account, this procedure has to be slightly modified.

At the start of the first time increment the inelastic strain is:

$$\varepsilon_x^{in}(y) = \varepsilon_x^{pl}(y) \tag{3.23}$$

where

ε_x^{pl} is the total accumulated plastic strain up to that instant (due to welding and heating)

As mentioned before, ε_x^{pl} will remain constant during the whole soaking period.

To get a first approximation of the total strain, ε_x, after Δt, from Eq. (3.18) it is now assumed that

$$\Delta\varepsilon_x^{in} = \Delta\varepsilon_x^{c} = 0 \tag{3.24}$$

This first approximation of the total strain, ε_x, is then substituted in Eq. (3.16) to obtain a first approximation of stress σ_x. Using this stress approximation and the appropriate creep law (Section 3.3.5), a second approximation for the creep strain increment, $\Delta\varepsilon_x^{c} = \Delta\varepsilon_x^{in}$, is obtained. This value is now again substituted in Eq. (3.18) for a new approximation of the total strain ε_x and the process is repeated until convergence is reached.

At the start of the second and any subsequent time increments, the total strains will be equal to the initial plastic strain plus the accumulated creep strain during the previous time increments:

$$\varepsilon_x^{in}(y) = \varepsilon_x^{pl}(y) + \sum_{i=1}^{n-1} \Delta\varepsilon_x^{c}(y) \tag{3.25}$$

Assuming again that $\Delta\varepsilon_x^c$ is zero during this time step, the process outlined above can be repeated.

3.3.5 Creep Laws

Creep, the time dependent deformation and fracture of materials, is probably the most general type of material behavior. The current state of the art in inelastic high-temperature analysis requires that plasticity and creep constitutive equations be formulated largely on independent bases. However, elevated-temperature deformation is, essentially, the result of time-dependent processes where both plastic and creep behaviors are present simultaneously. Prior creep deformations influence subsequent plastic behavior and vice versa. However, only limited information is available on these mutual interactions as outlined by Corum, et al.[25] For the purposed of this study the two behaviors were modeled separately, as already noted in the previous section.

Very limited information is available in the literature on the creep behavior of high-strength, quenched and tempered steels, as HY-80 and HY-130. Only some data on the minimum creep rupture time are reported (as by Domis[26]).

---

[25] Corum, J.M., et al., "Interim Guidelines for Detailed Inelastic Analysis of High-Temperature Reactor System Components", Oak Ridge National Laboratory Report ORNL-5014, Dec. 1974.

[26] Domis, W.F., "Creep and Creep Rupture Properties of HY-80 and HY-130 (T) Steels", U.S. Steel Applied Research Laboratory, Report No. 39.012-006 (1), July 15, 1968.

For stainless steels, on the other hand, numerous studies have been performed to investigate their elevated-temperature inelastic behavior. As reported by Clinard, et al.[27], uniaxial creep behavior (Figure 3.8) of stainless steels during the primary and secondary stage can be very well modeled by an equation of the form:

$$\varepsilon_x^c(\sigma_x,t,T) = f(\sigma_x,T)\left[1-e^{-r(\sigma_x,T)t}\right] + g(\sigma_x,T)\ .\ t \qquad (3.26)$$

where ε_x^c is the uniaxial creep strain, σ_x the applied stress, T the test temperature and t the time.

The functions $f(\sigma_x,T)$, $r(\sigma_x,T)$ and $g(\sigma_x,T)$ can be deduced from creep test data by curve fitting. Clinard, et al.[27], report for 304 stainless steels, the following representation at T = 1100°F (594°C).

$$\begin{aligned} f(\sigma_x) &= 5.436\times10^{-5}\sigma_x^{1.843} \\ r(\sigma_x) &= 5.929\times10^{-5}\exp(0.2029\sigma_x) \\ g(\sigma_x) &= 6.73\times10^{-9}\left[\sinh\ (0.1479\sigma_x)\right]^{3.0} \end{aligned} \qquad (3.27)$$

where

σ_x is expressed in Ksi, t in hours and the creep strain and ε_x^c in inches/inch.

Creep response to constant uniaxial compression is usually assumed identical to that in tension (actually a reflection of it with respect to the time axis).

For the complete description of the time dependent behavior of the material, a "hardening rule" is needed in order to predict the creep response when the stress levels are changing. The two most commonly used rules, time hardening and strain hardening, are schematically shown in Figure 3.9. It should be pointed out, however, that

[27] Clinard, J.A., et al., "Verification by Comparison of Independent Computer Program Solutions", Pressure Vessels and Piping Computer Program Evaluation and Qualification, Energy Technology Conference, Houston, Texas, September 1977, A.S.M.E., pp. 27-49.

these rules are strictly correct only in step changes of stress that are of long duration.

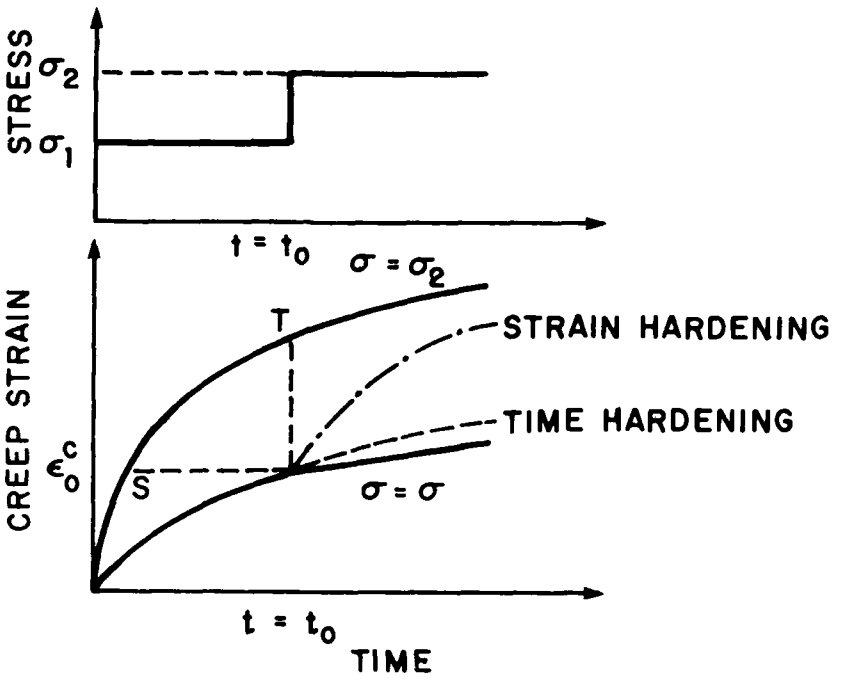

FIGURE 3.9 Strain-hardening and time-hardening models of creep response under a stepwise varying load

Experimental evidence tends to support a strain hardening formulation for the case of 304 and 316 stainless steels. In our problem, however, where small changes of stress take place at each infinitesimal time step, it was decided, for computational efficiency, to adopt time-hardening. Specifically the creep strain increment $\Delta e_x^c(y)$ accumulated between time t and t+ Δt (at each point along the cross section) is:

$$\Delta\varepsilon_x^c(y) = \varepsilon_x^c\left[\sigma_x(y),\ (t+\Delta t),\ T(y)\right] - \varepsilon_x^c\left[\sigma_x(y), t, T(y)\right] \qquad (3.28)$$

where

$T(y)$ = the temperature distribution, and

$\sigma_x(y)$ = the current approximation of the stress distribution

In Eq. (3.28) the creep strain rate $\Delta\varepsilon_x^c(y)/\Delta t$ is a function of stress, time and temperature. Time hardening was assumed in order to avoid the added computations of solving Eq. (3.26) for time, as a strain hardening formulation would require.

3.3.6 Computer Implementation and Results

It should be noted at this point that in the calculation of the temperature distribution during welding and non-uniform heat treating, a special iterative scheme is employed in order to account for the temperature dependence of the material properties.

In the stress calculation, all variables and formulas are non-dimensionalized and all the integrations are performed numerically. Finally, it is worth pointing out that the previously derived equations are considerably simplified in special cases. So, during butt or bead-on-plate welding, the temperature, and thus the strain and stress, distribution is symmetrical with respect to the weld line. Furthermore, during uniform heat treating the temperature is assumed to be constant over the whole plate during each time step. Further details of the above analysis, a complete listing of the modified one-dimensional program, and results of various sample cases are given in Agapakis' thesis.

The predictions of the one-dimensional program for the case of edge welding and subsequent stress relieving of 304 stainless steel plates are presented next in this section. Welding conditions were assumed exactly the same as in the experiments described in Section 3.4.1 of this report. Temperatures, strains and stresses were calculated across a center strip of the specimen throughout welding and stress relieving operations.

A range of values was found in the literature for the arc efficiency and the surface heat loss coefficient. Since, no experimental measurements of these parameters were made in this study, the actually selected values, within that range, were such as to minimize the deviation of the predicted temperature history from the experimentally measured one.

The predicted temperatures, mechanical strains and stresses during welding are plotted in Figures 3.10, 3.11, 3.12. For ease of comparison with experimental data, the same locations (0.5, 1.0, 1.5, 2.0 and 3.0 inches from the weld line) are selected.

During uniform stress relieving at 1000°F, the assumed temperature history is shown in Figure 3.13 and the predicted variations in mechanical strain and stress are plotted, versus time, in Figures 3.14 and 3.15. Comparisons of the predicted residual stress distribution after welding and after stress relieving are given in Figure 3.16.

Analytical results for HY-130 steel are given in Section 3.4.2, together with experimental measurements.

3.4 Experimental Study

To verify the analytical predictions, experiments were initially performed using 304 stainless steel plates. As already mentioned, this was decided since extensive creep data for HY-130 steel could not be located. Only uniform-temperature heat treatments were tested in this first phase.

Subsequently, further experiments were conducted using HY-130 steel plates. Both uniform and line heating treatments were tested.

A summary of the experimental procedures and results will be presented in the next few parts of this section.

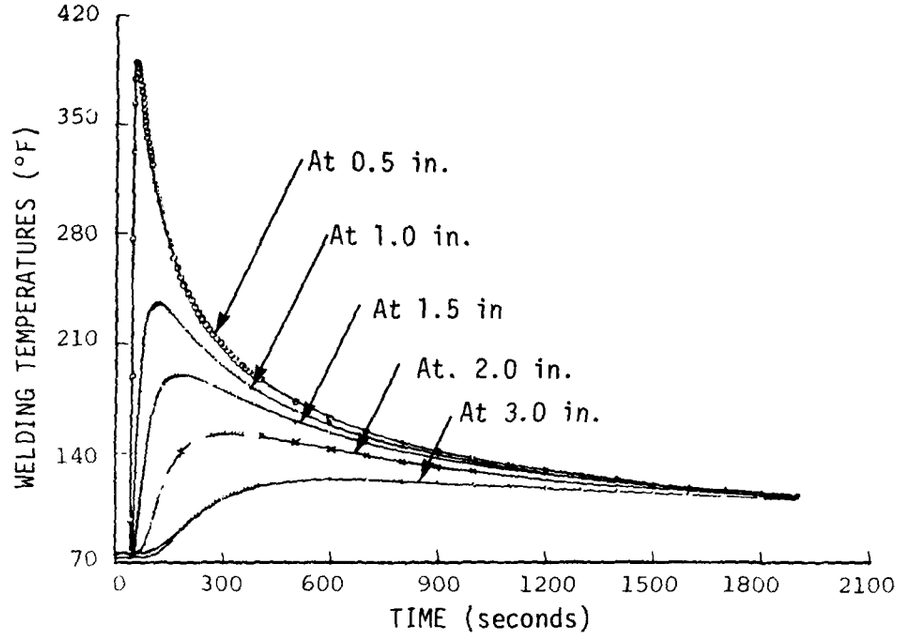

FIGURE 3.10 Temperatures during edge welding, as predicted by the one-dimensional program

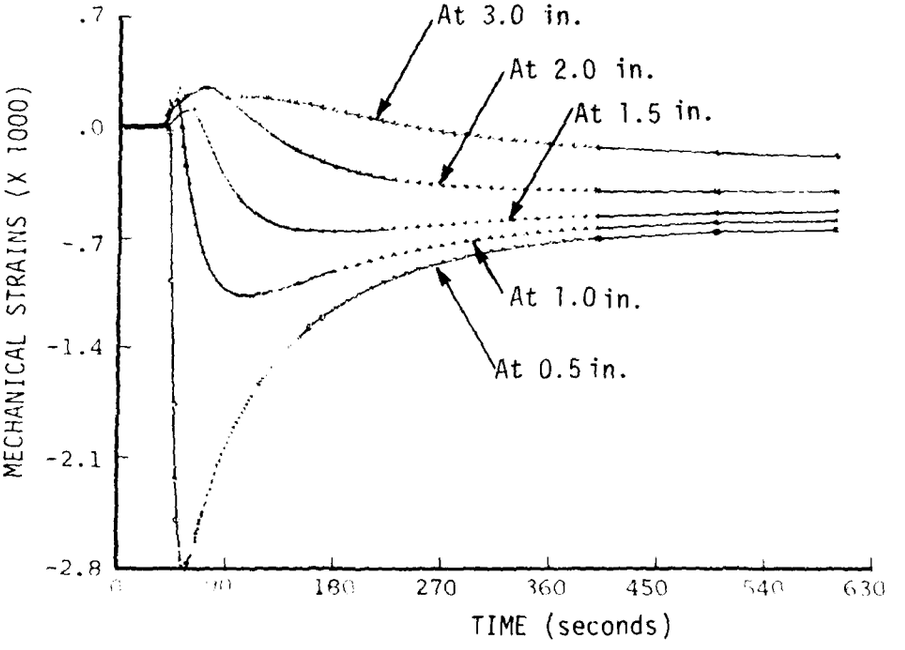

FIGURE 3.11 Mechanical strains during edge welding, as predicted by the one-dimensional program

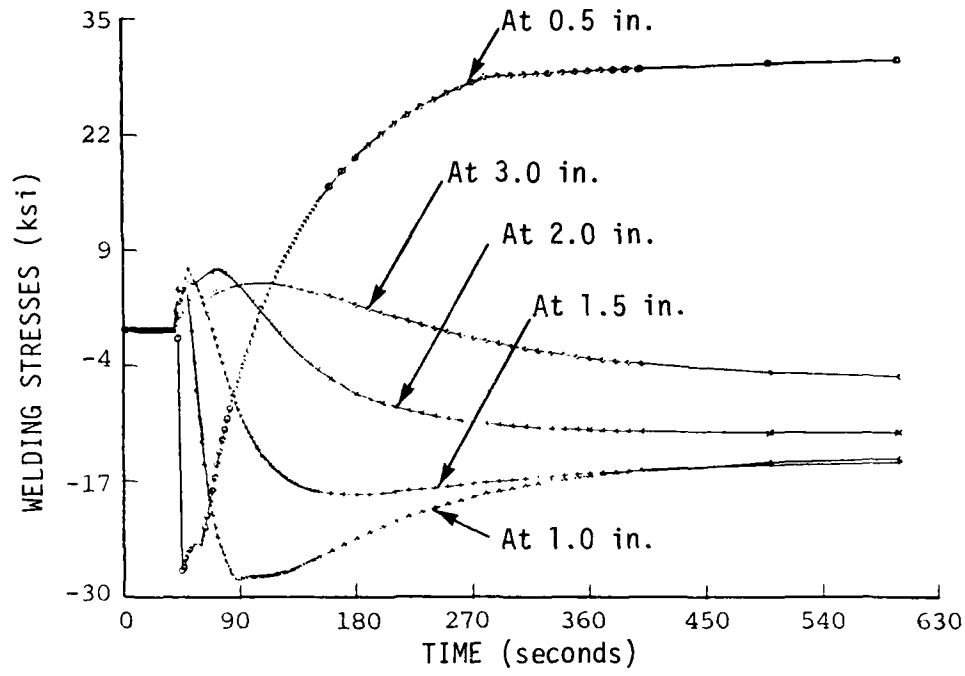

FIGURE 3.12 Stresses during edge welding, as predicted by the one-dimensional program

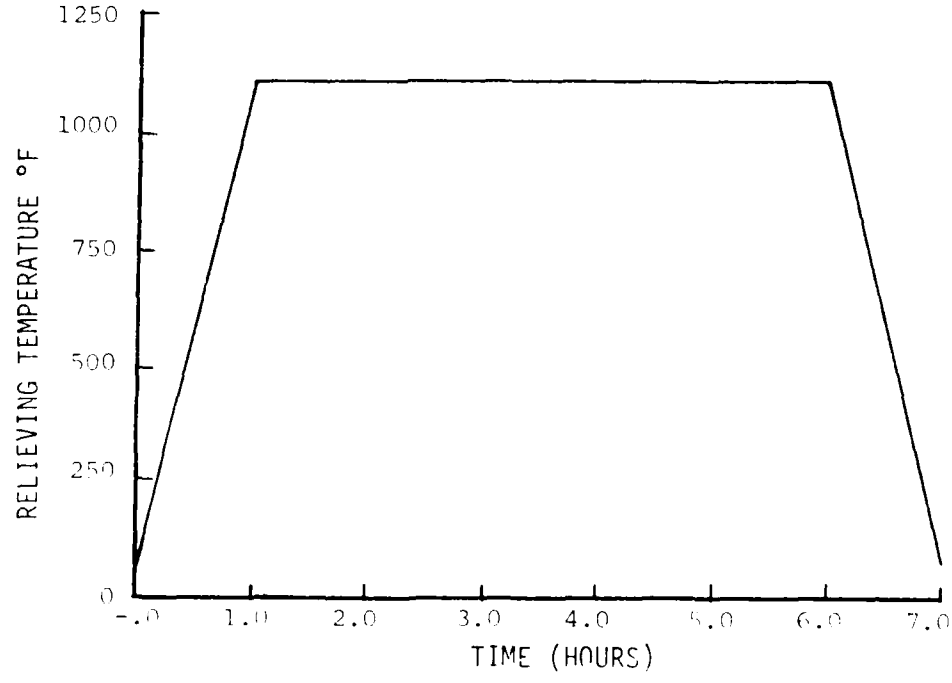

FIGURE 3.13 Assumed temperatures during uniform stress relieving at 1100°F

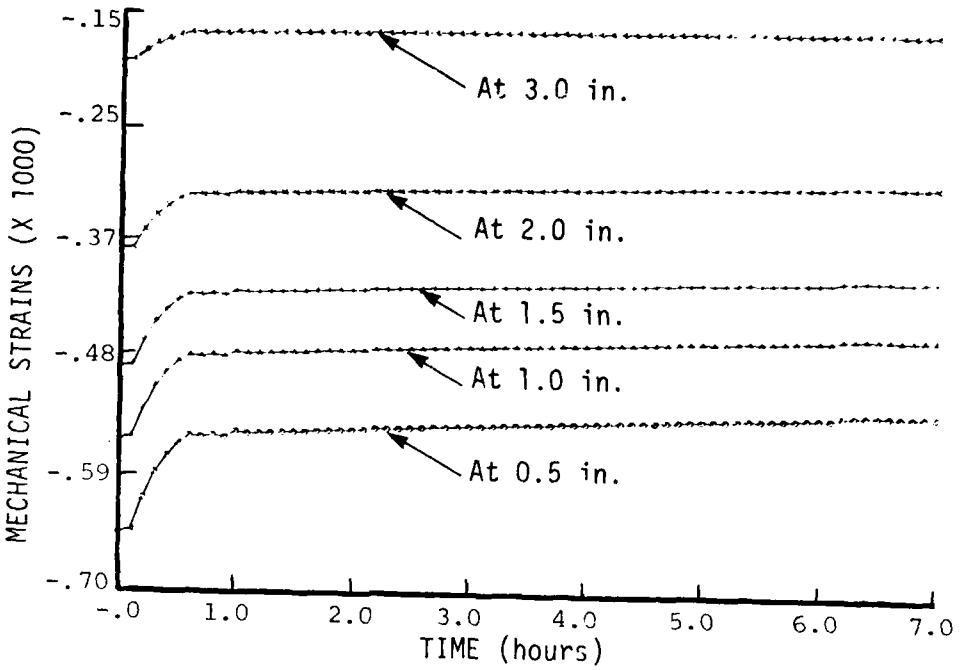

FIGURE 3.14 Mechanical strains during stress relieving at 1100°F, as predicted by the one-dimensional program (creep taken into account during holding)

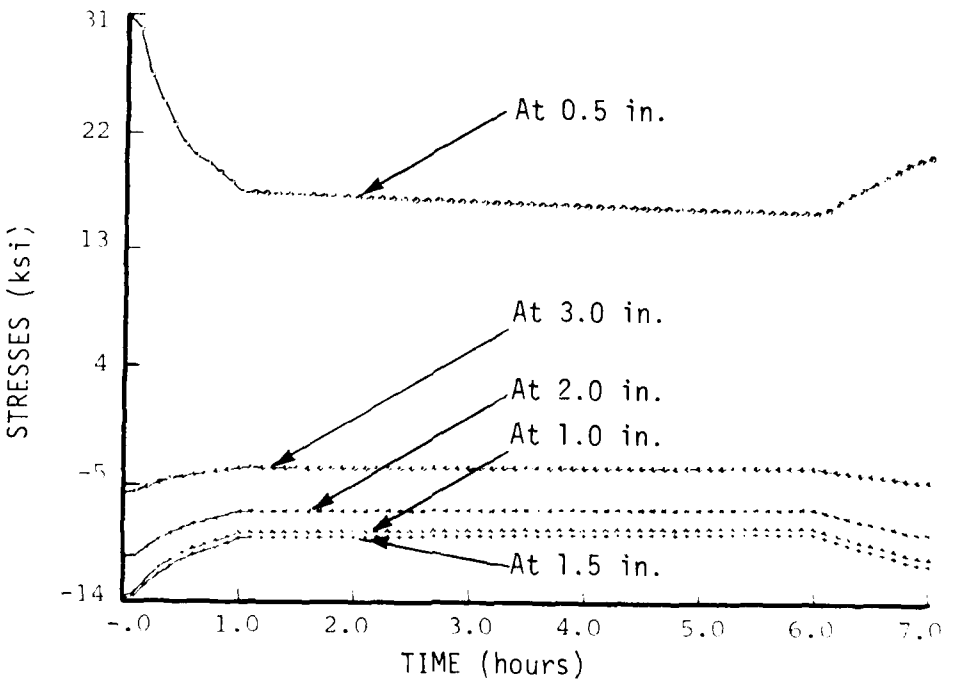

FIGURE 3.15 Stresses during stress relieving at 1100°F, as predicted by the one-dimensional program

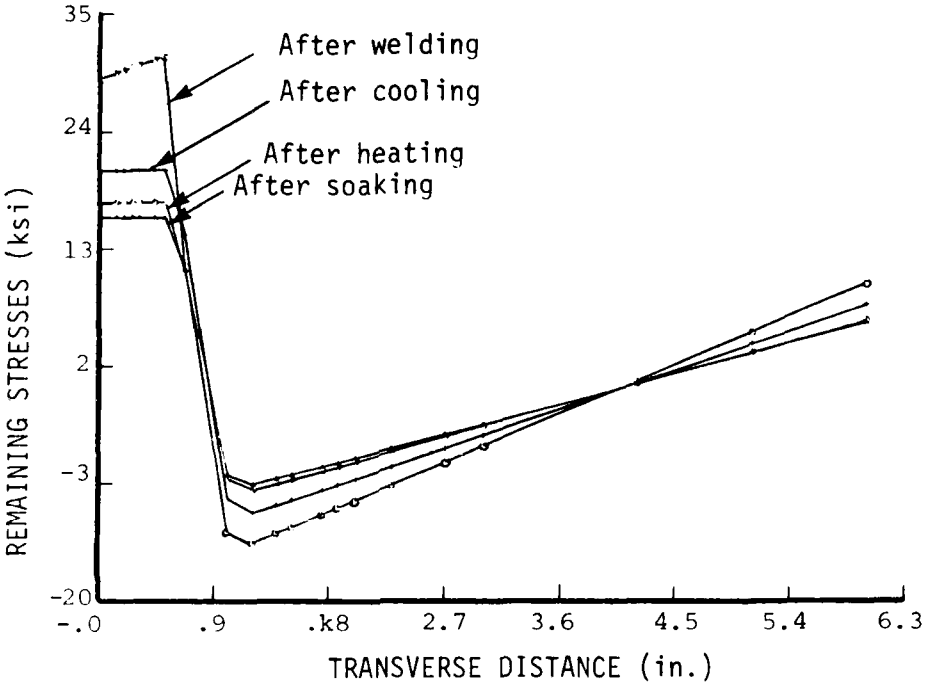

FIGURE 3.16 Comparison of residual stresses before, during and after stress relieving at 1100°F, as predicted by the one-dimensional program

3.4.1 Initial Verification Tests on 304 Stainless Steel Plates

The geometry and the dimensions of the four main[28] specimens are shown in Figure 3.17. All plates were edge welded and all but one were subsequently stress relieved in a furnace at different holding temperatures. The plates were finally sectioned and residual stresses were measured by stress relaxation.

The temperature and strain changes during welding and subsequent heat treatment were measured by thermocouples and electrical-resistance strain gages attached on the plates. The thermocouple and strain gage locations are also depicted in Figure 3.17. The total number of strain gages and their configuration is given in Table 3.1 for all specimens.

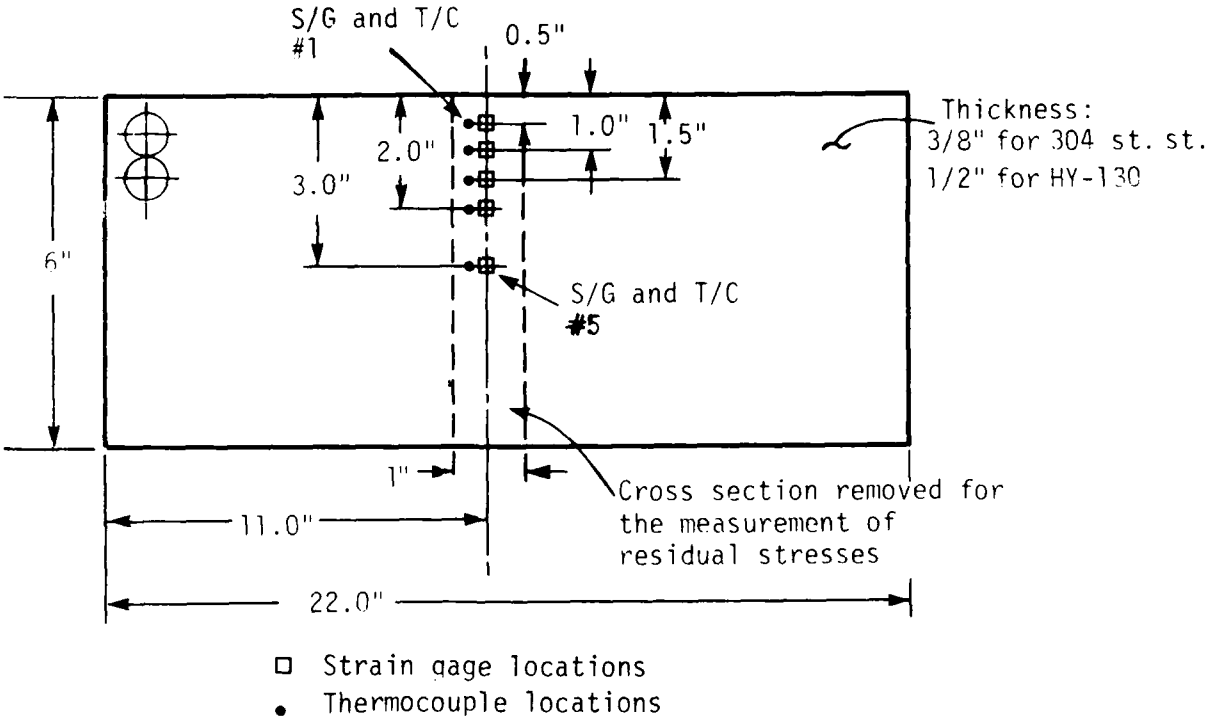

FIGURE 3.17 Specimen geometry and instrumentation

[28] Five more specimens were used during this phase, in order (a) to determine the appropriate welding conditions, (b) to evaluate the performance of the data acquisition system, and (c) to test the heating uniformity of the stress-relieving furnace.

Table 3.1: Arrangement of Strain Gages and Thermocouples for the Verification Tests

Specimen No.	Specimen Dimensions	Strain Gages		Thermocouples	
		Number	Configuration	Number	Configuration
1	22"x6"x3/8"	5	A	5	C
2	22"x6"x3/8"	5[1]	A	5	C
3	22"x6"x3/8"	10	B	5	C
4	22"x6"x3/8"	10[2]	B	5	C

Key: (A): Single gages in the longitudinal direction on the one side of the plate only

(B): Single gages in the longitudinal direction on both sides of the plate (to determine possible bending)

(C): Thermocouples located at the surface of the specimen on one side only

Notes: [1]Five additional gages were added in the transverse direction before cutting.

[2]Original strain gages were destroyed during stress relieving. Ten new gages were installed in both the longitudinal and transverse directions before cutting.

Straight polarity short circuiting, gas metal arc welding was performed on all specimens utilizing a 308 stainless steel wire (0.035" in diameter) and a 90% He - 7 1/2% A - 2 1/2% CO_2 gas mixture. The finally selected welding conditions were the same for all specimens:

Arc Voltage	23 volts
Arc Current	90 Amperes
Wire Feed Speed	175 inches/min
Weld Travel Speed	16 inches/min

Very similar temperature and strain distributions were observed on all specimens. This is evidenced in Figures 3.18 to 3.21, which depict the temperature and strain history at various distances from the weld line in specimens #2 and #4. Based on this similarity in the distribution of transient temperatures and strains, it is reasonable to assume that very similar residual stress distributions existed in all the specimens after welding.

After welding and cooling, specimen #2 was directly cut in order to determine the residual stresses in the as-welded condition whereas specimens #1, #3 and #4 were stress relieved at different holding temperatures before cutting. Details on the stress relieving conditions are given in Table 3.2.

The temperature history during stress relieving is depicted in Figures 3.22 and 3.23 for specimens #1 and #3 respectively. Strain measurements during stress relieving were only taken for specimens #1 and #3 since the gages were destroyed at temperatures above 550°F. Strains for specimen #3 are shown in Figures 3.24 and 3.25.

Finally, after stress relieving, the plates were sectioned and the obtained distribution of residual stresses was compared with the one in the as-welded case (Figure 3.26). More details on these experiments and the results can be found in Agapakis' thesis.

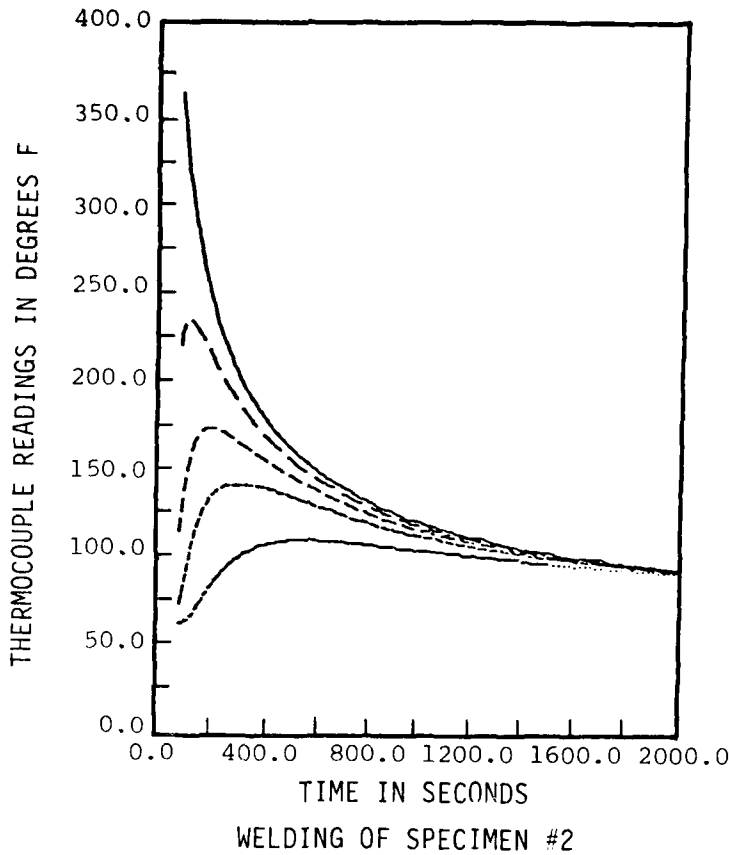

FIGURE 3.18 Thermocouple readings during welding of specimen #2

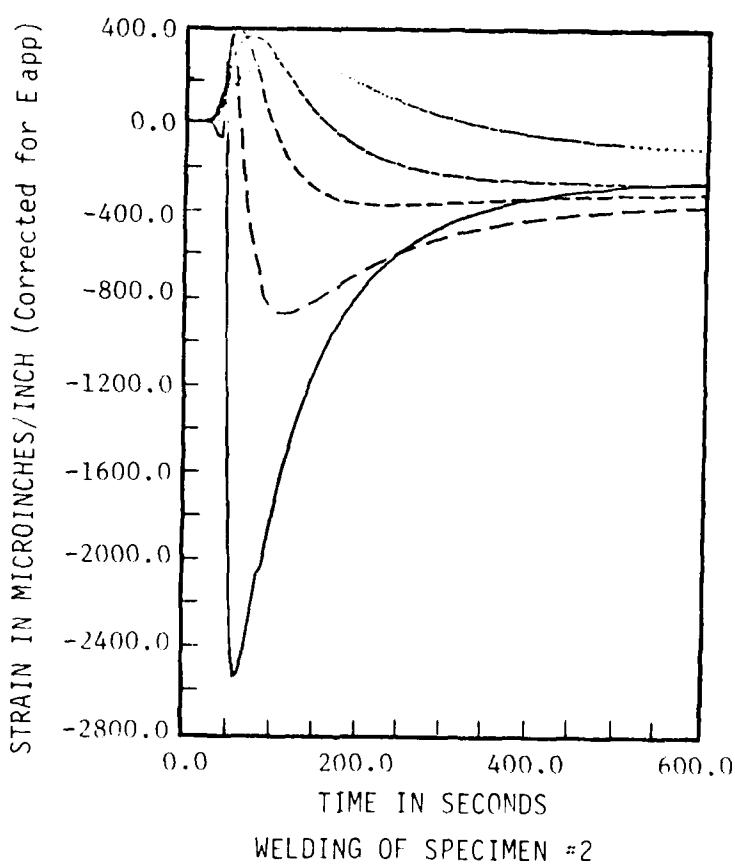

FIGURE 3.19 Strains during welding of specimen #2 (corrected for temperature-induced apparent strain and gage factor variations.

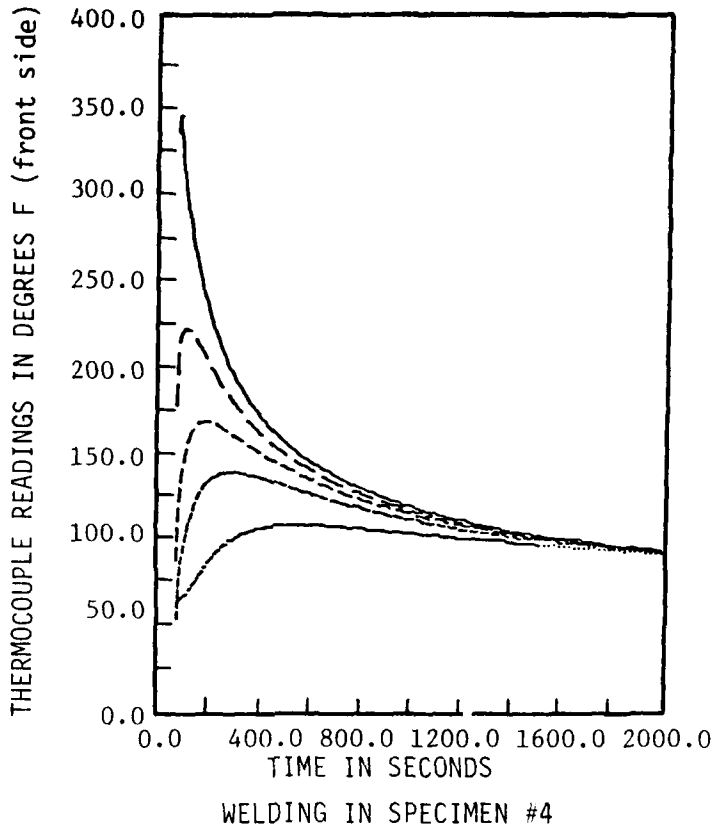

FIGURE 3.20 Thermocouple readings during welding of specimen #4

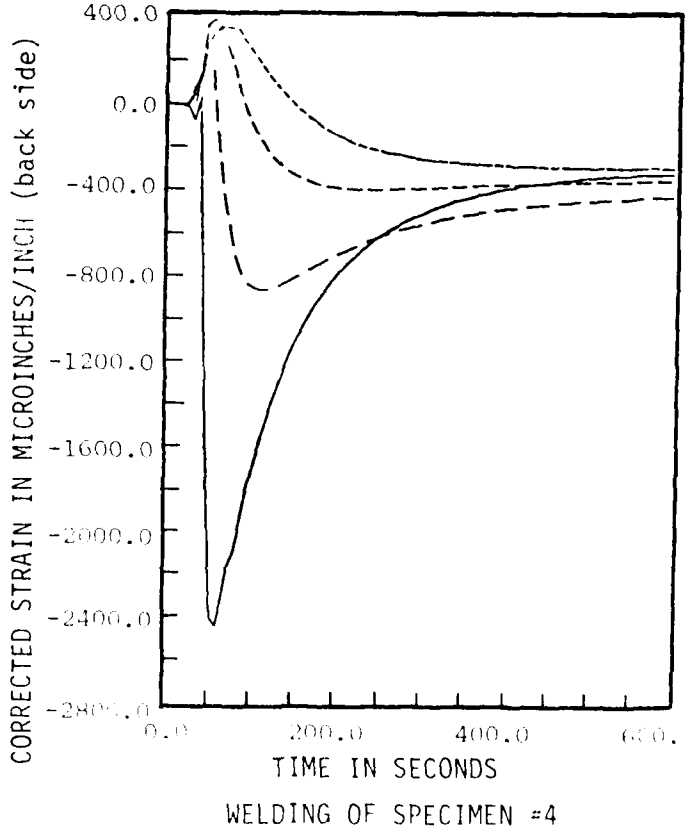

FIGURE 3.21 Strains during welding of specimen #4, back side (corrected for temperature induced apparent strain and gage factor variations)

Table 3.2: Stress Relieving Conditions for the Verification Tests

Specimen No.	Holding Temperature °F (°C)	Time in Furnace hr
1	500°F (260°C)	6
2	not stress relieved	-
3	approx. 370°F (188°C)	4
4	1100°F (593°C)	7
6	500°F (260°C)	2
	370°F (188°C)	

Note: All stress relieved specimens were cooled in air after heating.

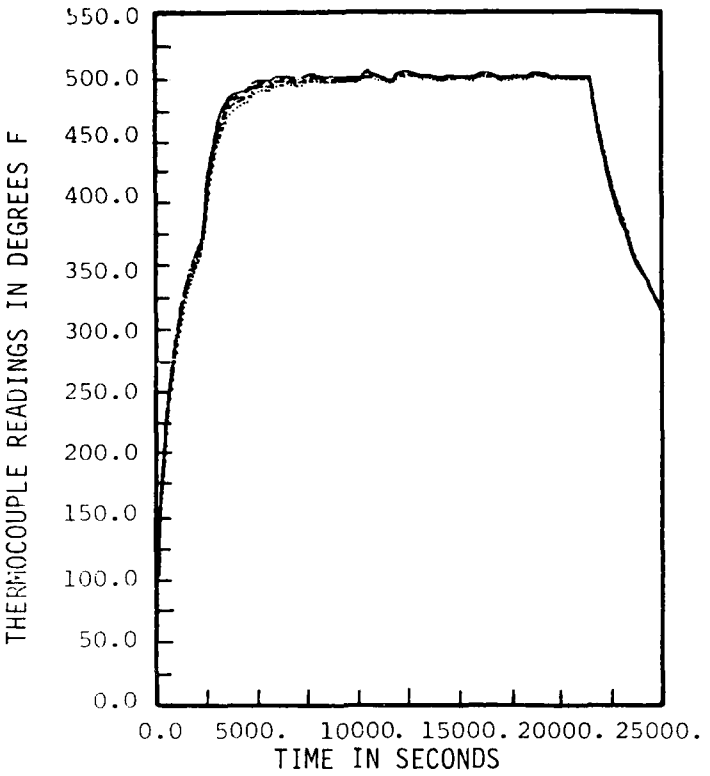

FIGURE 3.22 Thermocouple readings during stress-relieving of specimen #1

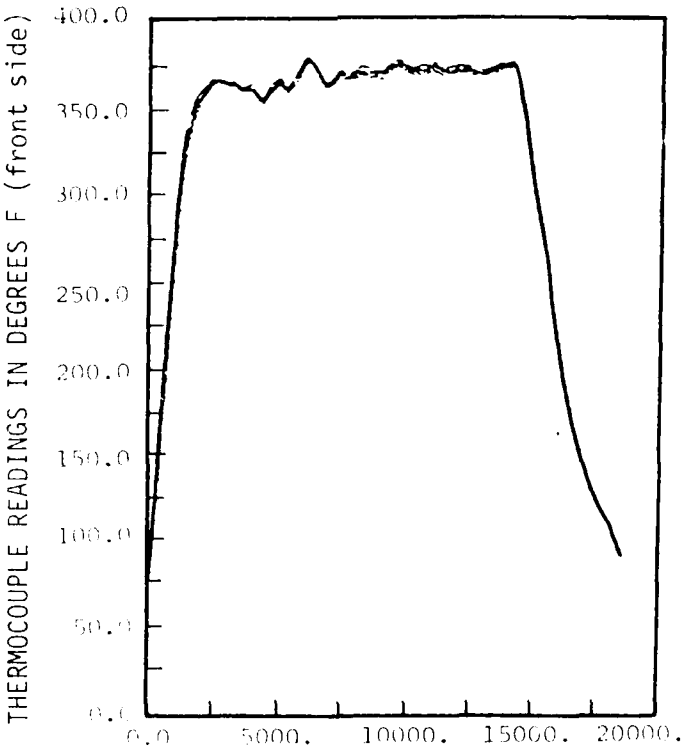

FIGURE 3.23 Thermocouple readings during stress-relieving of specimen #3

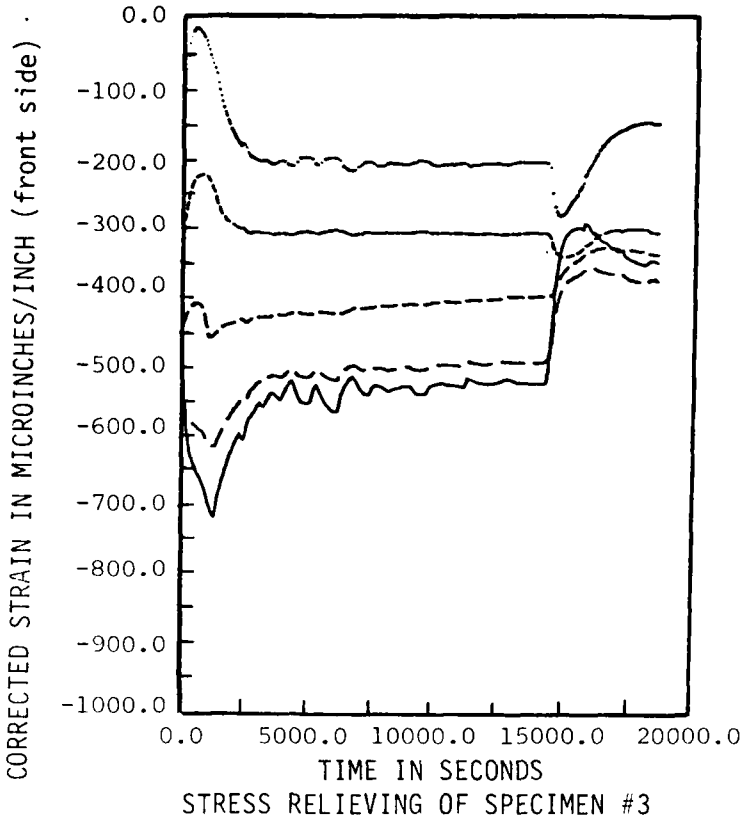

FIGURE 3.24 Strains during stress-relieving of specimen #3, front side (corrected for temperature induced apparent strain and gage factor variations)

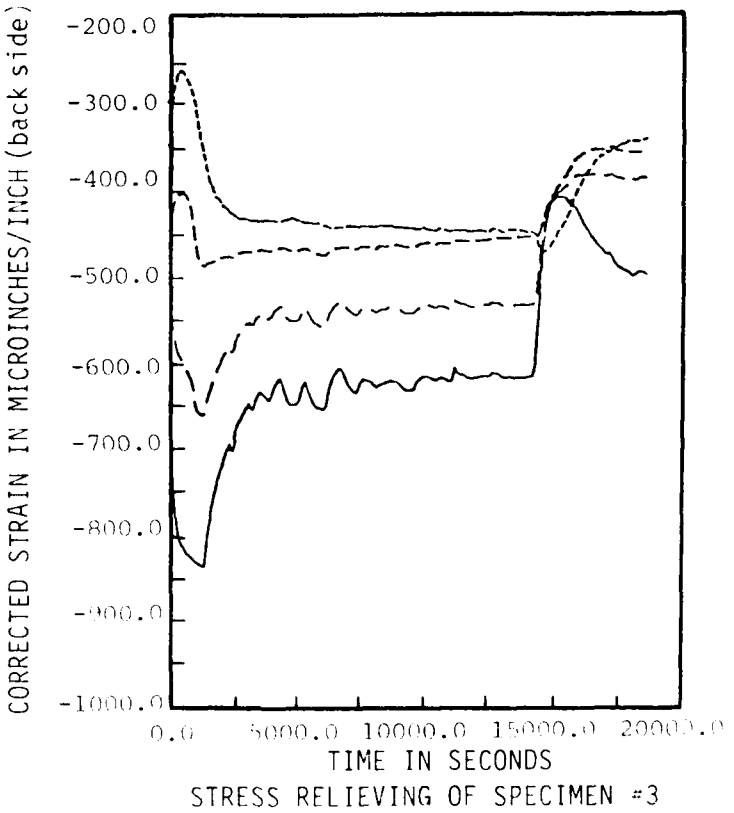

FIGURE 3.25 Strains during stress relieving of specimen #3, back side (corrected for temperature induced apparent strain and gage factor variations)

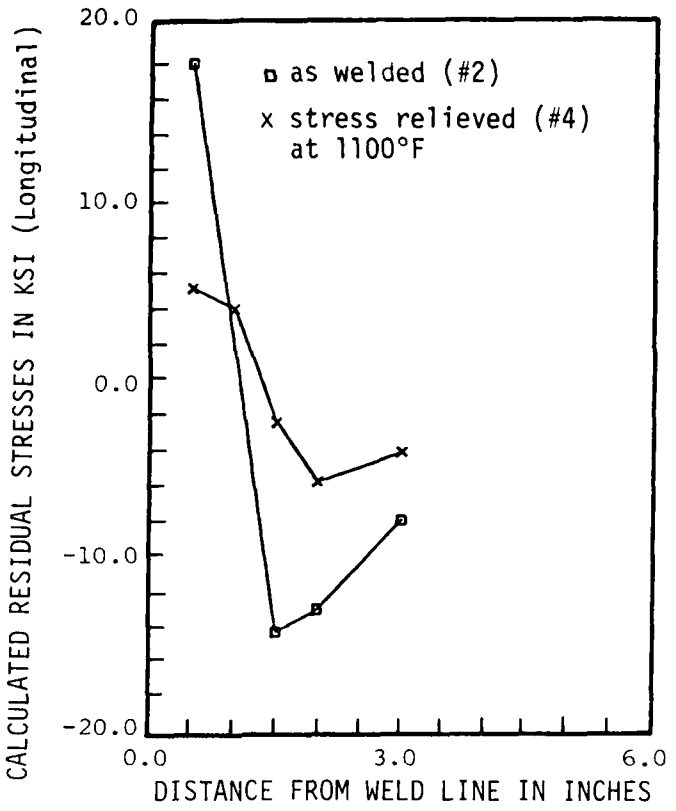

FIGURE 3.26 Comparison of longitudinal residual stresses after welding and stress relieving (1100°F)

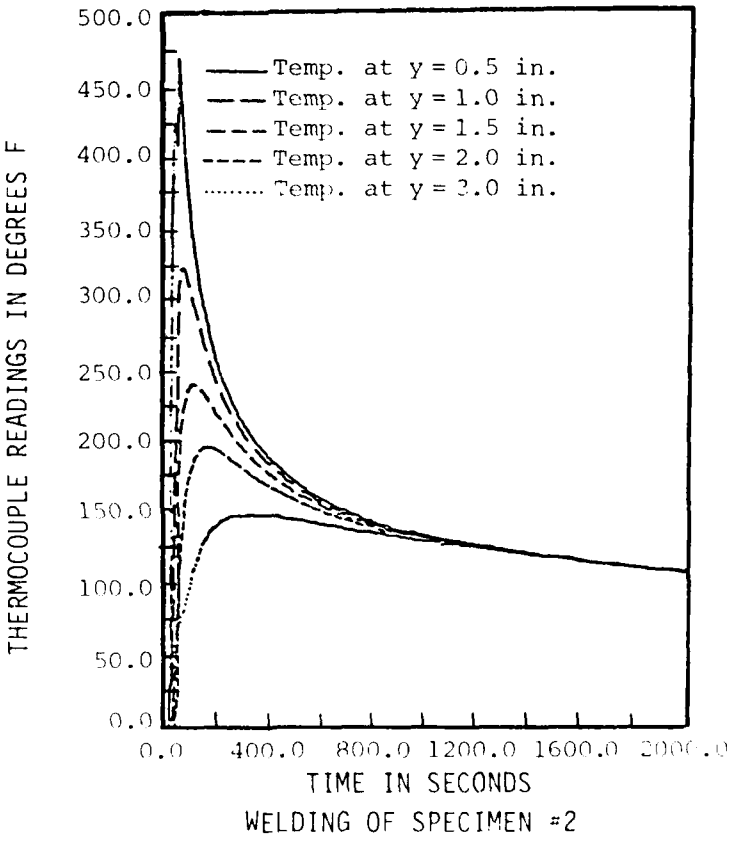

FIGURE 3.27 Time variation of temperature during welding

It should also be mentioned at this point that considerable effort has been recently devoted in upgrading our experimental data acquisition systems. A microcomputer (MINC-23, manufactured by the Digital Equipment Corporation) was purchased for this purpose, using funds not related to this research project, and was interfaced to the signal conditioning equipment for strain gages and thermocouples. Further details on the data acquisition system are considered outside the scope of this report, however, and can be found in:

Agapakis, J.E., "Fundamentals of Computer Aided Experimentation for Welding", Department of Ocean Engineering, M.I.T., December 1982.

3.4.2 Further Experiments on HY-130 Steel Plates

Four HY-130 steel specimens (22"x6"x1/2") were tested in this phase. Their geometry and configuration was the same as that of the stainless steel specimens (Figure 3.17). All plates were edge welded, and all but one were subsequently stress relieved (one in a uniform temperature furnace and the other two by line heating with an oxy-acetylene flame). The plates were then cut, and residual stresses were measured by stress relaxation.

Only temperatures were measured during welding and stress relieving operations. Strain gages were installed on all specimens (in both the longitudinal and the transverse direction) only before cutting. Their location is again depicted in Figure 3.17. Spray transfer, gas metal arc welding was performed on all specimens utilizing an AX-140 (0.045" in diameter) wire and a 98% A - 2% O_2 gas mixture. The selected welding conditions were (same for all specimens):

Arc Voltage	27 Volts
Arc Current	225 Amperes
Wire Feed Speed	285 inches/min
Weld Travel Speed	21 inches/min

The temperature distribution during welding for plate #2 is given in Figure 3.27. Very similar temperature distributions were observed on all plates.

After welding, specimen #1 was cut in order to determine the as-welded residual stress distribution. Specimen #2 was heated in a furnace at 1000°F[1] and air cooled to room temperature. Specimens #3 and #4, on the other hand, were flame heated using an oxyacetylene torch. The torch was moved at a constant speed of 1 inch/min along a line 1.64 inches (in specimen #3) and 4.30 inches (in specimen #4) away from the weld line. The temperature distribution during stress relieving is given in Figures 3.28 and 3.29 for specimens #2 and #4, respectively.

The selection of the torch velocity and location was based on computer predictions for maximum stress relaxation. The resulting residual stress distributions are given together with the computer predictions in Figures 3.30 to 3.33.

Further details on these experiments and their results can be found in Carpentier's thesis. It should be noted however, that due to the [illegible] number of experiments no definite conclusions can be drawn on the effectiveness of line heating as a stress relieving technique. At this point, further investigation is considered necessary.

[1] Since creep of HY-80 steel could not be handled by our model the plates were left in the furnace only for about an hour.

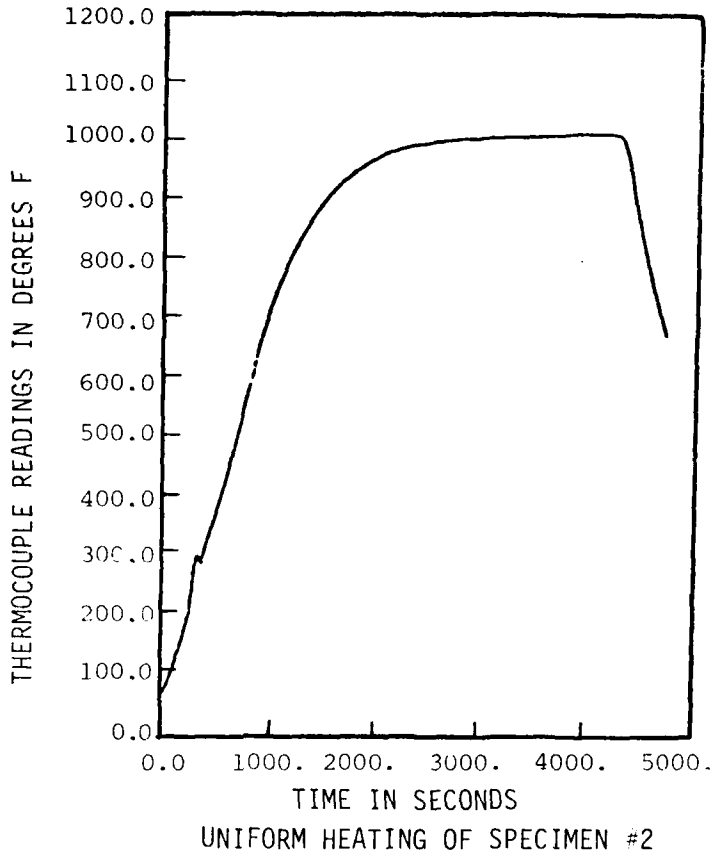

FIGURE 3.28 Time variation of temperature during uniform heating

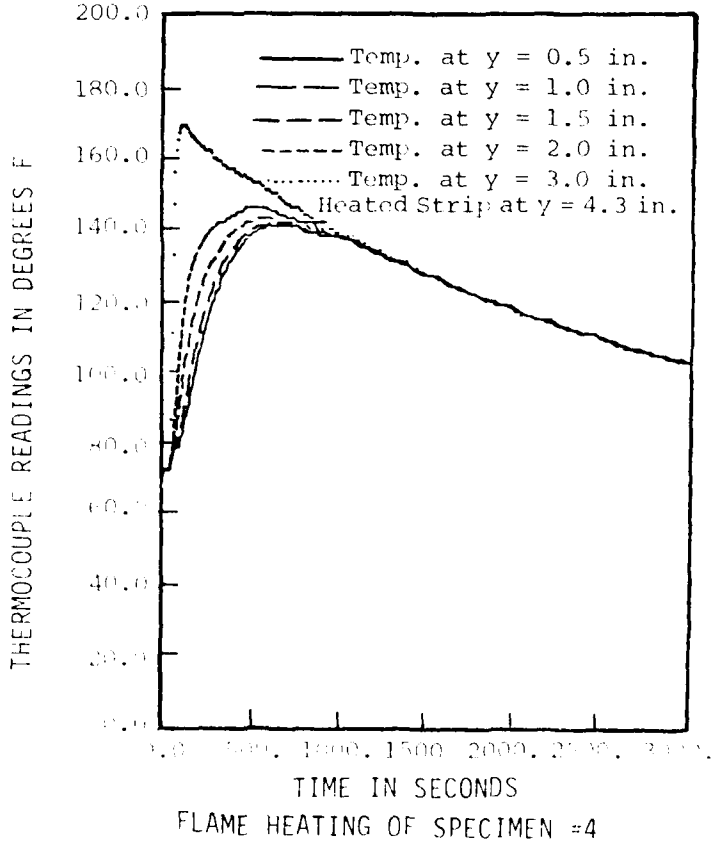

FIGURE 3.29 Time variation of temperature during strip heating (case #2)

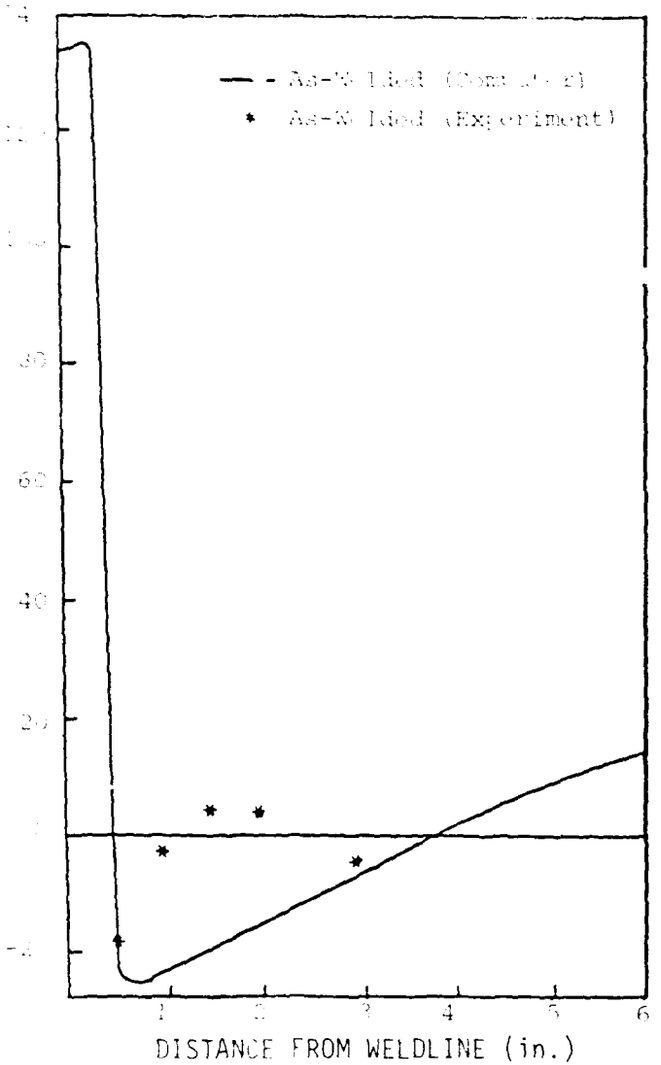

FIGURE 3.30 Empirical stress distribution. As-Welded case.

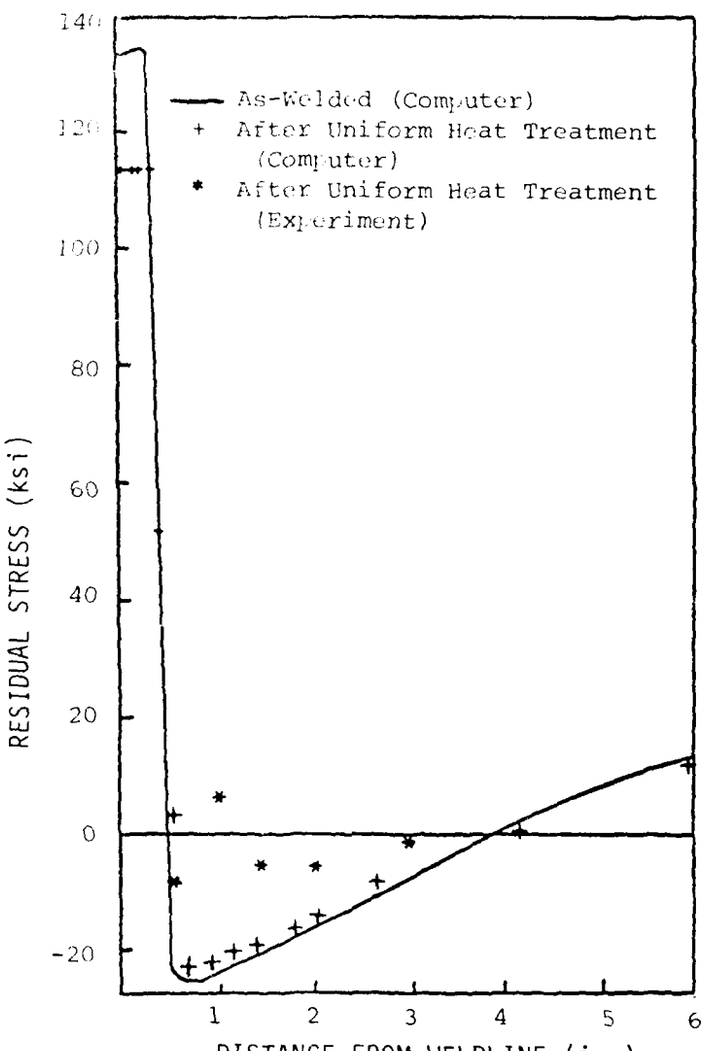

FIGURE 3.31 Empirical stress distribution. Uniform heat treatment case.

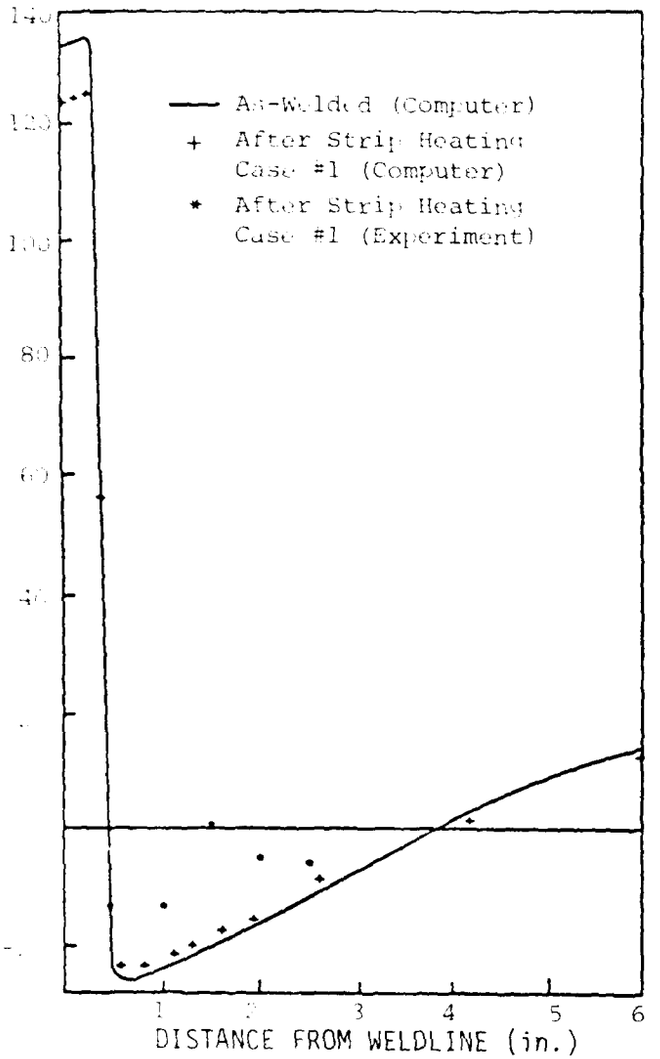

FIGURE 3.32 Empirical stress distribution. Strip heating case #1

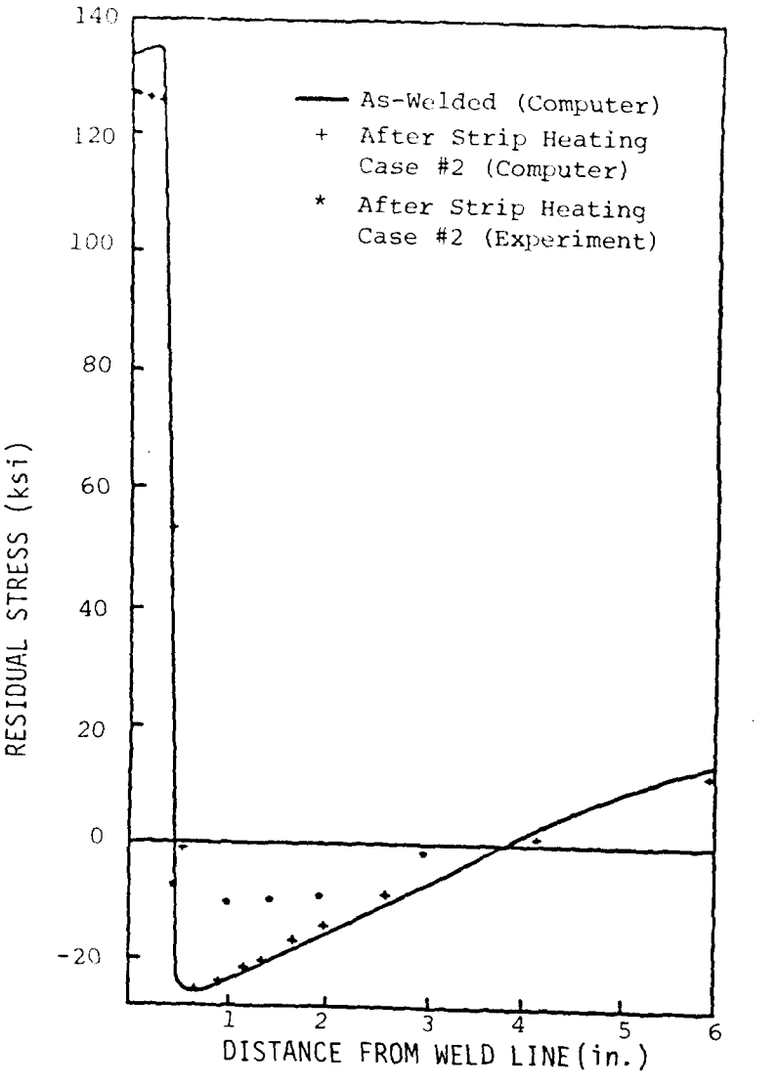

FIGURE 3.33 Empirical stress distribution. Strip heating case #2.

4. WORK ACCOMPLISHED ON TASK 5 - IMPROVED COMPUTER PROGRAMS

4.1 General Status

The objective of Task 5 of the current research program is to develop manuals of improved computer programs for analyzing (1) heat flow, (2) transient thermal stresses and metal movement, and (3) residual stresses and distortion of weldments. Although Task 5 includes some efforts at improving existing computer programs, it does not include major improvements of old computer programs or the development of new ones.

A unique feature of Task 5 is the revision of the programs in such a way that they can become more useful to practicing engineers. Moreover, a series of examples to aid engineers in understanding their use, capabilities, and limitations are also to be included.

Two subtasks to be performed under Task 5 have been identified in the proposal to O.N.R. dated November 1980, as follows:

Task 5.1: Development of Improved Manuals of Independent Welding Programs

Task 5.2: Development of Manuals of Programs which are Compatible with the ADINA Program

Details on the work done are included in the next two sections. Note, however, that all manuals are published separately from this final report.

4.2 Manuals of Independent Welding Programs

During the past decade M.I.T. researchers, under the direction of Professor K. Masubuchi, have developed a series of computer programs for analyzing various problems related to heat flow, transient thermal strains, residual stresses, and distortion in weldments. On some computer programs, manuals have already been prepared, some of which were included in the monograph prepared under Task 1 of a previous O.N.R. Sponsored Research Program. Since then, large amounts of experimental data have been obtained and compared with analytical

predictions. Considerable efforts have been made at the same time to improve these programs.

Among these programs, the one-dimensional program was proven to be very useful for the case of welding thin plates and T-shaped built-up beams. As a consequence, it was decided that a new manual for this program needs to be written. This new manual is published separately:

Imakita, A., Papazoglou, V.J., and Masubuchi, K., "Consolidated Manual of One-Dimensional Computer Programs for Analyzing Heat Flow, Transient Thermal Strains, Residual Stresses, and Distortion in Weldments", prepared under Contract N00014-75-C-0469 (M.I.T. OSP # 82558) for the Office of Naval Research, M.I.T., July 1982

In what follows a summary of the modifications made in these programs is described. For more details, one is referred to the aforementioned manual.

One-Dimensional Program. This computer program is capable of calculating the temperatures, thermal strains, and stresses developed in a thin plate during and after welding, assuming a one-dimensional state of stress. The following modifications, as compared to the earlier version of the program, were made prior to developing the revised manual:

(1) The numerical integration method was modified

(2) The number of integration points was increased to improve accuracy

(3) The temperature dependence of the surface heat loss coefficient was taken into account, and

(4) The output format was changed to facilitate easier handling of the results

A detailed sample analysis, accompanied by a number of comments, is also included in the manual.

One-Dimensional Program for T-shaped Beams. This computer program is an extension of the previous one and is aimed at calculating temperatures, thermal strains, residual stresses, and longitudinal bending distortion during the welding fabrication of built-up T-beams. The following modifications were made in this program:

(1) The temperature dependence of material properties was used in conjunction with a parabolic interpolation instead of the linear one previously used

(2) The heat flow between the web and the flange plates was taken into account

(3) The strain calculation procedure was changed to conform with the one used in the simple one-dimensional program

(4) The program is now capable to also perform calculations for the case of edge welds, and

(5) The output data format was changed, while at the same time more results can be printed out

The manual includes detailed sample analyses of both edge and T-beam welds.

No efforts have been or will be undertaken to develop manuals for the two-dimensional finite element programs that have been developed independently in the past by M.I.T. investigators. This decision was based on the availability of the much more sophisticated and efficient programs ADINAT and ADINA.

4.3 Manuals of Programs Compatible to ADINA

During the initial stages of the current research project, it was decided that all computer programs developed should be compatible with a general purpose finite element computer program, to facilitate easier integration with other kinds of numerical analyses, e.g., structural static and dynamic, fracture, etc. Upon consultation with representatives of the Office of Naval Research, the general purpose finite element codes ADINAT and ADINA, capable of performing nonlinear heat transfer and thermal-elastic-plastic stress analyses respectively, were

chosen. Both of these codes were developed by Professor K. J. Bathe and co-workers at the Department of Mechanical Engineering, M.I.T.

To make these programs capable of analyzing the welding problem, i.e., heat flow and stress calculations during welding, several modifications had to be made. Details of these modifications were presented in the third progress report to O.N.R. Efforts were made to publish manuals that explain in detail the programs developed and modified. These manuals also contain directions for the more efficient use of the programs as well as some sample analyses.

More specifically, the following manual is completed and published independently:

Imakita, A., "Heat Source Models Using Finite Element Method for Arc Welding", Dept. of Ocean Engineering, M.I.T., July 1982.

This manual gives details on the use of the general purpose finite element program ADINAT, for the calculation of temperature distribution during welding. A review of past work in the area is also included together with some sample cases and discussion on the effects of various model parameters.

Two more manuals are currently in the final stages of preparation:

Papazoglou, V.J., "Computer Programs for the Calculation of Schematic Continuous Cooling Transformation Diagrams", report to the Office of Naval Research (under preparation).

Papazoglou, V.J., "Numerical Calculation of Microstructure History and Phase Transformation Strains", report to the Office of Naval Research (under preparation).

The first one describes the programs developed to calculate schematic continuous cooling transformation (CCT) diagrams from isothermal data, i.e., from experimentally obtained time-temperature-transformation (TTT) diagrams.

The second describes the program developed to calculate the microstructure history of a material resulting from a given temperature history and based on an idealized CCT diagram of the material. It also

5. PUBLICATIONS AND DEGREES GRANTED

5.1 Publications

Work done under the present contract from the Office of Naval Research has resulted in the following publications:

(1) Masubuchi, K., "Models of Stresses and Deformation Due to Welding: A Review", presented at the Conference on Modeling of Casting and Welding Processes, Franklin Pierce College, Rindge, New Hampshire, August 4-8, 1980.

(2) Masubuchi, K., and Papazoglou, V.J., "Thermal Strains and Residual Stresses in Heavy HY-130 Butt Welds", Proceedings of 1980 Fall Meeting of SESA, Ft. Lauderdale, Florida, October 12-15, 1980.

(3) Papazoglou, V.J., and Masubuchi, K., "Analytical Methods for Determining Temperatures, Thermal Strains, and Residual Stresses Due to Welding", presented at the 1980 ASM Materials and Processes Congress, Cleveland, Ohio, October 28-30, 1980.

(4) Papazoglou, V.J., and Masubuchi, K., "Analysis of Thermal Strains and Residual Stresses in High Strength Steel Weldments", presented at the 62nd Annual Meeting of AWS, Cleveland, Ohio, April 6-9, 1981; submitted for publication in the Welding Journal.

(5) Masubuchi, K., "Welding Stresses", presented at the 28th Sagamore Army Materials Research Conference on Residual Stresses and Stress Relaxation, Lake Placid, New York, July 13-17, 1981.

(6) Masubuchi, K., and Agapakis, J., "Analysis and Control of Residual Stress, Distortion and their Consequences in Welded Structures", Proceedings of Conference on Trends in Welding Research in the United States sponsored by ASM, New Orleans, Louisiana, November 16-18, 1981.

(7) Papazoglou, V.J., and Masubuchi, K., "Numerical Analysis of Thermal Stresses during Welding Including Phase Transformation Effects", presented at the ASME Pressure Vessels and Piping Division Meeting, Orlando, Florida, June 27 to July 1, 1982; to appear in the Journal of Pressure Vessel Technology.

(8) Papazoglou, V.J., Masubuchi, K., Gonçalves, E., and Imakita, A., "Residual Stresses Due to Welding: Computer-Aided Analysis of their Formation and Consequences", presented at the SNAME 1982 Annual Meeting, New York, N.Y., November 18-20, 1982.

(9) Agapakis, J.E., and Masubuchi, K., "Thermal Stress Relieving of High Strength and Stainless Steel Weldments", to be presented at the 64th Annual Meeting of AWS, Philadelphia, Pennsylvania, April 25-29, 1983.

5.2 Degrees Granted

The following degrees in chronological order have been granted to students working on this project (note that some of these students were U.S. or allied countries' Navy Officers and so their services were furnished at no cost to the project):

Lipsey, M.D.: Ocean Engineer, and Master of Science in Naval Architecture and Marine Engineering.

Coneybear, G.W.: Master of Science in Naval Architecture and Marine Engineering.

Mylonas, G.A.: Master of Science in Naval Architecture and Marine Engineering, and Master of Science in Mechanical Engineering.

Rogalski, W.J.: Ocean Engineer, and Master of Science in Naval Architecture and Marine Engineering.

Mabry, J.P.: Ocean Engineer, and Master of Science in Naval Architecture and Marine Engineering.

Coumis, G.A.: Master of Science in Naval Architecture and Marine Engineering, and Master of Science in Mechanical Engineering.

Sousa Sá, P.A.: Ocean Engineer, and Master of Science in Mechanical Engineering.

Gonçalves, E.: Master of Science in Ocean Engineering, and Master of Science in Materials Science.

Suchy, A.F.: Ocean Engineer.

Papazoglou, V.J.: Ph.D. in Ocean Engineering.

Golçalves, E.: Ph.D. in Ocean Engineering.

McCord, R.S.: Ocean Engineer.

Agapakis, J.E.: Master of Science in Mechanical Engineering, and Master of Science in Ocean Systems Management.

Carpentier, K.P.: Master of Science in Naval Architecture and Marine Engineering.

5.3 Theses Completed

The following theses detailing the work performed under this research program have been completed:

1. Lipsey, M.D., "Investigation of Welding Thermal Strains in High Strength Quenched and Tempered Steel", Ocean Engineer Thesis, M.I.T., June 1978.

2. Coneybear, G.W., "Analysis of Thermal Stresses and Metal Movement during Welding", S.M. Thesis, M.I.T., May 1978.

3. Mylonas, G.A., "Experimental Investigation of Residual Stress Distributions in Thick Welded Plates", S.M. Thesis, M.I.T., July 1979.

4. Rogalski, W.J., "An Economic and Technical Study on the Feasibility of Using Advanced Joining Techniques in Constructing Critical Naval Marine Structures", Ocean Engineer Thesis, M.I.T., May 1979.

5. Mabry, J.P., "Prediction and Control of Residual Stresses and Distortion in HY-130 Thick Pipe Weldments", Ocean Engineer Thesis, M.I.T., May 1979.

6. Coumis, G.A., "An Experimental Investigation of the Transient Thermal Strain Variation and the Triaxial Residual Stress Field Generated due to Electron Beam Welding of Thick HY-130 Plates", S.M. Thesis, M.I.T., June 1980.

7. Sousa Sá, P.A., "Investigation of Triaxial Residual Stress Distribution Remaining after GMA Welding of Thick HY-130 Steel Plates", Ocean Engineer Thesis, M.I.T., January 1981.

8. Gonçalves, E., "Investigation of Welding Heat Flow and Thermal Strain in Restraint Steel Plates", S.M. Thesis, M.I.T., May 1980.

9. Suchy, A.F., "Investigation of Temperature Distribution and Thermally Induced Thermal Strains in Highly Restrained, Thick, HY-130 Steel Plate Weldments", Ocean Engineer Thesis, M.I.T., June 1980.

10. Papazoglou, V.J., "Analytical Techniques for Determining Temperatures, Thermal Strains, and Residual Stresses during Welding", Ph.D. thesis, M.I.T., May 1981.

11. Gonçalves, E., "Fracture Analysis of Welded Structures", Ph.D. thesis, M.I.T., May 1981.

12. McCord, R.S., "An Investigation of Strain, Distortion, and Heat Distribution during Welding of Nickel-Aluminum Bronze", Ocean Engineer thesis, M.I.T., June 1981.

13. Agapakis, J.A., "Welding of High Strength and Stainless Steels: A Study on Weld Metal Strength and Stress Relieving", S.M. Thesis, M.I.T., May 1982.

14. Carpentier, K.P., "Thermal Stress Relief of HY-130 Weldments", S.M. Thesis, M.I.T., May 1982.

APPENDIX A

THE AMERICAN SOCIETY OF MECHANICAL ENGINEERS
345 E. 47 St., New York, N.Y. 10017

82-PVP-44

APPENDIX A

Numerical Analysis of Thermal Stresses During Welding Including Phase Transformation Effects

V. J. Papazoglou
Postdoctoral Associate,
Assoc. Mem. ASME

K. Masubuchi
Professor,
Mem. ASME

Department of Ocean Engineering,
Massachusetts Intitute of Technology,
Cambrige, Mass. 02139

The problem of determining temperature distributions, transient thermal strains, and residual stresses during butt welding thick plates with the multipass GMAW process is solved using the finite element method. First, a nonlinear heat transfer analysis is performed taking into account the temperature dependence of the material properties, and convection and radiation surface heat losses. This is followed by a thermo-elastic-plastic stress analysis that incorporates phase transformation strains. Finally, the theoretical predictions are compared with experimentally obtained data showing good correlation.

Introduction

The welding processes have been and are extensively used for the fabrication of various structures ranging from bridges and machinery to all kinds of sea-going vessels to nuclear reactors and space vehicles. This is the case because of the many advantages they offer compared to other fabrication techniques - excellent mechanical properties, air and water tightness, and good joining efficiency, to name but a few.

At the same time, however, welding creates various problems of its own that have to be solved. In the past these problems have been tackled through experimental investigations resulting in the collection of extensive data on low-carbon steel using conventional arc welding techniques. Because of the large amount of manpower and the high cost required for such investigations, however, this method is rather inefficient when different materials (high-strength quenched and tempered steels, aluminum and titanium alloys, etc.) or modern welding techniques (electron beam, laser, etc.) need to be studied. Fortunately enough, since the advent of the computer, a new tool became available which, combined with limited experimental efforts, could give solutions to many of the welding problems.

One of the problems suitable for computer analysis is the one involving residual stresses and distortion during welding. The uneven temperature distribution produced during welding gives rise to incompatible strains which in turn result in self-equilibrating residual stresses that remain in the structure after it has cooled down to ambient temperature. The phenomena involved are very complex necessitating the use of numerical techniques for their solution. Moreover, the prediction of residual stresses is of paramount importance since these stresses adversely affect the service behavior of welded structures including their brittle fracture, stress corrosion cracking, fatigue, and buckling characteristics.

Contributed by the Pressure Vessels and Piping Division for presentation at the Pressure Vessels and Piping Conference, Orlando, Florida, June 27-July 2, 1982, of THE AMERICAN SOCIETY OF MECHANICAL ENGINEERS. Manuscript received at ASME Headquarters, April 2, 1982. Paper No. 82-PVP-44.
Copies will be available until March 1983.

Several investigators have contributed towards the solution of the welding residual stress prediction problem in the past ten or so years [1-12]. In most of these studies use is made of the powerful finite element method in two dimensions (plane stress, plane strain, and axisymmetric analyses). Moreover, the thermomechanical problem is assumed to be uncoupled, with the thermal and mechanical parts being treated separately [2]. Good correlation is generally observed between the obtained results and experimental data. In cases where poor agreement is found, the discrepancy is attributed to the fact that no consideration is given to the phenomenon of allotropic phase transformations [2, 5].

This paper describes a technique for analyzing temperatures, thermal stresses, and residual stresses using the finite element method. Particular emphasis is placed on the rational determination of the phase transformation strains. The computed results are then compared with experimental data obtained during butt welding 25.4-mm-thick HY-130 plates using the multipass Gas Metal Arc Welding (GMAW) process.

Heat Transfer Analysis

The problem of heat flow during welding was solved using the multipurpose finite element program ADINAT developed by Bathe and co-workers at the Department of Mechanical Engineering, M.I.T. [13]. Following is a discussion of the particular features of the program pertaining to the welding analysis.

Finite Element Formulation. The governing isoparametric finite element equations for the nonlinear heat transfer problem can be written in matrix form as follows:

$$t_{k}\,\Delta\theta^{(i)} = t + \alpha\Delta t_{Q}\,(i-1) \tag{1}$$

with

$$t + \alpha\Delta t_{\theta}\,(i) = t + \alpha\Delta t_{\theta}(1-1) + \Delta\theta^{(i)} \tag{2}$$

Equation (1) represents the heat flow equilibrium at time

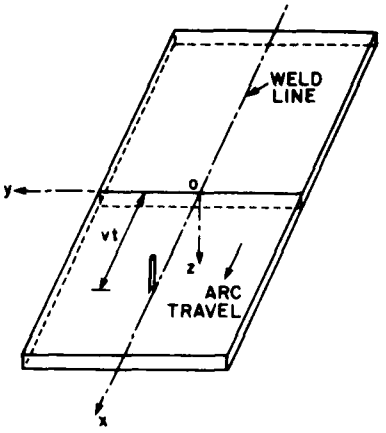

Fig. 1 Weldment configuration

$t+\alpha\cdot\Delta t$, where $0\le\alpha\le 1$ and α is chosen to obtain optimum stability and accuracy in the solution. Furthermore, the solution using these equations corresponds to the modified Newton-Raphson iteration scheme.

All boundary conditions relevant to the welding problem are incorporated in the matrices of equation (1). They include:

1 Convective heat losses from the plates' surfaces, modeled according to Newton's law.

2 Radiation heat losses which are very significant in the vicinity of the weld metal due to the large difference between the surface and environmental temperatures and which are modeled according to the well-known quartic Stefan-Boltzman law.

3 The heat input during welding is modeled using the concept of arc efficiency. For the space distribution of the heat input, a consistent formulation is adopted assuming a uniform distribution over the top of each weld bead. Finally, the time distribution of the heat input is modeled in such a way that the passing of the arc over the cross section examined can be simulated (a linear increase as the arc approaches, uniform as the arc travels over the cross section, followed by a linear decrease).

A family of one-step methods is considered for the time integration using the parameter α [14]. The scheme was found to be unconditionally stable for $\alpha \ge 1/2$ and to generally give better solution accuracy when $\alpha = 1$ (Euler backward method). Finaly, the modified Newton iteration is guaranteed to converge provided the time step Δt is small enough.

Two-Dimensionality of Problem. Assuming that the welding heat source (arc) is moving at a constant speed along a regular path (e.g., a straight line in a planar weld), that the weld speed is sufficiently high relative to the material's characteristic diffusion rate, and that end effects resulting from either initiation or termination of the heat source can be neglected, the three-dimensional character of the heat transfer problem can be simplified [3, 6, 15]. This can be achieved by analyzing a cross section of the weldment of unit thickness and located in the mid-length region of the weld (see Fig. 1).

Modeling of Weld Metal. The heat transfer mechanism in the weld metal, when molten, is extremely complex and its physics are not well understood as of today. These complexities arise from the difficulties in adequately modeling the convective motion of the molten metal, the electric heating due to the current flow in the base metal, the boundary conditions for heat losses, etc.

Although some progress has recently been made towards a proper modeling of the fluid flow and the convective heat transfer [16], these efforts are still directed towards simple cases and are rather inconclusive. As a consequence, most investigators try to simulate the convective heat transfer mechanism in the molten metal by assuming a higher [3, 6] or lower [2] value for the thermal conductivity than that for the material at the solidus temperature. In this study a higher value is used, since it is believed that it better approximates the actual phenomena.

Finally, since the cases analyzed involve multipass welding, it is necessary to find a way to model the laying of the various beads during the welding cycle. This is made possible by the element birth-and-death capabilities of the code used.

Transient Strain and Residual Stress Analysis

Using the predicted temperature distributions obtained from the heat transfer analysis, the transient stresses, and residual stresses can be calculated. In the present study these calculations were performed using the multipurpose finite element nonlinear stress analysis computer program ADINA [17], properly modified to take into account the transformation strains [15]. Details of the method used are presented in the forthcoming.

Finite Element Formulation. The thermal-elastic-plastic constitutive model (with the phase transformation modifications discussed later) is used to study the mechanical part of the welding problem for the case of plane strain. The governing incremental finite element equations can be written as

$$\tau_{\mathbf{K}}\Delta\mathbf{U}^{(i)} = t+\Delta t_{\mathbf{R}} - t+\Delta t_{\mathbf{F}}(i-1) \qquad (3)$$

The solution using equation (3) corresponds to the modified Newton-Raphson iteration procedure which is helpful in improving the solution accuracy and in many cases in preventing the development of numerical instabilities. The convergence of the iteration can be accelerated using the

Nomenclature

B = bainite transformation temperature
$\bar{\epsilon}^p$ = effective plastic strain
e_1 = thermal strain, mixture of phases
e_2 = transformation strain
e_3 = thermal strain, single phase
f = fraction transformed at θ
f_B = fraction transformed at θ_f
$\mathbf{F}$ = vector of nodal point forces
h = heat convection coefficient
$\mathbf{K}$ = stiffness matrix
M = martensite transformation temperature
$\hat{\mathbf{Q}}$ = effective heat flow vector
$\mathbf{R}$ = external force vector
t = time
t_{B_s} = bainite transformation starting time
$\mathbf{U}$ = displacement vector
v = welding speed
x,y,z = Cartesian coordinates
α = time integration parameter
$\Delta\theta$ = temperature increment
$\Delta\mathbf{U}$ = displacement increment
Δt_B = bainite transformation time interval
δ_{rs} = Kronecker delta
ϵ_{rs}^{TH} = thermal and transformation strain
η_a = arc efficiency
$\boldsymbol{\theta}$ = temperature vector
θ = temperature

Subscripts

s = start
f = finish

Superscripts

left = time at which a quantity occurs
right = iteration counter

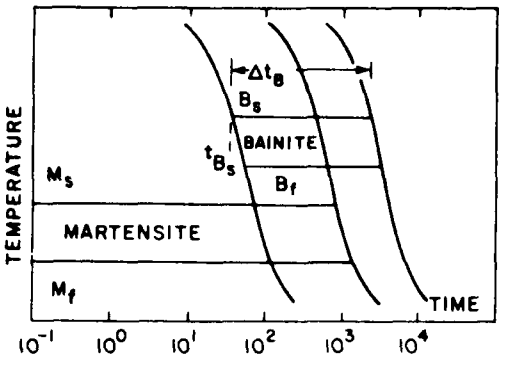

Fig. 2 Idealized CCT diagram

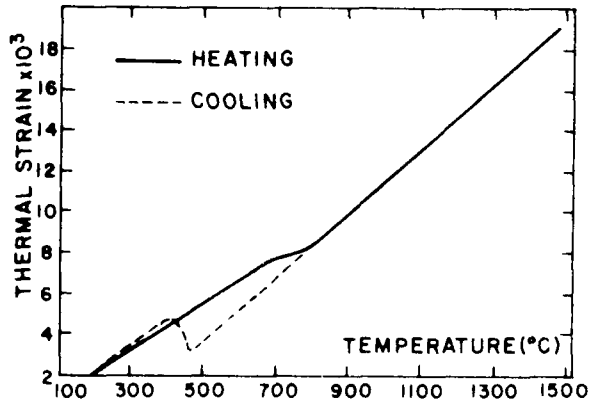

Fig. 3 Typical dialatational curve including phase transformation effects

Aitken method or, in complex material nonlinear cases (like the welding problem), improved using the BFGS (Broyden-Fletcher-Goldfarb-Shanno) matrix updating method.

The usual small strain assumption of decomposing the total strain at any time instance in its elastic, plastic, and thermal components is used. Creep is neglected, given that in the welding problem the time intervals at high temperature are short. The plastic strain component is calculated using the von Mises yield criterion, modified for temperature dependence, and the associated flow rule. Kinematic hardening, thought by many to better model the phenomena involved, is used; it is based on the assumption that the size of the yield surface depends on temperature only, whereas its translation rate in the stress space depends on the plastic strain rate.

Phase Transformation Effects. In most previous stress analyses of the welding problem no consideration is given to the phenomenon of phase transformations. The limited efforts reported in the literature are based on the use of a small number (usually three) of experimentally obtained dilatational curves for specific cooling rates and do not concentrate on the fundamentals of the phenomena involved [10]. A rational model developed to calculate the phase transformation strains is discussed in this section.

The model starts from the Continuous Cooling transformation (CCT) diagram of the material under consideration which is either known experimentally or can be derived from isothermal data (TTT diagram). Methods for the latter case are reported in the literature by considering linear cooling rates [18, 19]. Based on the fact, however, that the welding cooling rates resemble log-linear curves some modifications to the available methods had to be made to take this fact into account [15].

Using the CCT diagram (see Fig. 2 for an idealized version of it) and the temperature distribution during welding, the history of microstructure formation during the cooling stages can be predicted for each point in the HAZ and the weld metal.

To predict the microstructures during the cooling stage of the welding process an incremental strategy is involved so that the model can be compatible with the step-by-step solution of the nonlinear stress analysis using ADINA. A procedure has therefore to be established that will enable one to calculate the proceeding of each transformation. The following equation has been used for this purpose:

$$f = f_F \cdot \left[1 - \left(\frac{\theta - \theta_f}{\theta_s - \theta_f}\right)^2\right] \tag{4}$$

Equation (4) is applied separately for each allotropic transformation, namely for the martensite to austenite one upon heating and for the austenite to bainite and austenite to martensite ones upon cooling [15].

Based on the microstructure predictions calculated by the methodology outlined in the foregoing, the combined thermal and transformation strains, e_{rs}^{TH}, developed during the welding thermal cycle can then be found from

$$e_{rs}^{TH} = (e_1 + e_2 + e_3) \cdot \delta_{rs} \tag{5}$$

The estimation of the thermal strains e_1 and e_3 requires knowledge of the microstructures present and of the average thermal expansion coefficients of austenite, bainite, and martensite. Similarly, to calculate the transformation strain, e_2, one has to also know the transformation strains for each separate phase change, namely from martensite to austenite, from austenite to bainite, and from austenite to martensite.

To show the impact the inclusion of phase transformation effects has on the thermal strain of a section which is free to expand or contact, Fig 3 is constructed. The solid line depicts for a specific temperature history the thermal strain during the heating stage of this history, including the phase transformation effects (phase change from martensite to austenite). This is the usual curve assumed as input in previous stress analyses using the finite element method. Upon cooling, the same curve was usually assumed, thus neglecting the phase changes from austenite to bainite and/or martensite. By contrast, the intermittent line shows clearly the effect the expansion accompanying these transformations has on the thermal strain.

Welding Model. A cross section of the weldment at its midlength is used in this study under plane strain conditions. This is rationalized by the fact that for relatively long plates the maximum stresses are developed in this region.

The boundary conditions used in the analysis allow free expansion of the weldment in the transverse direction as well as bending. At the same time the structure should be properly restrained to eliminate all possible modes of rigid body motion; otherwise the stiffness matrix will not be positive definite.

An important point is the accumulation of plastic strains in the regions that become molten during the welding cycle. When the temperature reaches the liquids these plastic strains are physically relieved, starting to accumulate again when the metal solidifies. The presence of nonzero material properties above the liquidus, however, would cause the plastic strains not only to continue accumulating but also to reach artificially high values owing to the very low magnitude of the mechanical properties at these temperatures. It was, therefore, necessary to modify ADINA by imposing a total relief of plastic strains when the material melts.

Finally, one of the most important decisions an analyst has to make when performing a nonlinear incremental stress analysis is the solution strategy to be followed, because the accuracy and the convergence characteristics of the solution depend very much on it. This is especially true for complex

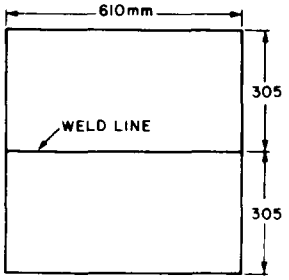

Fig. 4 Test plate arrangement

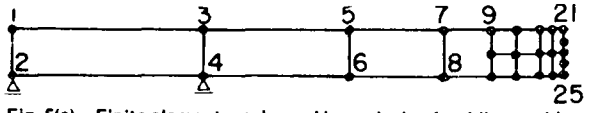

Fig. 5(a) Finite element mesh used in analysis of welding problem

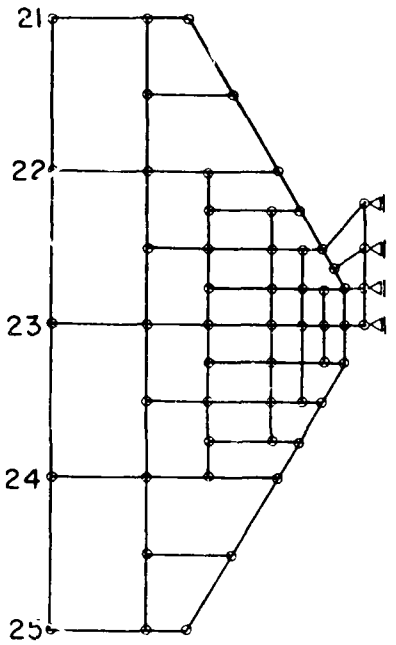

Fig. 5(b) Finite element mesh, continued (12.7 mm to the right of weld centerline)

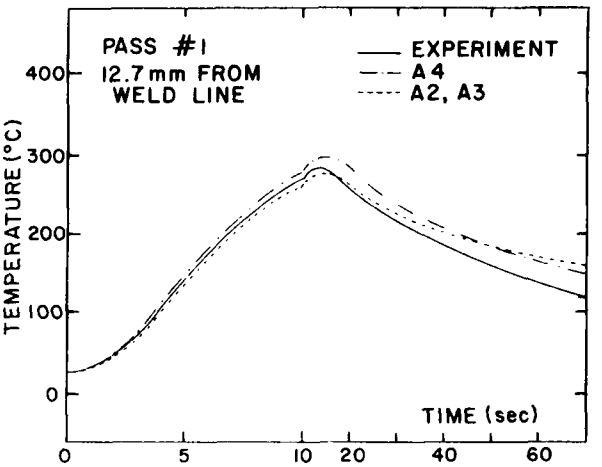

Fig. 6 Comparison of finite element results with experimental data (weld pass No. 1)

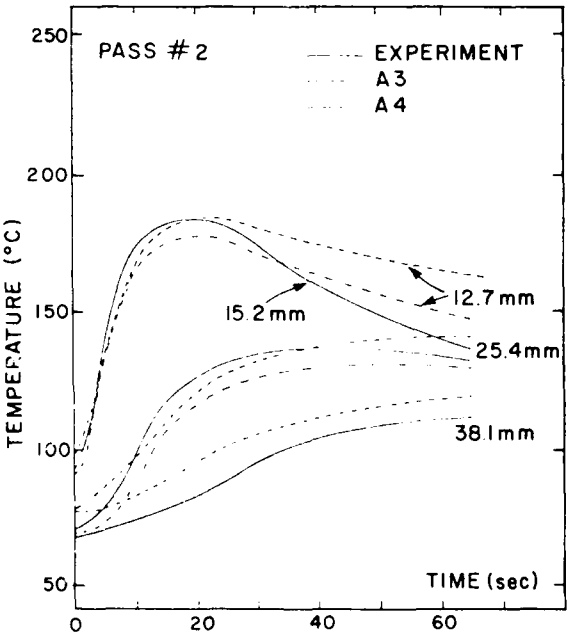

Fig. 7 Comparison of finite element results with experimental data (pass No. 2)

situations involving highly nonlinear material behavior like the one encountered in the welding problem. In this study these parameters were chosen based on previous experience and on a number of numerical experiments.

Experimental Program

A series of experiments consisting of butt welding HY-130 steel plates using the GMAW process were performed. Each plate measured 305 mm × 610 mm × 25.4 mm resulting, after welding, in the configuration shown in Fig. 4. The weld joint consisted of a double-V groove with a 60-deg included angle in accordance with U.S. Navy specifications. All welding experiments were performed with the plates resting on knife edge supports in order to better simulate the completely unrestrained condition. For more details on the experimental procedures used see [15].

Temperatures and strains were measured throughout the welding operation using Chromel/Alumel adhesively bonded thermocouples and 90-deg Rosette electric resistance strain gages cemented on the plates' surface respectively, and recorded at various distances from the weld centerline [15].

Comparison of Numerical and Experimental Results

The finite element mesh used for the numerical calculations is shown in Fig. 5, where only the left half of the plate and the weld metal is shown, the right half being exactly symmetric. This mesh represents the unit thickness cross section of the plate at its midlength. Four to six-node isoparametric quadrilateral elements were used, taking special care not to include any triangular elements in the mesh since they are considered by many as inefficient. A total of 77 nodes and 47 elements were utilized with the mesh being finer near the weld centerline because of the large gradients of temperature and stresses present in this region. The temperature dependence of all material properties was considered in the analyses [15].

Temperature Distributions. The heat transfer analysis was performed for the first three welding passes only. A total of four analyses (A1 to A4) were made by varying the arc efficiency and the temperature variation of the heat convection coefficient [15].

Cases A2, A3, and A4 are compared with the experimentally obtained results in Fig. 6 for a point on the

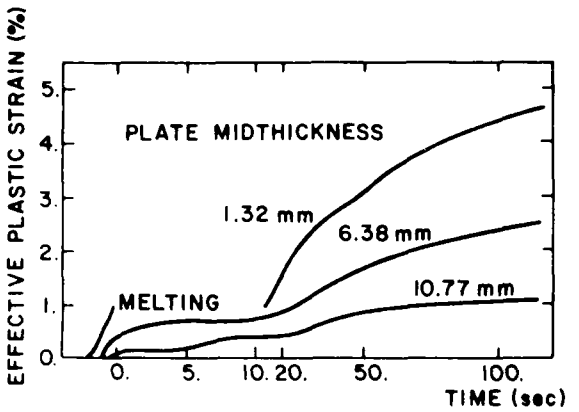

Fig. 8 Accumulated effective plastic strain history at various distances from the weld centerline

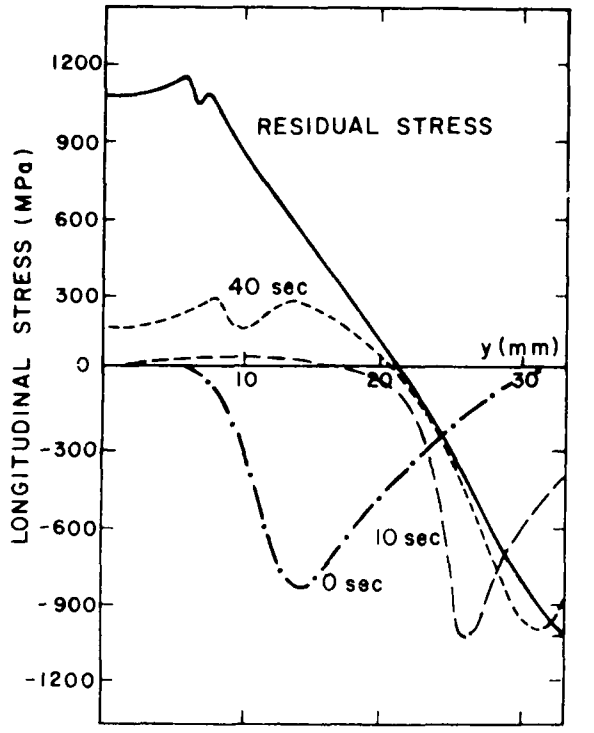

Fig. 9 Longitudinal stress distribution at several time instances

plate's top surface 12.7 mm away from the weld centerline and for the first welding pass. Considering the same heat input (η_a = 0.60), little difference is found between cases A2 and A3. This is due to the fact that although higher values for the convection coefficent were chosen in analysis A3, these values were not high enough to significantly alter the heat losses from the top and bottom surfaces of the plate and consequently the temperature distribution. A substantial increase in the convection coefficient was therefore chosen for case A4; at the same time, however, an increase in the arc efficiency was made (η_a = 0.70) to partially compensate for the higher h, and thus to obtain a good estimate of the maximum temperature rached. As seen in Fig. 6 the combination of values used in this latter analysis succeeded in bringing the cooling rate much closer to the experimental one. At the same time a 4-percent overprediction of the maximum temperature is observed. The difference, however, was very small so that any further analysis was not felt necessary.

Similar results were found at other points of the plate, and for other passes. Case A4 came always closest at matching the experimentally obtained results (see Fig. 7).

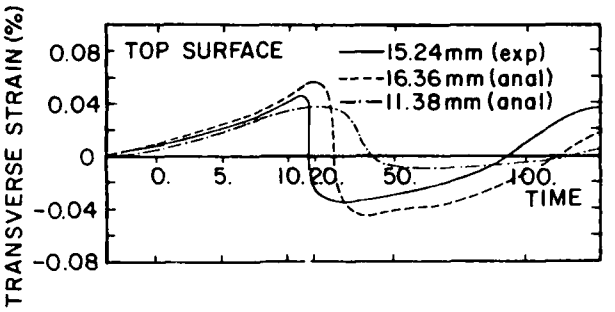

Fig. 10 Comparison of experimentally measured transverse transient strains on the plate's top surface with numerical predictions

Strain and Stress Distributions. Due to the high costs involved in performing the numerical stress analysis, only the first welding pass was thoroughly analyzed. The results obtained are discussed below.

Figure 8 shows the accumulation of the effective plastic strain, e^{-p}, for the first welding pass at three points located on the plate's midthickness and at various distances away from the weld centerline. In the weld metal zone, plastic strain is built up rapidly as the material yields in compression. At the melting region this plastic strain is completely relieved, to rapidly reach again a level in close proximity to that existing prior to melting upon solidification. As cooling continues and yielding in tension progresses, the plastic strain steadily increases but at a smaller rate than before. In the heat-affected zone, plastic strain is accumulated during heat-up in much the same way as in the weld metal zone but not quite as rapidly. As the material cools, it yields in tension and further plastic strain is accumulated.

Figure 9 shows calculated transient longitudinal stress distributions. Compressive stresses exist in the weld metal prior to melting. When the metal is in its molten stage, negligible compressive or tensile stresses were calculated. As cooling commences, tensile stresses start appearing in the weld metal. These stresses then build up to the residual stress pattern when ambient temperature is reached. For self-equilibrating purposes, compressive stresses exist in areas removed from the weld centerline. Note in Fig. 9 the effect of phase transformation, causing a sudden decrease in the tensile stresses.

Comparison of the experimentally measured transverse transient strain history at a point located on the top surface of the plate is made with the numerically obtained results in Fig. 10. The correlation is relatively good if one takes into account the various assumptions involved in modeling the complex welding problem. A delay in the transition from tensile to compressive and again from compressive to tensile strains is observed in the analysis. The same delay as far as the occurrence of the maximum strain is also exhibited. It is believed that this phenomenon is primarily due to the relative coarseness of the finite element mesh, and the complex loading history present in the welding problem.

Conclusions

This paper presented a methodology for predicting temperatures, transient strains, and residual stresses due to welding using the finite element method. Particular emphasis was placed on the incorporation of phase transformation effects in the analysis, an important parameter when welding quenched and tempered steels. Comparison of the computed results with experimentally obtained data showed the importance of considering these effects.

Finally, it should be noted that the analysis presented is a rather expensive one. It is thus recognized that it cannot be used in everyday practice. The authors believe, however, that

benefits can accrue in the case of manufacturing critical structures when an accurate estimation of the metallurgical microstructures and residual stresses that result from the welding operation is very essential.

Acknowledgments

The work described in this paper is part of a four-year research project at M.I.T. from the Office of Naval Research (Contract Number N00014-75-0469) entitled "Study of Residual Stresses and Distortion in Structural Weldments in High-Strength Steels," The authors gratefully acknowledge the financial support provided by O.N.R. The authors would also like to thank Professor K. J. Bathe of the Department of Mechanical Engineering, M.I.T. for his interest and valuable help.

References

1 Ueda, Y., and Yamakawa, T., "Analysis of Thermal-Elastic-Plastic Stress and Strain Analysis During Welding by Finite Element Method," *Transactions of Japan Welding Society*, Vol. 2, No. 2, Sept. 1971, pp. 90-100.

2 Hibbitt, H. D., and Marcal, P. V., "A Numerical Thermo-Mechanical Model for the Welding and Subsequent Loading of a Fabricated Structure," *Computers and Structures*, Vol. 3, No. 5, Sept. 1973, pp. 1145-1174.

3 Frieman, E., "Thermomechanical Analysis of the Welding Process Using the Finite Element Method," ASME JOURNAL OF PRESSURE VESSEL TECHNOLOGY, Aug. 1975, pp. 206-213.

4 Muraki, T., Bryan, J. J., and Masubuchi, K., "Analysis of Thermal Stresses and Metal Movement During Welding," ASME *Journal of Engineering Materials and Technology*, Vol. 97, No. 1, Jan. 1975, pp. 81-91.

5 Masubuchi, K., "Numerical Modeling of Thermal Stresses and Metal Movement during Welding," *Proceedings of 1977 ASME WAM, Numerical Modeling of Manufacturing Processes*, PVP-PB-025, Dec. 1977, pp. 1-17.

6 Friedman, E., "Numerical Simulation of the Gas Tungsten Arc Welding Process," *Proceedings of 1977 ASME WAM, Numerical Modeling of Manufacturing Processes*, PVP-PB-025, Dec. 1977, pp. 35-47.

7 Rybicki, E. F., Schmuesser, D. W., Stonesifer, R. B., Groom, J. J., and Mishler, H. W., "A Finite Element Model of Residual Stresses in Girth-Butt Welded Pipes," *Proceedings of 1977 ASME WAM, Numerical Modeling of Manufacturing Processes*, PVP-PB-025, Dec. 1977, pp. 131-142.

8 Ueda, Y., Fukuda, K., and Nakacho, K., "Basic Procedures in Analysis and Measurement of Welding Residual Stresses by the Finite Element Method," *Proceedings of International Conference on Residual Stresses in Welded Construction and Their Effects*, The Welding Institute, London, 1977, pp. 27-37.

9 Masubuchi, K., "Applications of Numerical Analysis in Welding: Present State-of-the-Art and Future Possibilities," International Institute of Welding Annual Assembly, Colloquium on Application of Numerical Analysis in Welding, Dublin, Ireland, 1978.

10 Andersson, B. A. B., "Thermal Stresses in a Submerged-Arc Welded Joint Considering Phase Transformations," ASME *Journal of Engineering Materials and Technology*, Vol. 100, No. 3, pp. 356-362.

11 Fujita, Y., Nomoto, T., and Hagesawa, H., "Thermal Stress Analysis Based on Initial Strain Method," *International Institute of Welding Document* No. X-926-79, Apr. 1979.

12 Rybicki, E. F., and Stonesifer, R. B., "Computation of Residual Stresses due to Multipass Welds in Piping Systems," ASME JOURNAL OF PRESSURE VESSEL TECHNOLOGY, Vol. 101, No. 2, May 1979, pp. 149-154.

13 Bathe, K. J., "ADINAT—A Finite Element Program for Automatic Dynamic Incremental Nonlinear Analysis of Temperature," AVL Report 82448-5, Mechanical Engineering Department, M.I.T., May 1977 (revised Dec. 1978).

14 Hughes, T. J. R., "Unconditionally Stable Algorithms for Nonlinear Heat Conduction," *Computer Methods in Applied Mechanics and Engineering*, Vol. 10, 1977, pp. 135-139.

15 Papazoglou, V. J., "Analytical Techniques for Determining Temperatures, Thermal Strains, and Residual Stresses During Welding," Ph.D. thesis, M.I.T., May 1981.

16 Dilawari, A. H., Szekely, J., and Eagar, T. W., "Electromagnetically and Thermally Driven Flow Phenomena in Electroslag Welding," *Metallurgical Transactions B*, Vol. 9B, 1978, pp. 371-381.

17 Bathe, K. J., "ADINA—A Finite Element Program for Automatic Dynamic Incremental Nonlinear Analysis," AVL Report 82448-1, Mechanical Engineering Department, M.I.T., September 1975 (revised Dec. 1978).

18 Grange, R. A., and Kiefer, J. M., "Transformation of Austenite on Continuous Cooling and its Relation to Transformation at Constant Temperature," *ASM Transactions*, Vol. 29, No. 3, 1941, pp. 85-115.

19 Manning, G. K., and Lorig, C. H., "The Relationship Between Transformation at Constant Temperature and Transformation during Cooling," *AIME Transactions*, Vol. 167, 1946, pp. 442-463.

Printed in U.S.A.

APPENDIX B

THE SOCIETY OF NAVAL ARCHITECTS AND MARINE ENGINEERS
One World Trade Center, Suite 1369, New York, N.Y. 10048

no. 12

Advance copy of paper to be presented at the Annual Meeting, New York, N.Y., November 17-20, 1982

APPENDIX B

Residual Stresses Due to Welding: Computer-Aided Analysis of Their Formation and Consequences

Vassilios J. Papazoglou,[1] Associate Member, **Koichi Masubuchi,**[2] Member, **Edison Gonçalves,**[3] Visitor, and **Akihiko Imakita,**[4] Visitor

Results of recent investigations at M.I.T. on the subject of residual stresses due to welding are summarized. Part 1 deals with the computer-aided prediction of residual stress distributions. Both closed-form analytical and numerical solutions, the latter based on the finite-element method, to the problems of determining temperature, transient strain, and residual stress distributions are presented. Experimentally obtained data are then compared with predictions obtained by the developed computer programs to test their validity. Guidelines for the applicability of each model are also included. Part 2 discusses the computer-aided analysis of the effects of residual stresses on the service behavior of welded structures. A finite-element analysis of the fracture characteristics of high-strength steel weldments is described in some detail as a case study. The obtained results are also compared with experimental data.

Introduction

THE PROBLEM of predicting residual stresses due to welding has long been recognized by ship designers and fabricators as very important but at the same time as a very difficult one to analyze. This difficulty has its origin in the complex mechanism of residual stress formation which starts from the uneven temperature distribution caused by the intense, concentrated heat source associated with all fusion welding processes. The incompatible strains that are formed as a consequence give rise in turn to self-equilibrating stresses that remain in the welded structure after it has cooled down to ambient temperature, thus producing the so-called residual stresses.

To effectively analyze the problem and account for the nonlinear phenomena associated with it, one has to draw upon knowledge from a variety of scientific disciplines, including heat transfer, applied mechanics, numerical analysis, and materials science. On top of that, the lengthy calculations required make the solution prohibitive unless one has access to a fast electronic digital computer. It is therefore no coincidence that researchers became actively involved in the field only during the past decade or so, during which time computers and the powerful numerical techniques developed in association with them have started to be more widely used.

A logical question that could come to one's mind at this point is why should one be concerned with the prediction of residual stresses in welded structures, especially since it is such a formidable problem. The answer is that the effect they have on the service behavior of these structures can be detrimental. Brittle fracture can occur earlier because the presence of residual stresses, combined with any external loading, can substantially decrease the critical flaw size of the weldment. Compressive residual stresses located in the regions some distance away from the weld line can substantially decrease the critical buckling stress of a structure, especially if it is composed of thin plates, causing structural instabilities. Similar effects occur in the areas of fatigue fracture, stress-corrosion cracking, hydrogen embrittlement, and others.

It thus becomes evident that the practicing engineer would like to have a design tool to account for residual stresses and their effects. More specifically, what he wishes to do is to change design and fabrication parameters, such as plate thickness, joint design, welding conditions, and welding sequence, so that the adverse effects of residual stresses (and the associated distortion) can be reduced to acceptable levels from the point of view of reliability. It is generally much better to achieve this goal during an early stage of design and fabrication rather than confronting the problem at later stages of fabrication. This is especially true when critical structures, such as submarines and other types of deep-sea submersibles, are to be built using new materials (for example, HY-130 steel, titanium alloys) or unconventional welding processes (for example, electron beam, laser beam) or both.

One of the most comprehensive sources of information regarding the problem of residual stresses and their consequences is a recently published book by Masubuchi [1][5]. This book, which can be of great value to both designers and fabricators of welded structures, represents a systematic presentation of knowledge on the subject accumulated over the past 30 or so years mainly on the basis of extensive parametric experimental investigations, which can collectively be thought of as "first generation" or "pre-computer age" methodologies. These methodologies have served and still serve their purpose in cases

[1] Postdoctoral associate, Department of Ocean Engineering, Massachusetts Institute of Technology, Cambridge, Massachusetts.

[2] Professor of ocean engineering and materials science, Massachusetts Institute of Technology, Cambridge, Massachusetts.

[3] Assistant professor, Department of Naval Architecture and Marine Engineering, University of Sao Paulo, Sao Paulo, Brazil.

[4] Visiting research engineer, Department of Ocean Engineering, Massachusetts Institute of Technology, Cambridge, Massachusetts, also with Mitsui Engineering and Shipbuilding Co., Tokyo, Japan.

For presentation at the Annual Meeting, New York, N.Y., November 17-20, 1982, of THE SOCIETY OF NAVAL ARCHITECTS AND MARINE ENGINEERS.

[5] Numbers in brackets designate References at end of paper.

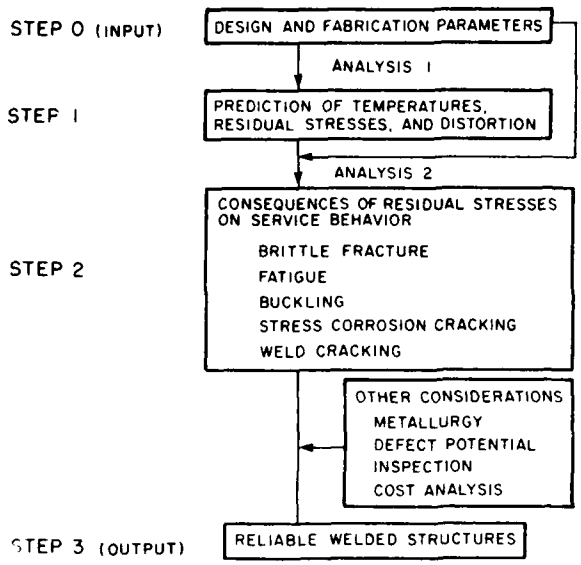

Fig. 1 Systematic approach for predicting residual stresses due to welding and their consequences

that have already been extensively investigated, for example, joining of mild steel structures using conventional arc welding techniques. Time and cost requirements in today's competitive world, however, do not allow them to be used when new materials and processes have to be effectively used in the construction of seagoing vessels and offshore structures. The need therefore exists for a new, more versatile and efficient computer-age methodology.

This paper discusses such a methodology based on the extensive use of computers in a very systematic way as shown in Fig. 1. Part 1 of the paper discusses state-of-the-art methods for predicting residual stresses (and distortion) due to welding; it thus corresponds to Analysis 1 between Steps 0 and 1 in Fig. 1. The methods presented range from relatively simple one-dimensional analyses to more complicated ones based on the finite-element method with nonlinearities. Comparing the obtained results with data collected through series of experiments, the predictive capabilities of the various methods are finally assessed.

In Part 2 of the paper the subject of analyzing the consequences of residual stresses on the service behavior of welded structures is addressed (Analysis 2 between Steps 1 and 2 in Fig. 1). To demonstrate how the computer can help in this respect, details of the special case of analyzing the fracture characteristics of weldments are presented. The numerical results obtained using the finite-element method are finally compared with exerimentally obtained data.

It is not the intent of the authors to present in detail all the mathematics involved in the discussed methodologies. The interested reader is referred for this purpose to other sources [2-5]. The emphasis will rather be placed on how the ship designers and fabricators can effectively use the state-of-the-art methodologies available today for solving the residual stress problem.

Part 1

Prediction of welding residual stresses

In this part of the paper the problem of predicting residual stresses due to welding is addressed. After a brief introduction on the physical aspects of residual stress formation, the various methodologies available for calculating residual stress distributions are discussed. Particular emphasis is placed on the method based on a computer simulation of the welding process as it relates to residual stress formation. This consists of first solving the heat-transfer problem and then utilizing the obtained results to perform the stress analysis.

Throughout the discussion special reference is made to the prediction capabilities of the analyses by comparing analytical results with experimental data collected from series of experiments conducted over the past several years by Massachusetts Institute of Technology (M.I.T.) investigators.

General information on residual stresses

Residual stresses are defined as these stresses that exist in a body if all external loads are removed. Various alternative technical terms have been used and can still be found in the literature that refer to residual stresses, including internal stresses, initial stresses, inherent stresses, reaction stresses, and locked-in stresses.

Areas in which residual stresses can exist vary greatly in scale from a large portion of a metal structure down to areas measurable only on the atomic scale [1]. Regarding the former case, macroscopic residual stresses can occur in scales ranging from ships heated by solar radiation from one side to a small area on the top of a plate where grinding took place. On the other hand, microscopic residual stresses can be produced on the atomic scale during a phase transformation or near a dislocation. Furthermore, residual stresses can also be classified, according to the mechanism of formation, to those produced by structural mismatching and those produced by an uneven distribution of nonelastic strains (including plastic and thermal strains).

In the case of welding, with which this paper is concerned, residual stresses can be classified as being macroscopic in scale and as being produced by uneven distributions of nonelastic strains. Finally, it should be noted that since residual stresses exist without any external loads they should always satisfy force and moment equilibrium, that is, they should be self-equilibrating.

Welding residual stress formation

To physically understand how residual stresses are formed during welding, the simple case of a straight bead-on-plate weld will be described in some detail [1]. Figure 2 shows schematically the changes of temperature and stresses that occur during such a process. The welding arc, which is moving at a speed v, is presently located at the origin O, as shown in Fig. 2(*a*).

Figure 2(*b*) shows the temperature distribution along several cross sections. Along Section A-A, which is ahead of the welding arc, the temperature change due to welding, $\Delta\theta$, is almost zero. Along Section B-B, which crosses the welding arc, the temperature change is extremely rapid and the distribution is very uneven. Along Section C-C, which is some distance behind the welding arc, the distribution of temperature change is as shown in Fig. 2(*b*) 3. Along Section D-D, which is very far from the welding arc, the temperature change due to welding again diminishes.

Figure 2(*c*) shows the distribution of stresses along these sections in the x-direction, σ_x. Stress in the y-direction, σ_y, and shearing stress, τ_{xy}, also exist in a two-dimensional stress field.

Along Section A-A, thermal stresses due to welding are almost zero. The stress distribution along Section B-B is shown in Fig. 2(*c*) 2. Because molten metal will not support a load, stress underneath the welding arc is close to zero. Stresses in regions a short distance from the arc are compressive, because the expansion of these areas is restrained by the surrounding metal where the temperatures are lower. Since the temperatures of

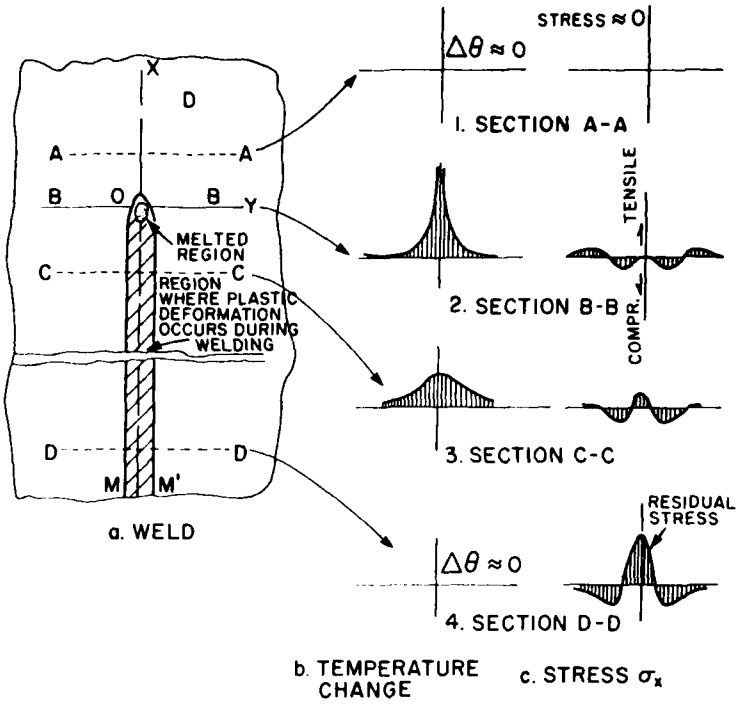

Fig. 2 Schematic representation of changes in temperature and stresses during welding

these areas are high and the yield strength of the material low, stresses in these areas are as high as the yield strength of the material at corresponding temperatures. The magnitude of compressive stress passes through a maximum with increasing distance from the weld or with decreasing temperature. However, stresses in areas away from the weld are tensile and balance with compressive stresses in areas near the weld. In other words

$$\int \sigma_x dy = 0$$

across Section B-B.[6] Thus, the stress distribution along Section B-B is as shown in Fig. 2(*c*)-2.

Stresses are distributed along Section C-C as shown in Fig. 2(*c*)-3. Since the weld metal and base metal regions near the weld have cooled, they contract and cause tensile stresses in regions close to the weld. As the distance from the weld increases, the stresses first change to compressive and then become tensile.

Figure 2(*c*)-4 shows the stress distribution along Section D-D. High tensile stresses are produced in regions near the weld, while compressive stresses are produced in regions away from the weld. This is the usual distribution of residual stresses that remain after welding is completed.

The cross-hatched area, M-M', in Fig. 2(*a*) shows the region where plastic deformation occurs during the welding thermal cycle. The egg-shaped region near the origin O indicates the region where the metal is melted.

The region outside the cross-hatched area remains elastic during the entire welding thermal cycle.

Sources of residual stresses—In the previous section the difference in shrinkage of differently heated and cooled areas of a welded joint was identified as the primary cause of residual stress formation, resulting in high longitudinal stresses, σ_x, in the weld metal. Similar tensile stresses, σ_y, arise in the transverse direction, too, but of smaller magnitude.

This situation is typical for the case examined. If, however, one is also interested in the through-thickness distribution of residual stresses or in materials exhibiting phase transformations, or both, two additional residual stress sources can be identified [6].

One source is the uneven cooling in the thickness direction of the weld. Surface layers of the weld and the highly heated areas close to it usually cool more rapidly than the interior, especially in the case of thick plates. Thermal stresses thus arise over a cross section which can lead to heterogeneous plastic deformation and hence to residual stresses. These "quenching" residual stresses are expected to be compressive at the surface of the highly heated areas and to self-equilibrate with the tensile ones in the inner regions.

The other source of residual stresses comes from the phase transformations that occur during cooling; in the case of steel, for example, austenite is transformed into ferrite, bainite, or martensite, or a combination of them. These transformations are accompanied by an increase in specific volume, causing the material being transformed (in the weld metal and the heat-affected zone) to tend to expand. This expansion, however, is hindered by the cooler material which is not being transformed, inducing compressive stresses in the transformed material and tensile stresses in the other regions.

The total residual stresses due to welding can thus be found by combining the effects of the aforementioned three sources.

Methods for predicting residual stresses

The incompatible nonelastic strains produced in the weldment as a result of the nonuniform temperature distribution are formed in a very complex manner as discussed in previous sections. The computational efforts required to analyze the phenomena involved, including high-temperature plasticity calculations in a multidimensional stress space, have limited investigators' efforts in the past to such simple cases as

[6] This equation neglects the effect of σ_y and τ_{xy} on the equilibrium condition

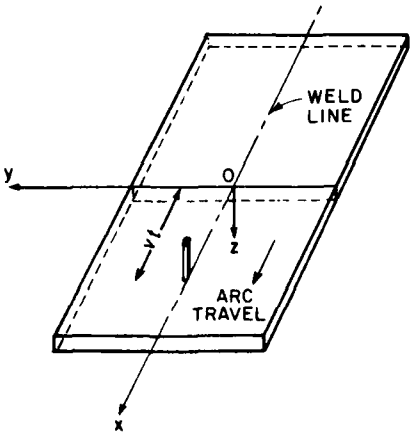

Fig. 3 Weldment configuration

1. Spot welding in which temperature and strain changes are axisymmetric.
2. Instantaneous heating along the edge of a strip in which temperature and stress changes occur in one dimension only.

In more complex cases, however, and before the advent of the era of powerful digital computers, a method had to be devised for the prediction of residual stresses. Such a method was developed by Masubuchi in the late 1950's [7,8] on the basis of Moriguchi's theory of incompatible strains [9]. This method consists of assuming an incompatible strain distribution in the weldment and calculating the residual stresses on the basis of the theory of elasticity, recognizing that this incompatibility is a form of singularity in an elastic stress field. Analyses using singular points, such as a concentrated load or a center of dilation, for solving stress problems under various boundary conditions are well established and can thus be very useful for analyzing residual stresses under similar boundary conditions.

One major drawback of this method, however, is that it is very difficult to estimate the distribution of the incompatible strains. In some representative cases the distribution has been found experimentally [10]. On that basis, estimates can then be made for other similar situations.

It is nevertheless felt that since the advent of the modern digital computer a more accurate prediction of the residual stress distribution can be made by simulating the phenomena that occur during the welding process.

Computer simulation—To accurately simulate the thermo-mechanical behavior of a weld, or for this matter any phenomenon that involves both thermal and stress analysis, one should start from first principles, which in this case is the first law of thermodynamics. This would mean that one would have to solve a problem containing mechanical and thermal coupling, a fact that makes the analysis extremely complicated, if not impossible, on the basis of the present state of knowledge, except in cases where thermoelastic modeling is sufficient. Initial attempts at formulating and investigating the more complex problem of coupled thermoplasticity have been undertaken by Mróz [11,12], but the whole subject area is still at its initial stages of development.

It becomes necessary, therefore, to uncouple the thermal and mechanical parts of the welding problem and solve each one separately. The assumptions required for this uncoupling have been examined by Hibbitt and Marcal [13]; the most critical ones are the neglect of dimensional changes and the neglect of cross-coupling between thermal and mechanical work.

Based on these assumptions the problem can be solved in two steps. First, the heat flow during welding is analyzed. The obtained temporal and spatial temperature distributions are then used as one of the inputs for the subsequent strain and stress analysis. Various analytical and numerical methods that can be used in each step are examined in the next sections of this part of the paper.

Problem characteristics—Figure 3 shows the physical phenomenon to be examined. A welding arc is traveling with a speed v between two plates, causing them to coalesce by providing filler metal.

The four parts of a weld that are subjected to different thermal histories are shown in Fig. 4. Part 1 constitutes the filler metal which is deposited molten and later solidifies as cooling begins. Part 2 is the part of the joint that melts and later resolidifies during cooling. Both these parts define the weld metal. Part 3 is the heat-affected zone (HAZ), defined for steel as that part of the joint in which the maximum temperature reached is above the A_1 but below the solidus temperature.[7] Finally, Part 4 is the base metal.

These four thermal histories and the related changes in physical properties are shown in Fig. 5 for the case of a single-pass weld [14].

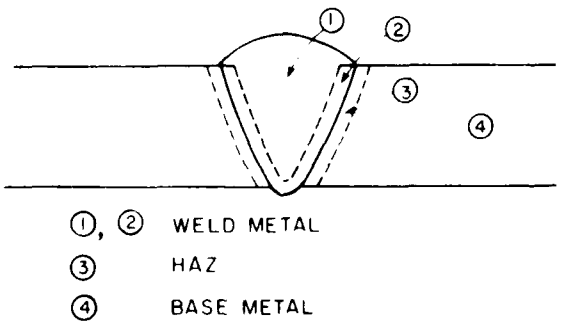

Fig. 4 The four parts of a weld subjected to different thermal histories

Analysis of heat transfer during welding

The importance of accurately predicting the temperature distribution during welding has been recognized for many years by both scientists and engineers working with welding problems. This importance stems from the fact that most of the phenomena subsequently encountered, such as residual stresses, distortion, and metallurgical changes, have their origin in the uneven temperature distribution and the fast heating and cooling rates that occur during the welding operation.

All of the early attempts at solving the problem of heat flow during welding were analytical in nature since they were performed before the advent of the computer. As a consequence several simplifying assumptions had to be made to allow for the solution of the highly nonlinear governing partial differential equation and the accompanying boundary conditions. Starting in the mid-sixties, however, several investigators from around the world have used the computer to numerically predict the thermal history during welding with much greater accuracy.

As with any complex engineering problems, the choice of whether to use an analytical or a numerical solution has to be based on a cost versus accuracy tradeoff. Analytical solutions are much more inexpensive and, though not as accurate as the numerical ones, provide nevertheless for the establishment of the general laws and thus facilitate a good understanding of the

[7] A_1 temperature is defined for steel as that temperature at which the eutectoid reaction takes place. Under equilibrium conditions this temperature is equal to 725 C (1333 F). Solidus is defined as that temperature above which the liquid phase is also present.

phenomena involved. On the other hand, the more expensive numerical solutions are necessary whenever accuracy is of paramount importance, as for example when a metallurgical characterization of the weld metal and the HAZ is needed, or when a subsequent stress analysis to determine the transient strains and residual stresses is required.

Closed-form analytical solutions

Fundamental solutions—The first exact analytical solutions of the problem of heat flow during welding were obtained by Rosenthal [15–17] in the late 1930's and early 1940's, although a particular case was considered independently at around the same time by Boulton and Lance Martin [18]. Rosenthal solved the conventional heat conduction differential equation for constant point, line, and plane heat sources moving at a constant speed with respect to a fixed Cartesian coordinate system. To facilitate easier handling of the problem, he assumed that welding was performed over a sufficient length so that the temperature distribution around the heat source would not change if viewed from a coordinate system moving with the heat source. This phenomenon is called quasi-stationary or quasi-steady state. Additional assumptions were made as follows:

1. The physical properties of the conducting medium are constant.
2. The heat losses through the surface of the conducting medium to the surrounding atmosphere are neglected.
3. Heat created in electric welding by the Joule effect is negligible.
4. The phase changes and the accompanying absorption or release of latent heat in the conducting medium are neglected.
5. The conducting medium is infinitely large in the two-dimensional case (line heat source) and semi-infinitely large in the three-dimensional case (point source).

Based on the foregoing assumptions Rosenthal developed the following exact solutions for the two- and three-dimensional cases, respectively (see Fig. 3):

$$\theta - \theta_0 = \frac{Q}{2\pi kH} \cdot e^{-\lambda v \xi} \cdot K_0(\lambda v r) \tag{1}$$

$$\theta - \theta_0 = \frac{Q}{2\pi k} \cdot e^{-\lambda v \xi} \cdot \frac{e^{-\lambda v R}}{R} \tag{2}$$

where

θ_0 = initial temperature
Q = total heat input
H = plate thickness
$\xi = x - vt$
v = welding (or arc travel) speed
t = time
(x,y,z) = fixed Cartesian coordinate system
$r = (\xi^2 + y^2)^{1/2}$
$R = (\xi^2 + y^2 + z^2)^{1/2}$
k = thermal conductivity
$\frac{1}{2}\lambda = k/\rho c = \kappa$ = thermal diffusivity
ρ = density
c = specific heat
$K_0(x)$ = modified Bessel function of second kind and zero order

For the case of thin plates (two-dimensional solution) Rosenthal [16] and other investigators have suggested that heat losses through the surface to the surrounding atmosphere might have to be taken into account by replacing in the Bessel function of equation (1) the factor λr by

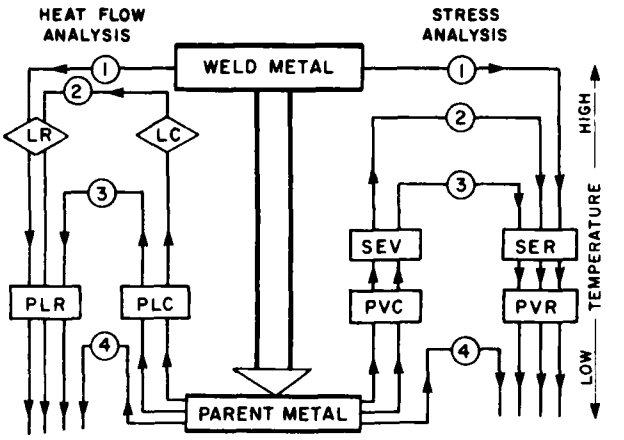

LC - ABSORPTION OF LATENT HEAT DURING MELTING
LR - RELEASE OF LATENT HEAT DURING SOLIDIFICATION
PLC - ABSORPTION OF LATENT HEAT DURING PHASE TRANSFORMATION
PLR - RELEASE OF LATENT HEAT DURING PHASE TRANSFORMATION
PVC - VOLUME SHRINKAGE DURING PHASE TRANSFORMATION
PVR - VOLUME EXPANSION DURING PHASE TRANSFORMATION
SEV - YIELD STRESS AND YOUNG'S MODULUS VANISH
SER - YIELD STRESS AND YOUNG'S MODULUS RECOVER

Fig. 5 Thermal histories and related changes of physical properties of the four weld parts

$$\left[(\lambda v)^2 + \frac{h_1 + h_2}{kH}\right]^{1/2} \tag{3}$$

where h_1 and h_2 are the heat-transfer coefficients, assumed constant, at the top and bottom of the plate, respectively.

Furthermore, by using the so-called "method of images" or "image source method" [16], one can get solutions for the cases of large but finite thickness and/or finite breadth plates. For example, a three-dimensional solution for laying a weld bead on the top of a finite-thickness plate with adiabatic boundary conditions can be obtained by adding an infinite series to equation (2), yielding

$$\theta - \theta_0 = \frac{Q}{2\pi k} \cdot e^{-\lambda v \xi} \cdot \left\{ \frac{e^{-\lambda v R}}{R} + \sum_{n=1}^{\infty} \left[\frac{e^{-\lambda v R_n}}{R_n} + \frac{e^{-\lambda v R_n'}}{R_n'} \right] \right\} \tag{4}$$

where

$$R_n = [\xi^2 + y^2 + (2nH - z)^2]^{1/2}$$

$$R_n' = [\xi^2 + y^2 + (2nH + z)^2]^{1/2}$$

Following these initial developments many investigators tested the validity of the proposed equations experimentally. A thorough exposition of these works can be found in Myers et al [19]. Comments on this subject are reported in a later section.

Modifications to fundamental solutions—Looking at data on thermal conductivity, specific heat, and density one finds that all these parameters are highly dependent upon temperature, thus making the constant-properties assumption of the analytical solutions unrealistic, especially for the regions close to the heat source where the material exhibits very high tem-

Table 1 Values of arc efficiency for various processes

	Christensen [23]	Rykalin [25]	Tsai [26]
GMAW	...	0.65 to 0.85	...
mild steel	0.66 to 0.70	...	0.80 to 0.90
aluminum	0.70 to 0.85	...	...
SAW	0.90 to 0.99	0.90 to 0.99	0.85 to 0.98
SMAW	...	...	...
mild steel, ac	0.66 to 0.85	0.65 to 0.85	0.55 to 0.90
GTAW	...	...	...
mild steel, ac	0.22 to 0.48	0.20 to 0.50	...
mild steel, dc	0.36 to 0.46	0.45 to 0.75	...
aluminum, ac	0.21 to 0.43	0.20 to 0.50	...

GMAW = gas metal arc welding.
SAW = submerged arc welding.
SMAW = shielded metal arc welding.
GTAW = gas tungsten arc welding.

peratures. It is desirable to predict the high-temperature region as accurately as possible, however, since it is this region that is directly related to the size of the plastic zone and the accompanying residual stresses and distortion.

Researchers at M.I.T. [20–22] adopted the iteration method to take into account the temperature dependence of material properties. The fundamental heat source solution with material properties at some temperature, say 300°C (572°F), provides the first approximate solution at a particular point. This temperature is compared with the initial guess and if the two temperatures disagree by more than 0.5°C, new properties are found for a temperature halfway in between. The new values are used to obtain a new temperature estimate. The process is repeated until convergence is reached. It should be pointed out that although this iteration method generally gives good predictions outside the fusion zone, there is no guarantee that it will converge to the correct solution since the approximation used may not satisfy the energy conservation law.

In addition, the conventional point heat source closed from solution fails to give good results in the case of multipass welding. This is due to the fact that the solution is based on the point source being located at the top surface of the plates being welded.

To accommodate the multipass welding case, a modification of the solution was made [2] enabling one to locate the heat source at any point through the plate's thickness. It thus becomes possible to simulate each welding pass by positioning the point source at the center of the pass.

The basic assumptions of the conventional solution were kept the same. Furthermore, the adiabatic boundary conditions on the top and bottom surfaces of the plate were satisfied by using the method of images. The obtained solution can then be expressed by the following equation:

$$\theta = \theta_0 + \frac{Q}{4\pi k} \cdot e^{-\lambda r\xi} \cdot \left\{ \frac{e^{-\lambda rR}}{R} + \sum_{n=1}^{\infty} \left[\frac{e^{-\lambda rR_n}}{R_n} + \frac{e^{-\lambda rR_n}}{R_n} \right] \right\} \quad (5)$$

where

$$R_n = \sqrt{\xi^2 + y^2 + (OT_n + z)^2}$$

$$R_n = \sqrt{\xi^2 + y^2 + (OB_n - z)^2}$$

$$OT_n = \sqrt{OB_{n-1} + 2F}$$

$$OB_n = \sqrt{OT_{n-1} + 2G}$$

with F and G being the distances of the point heat source from the top and bottom surfaces of the plate, respectively, and OT_n and OB_n the distances of the point heat source from the nth imaginary ones with respect to the top and bottom surfaces, respectively. All other quantities have been previously defined.

Three-dimensional finite heat source model—Most investigators agree that perhaps the most critical input required for the welding thermal analysis is the power, Q, that enters the plate or section being welded. It is customary to express this total heat input by the formula

$$Q = \eta_a \cdot V \cdot I \quad (6)$$

where V and I are the arc voltage and current, respectively, their product giving the electric arc power. The other parameter in the equation (6), η_a, is called arc efficiency; it represents the ratio of the power introduced by the arc into the metal to the total electric arc power. In other words it provides a semi-empirical way of taking into account the various heat losses that occur through electrode tip heating, radiation to the surrounding atmosphere, metal spatter, etc.

Arc efficiency, η_a, is heavily dependent on the welding process used, the penetration achieved, the shielding gas and many other factors that make it very difficult to predict. It is therefore estimated either through experimental measurements using the calorimetry method [23–25] or through semiempirical correlations with the weld width in the case of single-pass welding [26]. Values of the arc efficiency for various welding processes as proposed by several investigators are given in Table 1.

Of equal importance to the magnitude of the total heat input is its distribution. At the solutions presented earlier a point or line heat source was assumed. As Rykalin [25] and other investigators report, however, a more realistic approach is to assume a Gaussian radial heat flux distribution of the form

$$q(r) = q_0 \cdot e^{-Cr^2} \quad (7)$$

where

q_0 = maximum heat flux at center of heat spot
$= CQ/\pi$, [W/cm^2]
C = heat flux concentration coefficient $= 3/r_h^2$, [cm^{-2}]
r = radial distance from center of heat spot, [cm]
r_h = radius of heat spot, [cm]

Equation (7) is valid for a stationary arc. High-speed cinematography reveals, however, that during welding, when the arc is moving, the arc column is not radially symmetric but rather distorted backwards. This observation led Tsai [26] to propose the following equation for the arc heat distribution instead of equation (7):

$$q(r,\xi) = q_0 \cdot e^{-Cr^2 - \lambda r\xi} \quad (8)$$

where all the symbols have been previously defined.

Based on the preceding discussion it is evident that in order to more accurately describe the temperature distribution and cooling rates in the region close to the weld, more realistic assumptions should be employed. A three-dimensional finite heat source model for solving the governing partial differential equation of heat transfer was thus developed [2] under the following assumptions:

1. Quasi-stationary state, that is, steady-state conditions with respect to a coordinate system moving with the heat source.

2. The heat input is provided by a moving three-dimensional skewed normally distributed heat source moving on the surface of the plate and given by equation (8).

3. The thermal conductivity of the material, k, is assumed to be a linear function of temperature, θ, given by

$$k(\theta) = k_0 \cdot [1 + \gamma(\theta - \theta_0)] \quad (9)$$

where k_0 is the value of the thermal conductivity at the initial plate temperature θ_0 and γ the proportionality coefficient.

4. The thermal diffusivity of the material, κ, is assumed to be constant.

5. Convective and radiation boundary heat losses from the plate's surface are taken into account through a constant average "effective" heat-transfer coefficient, h, which can be different for the top and bottom surfaces of the plate.

6. The initial temperature of the plate, θ_0, can be different from the environmental (ambient) temperature, θ_e, to allow for preheating.

7. Phase transformation and Joule heating effects can be neglected.

The final result obtained from this model is given in Appendix 1.

Numerical solutions

Since the advent of the electronic digital computer several serious efforts have been made to numerically solve field, and in particular, heat-transfer, problems. And although the finite difference method had initially the edge, the advantages of the finite-element method, especially if coupled with thermal stress analysis, are more and more recognized today.

Over the years many finite-element programs have thus been developed that are capable of performing heat-transfer analyses. Several of these codes can take various nonlinearities into account in a more or less sophisticated manner. One of the most sophisticated ones is ADINAT (Automatic Dynamic Incremental Nonlinear Analysis for Temperatures) developed by Bathe and co-workers [27,28] over a period of years. Some details of this program will be discussed later. It suffices here to mention that ADINAT can take into account temperature-dependent material properties as well as nonlinear convection and radiation boundary conditions.

The discussion so far dealt with multipurpose heat-transfer finite-element method (FEM) programs. Concurrently, however, several investigators concerned with the welding problem have developed similar programs. Hibbit and Marcal [13] developed such a program in 1973 which was later used by other investigators too. At M.I.T. a team headed by Masubuchi also developed similar programs in the early 1970's [20, 29,30]. Friedman [31-33] has also made substantial contributions in the case of GTA welding working at the Westinghouse Electric Corporation's Bettis Atomic Power Laboratory.

The way each of the aforementioned individuals approached the various aspects of the welding problem are discussed at the appropriate places in the next subsections, where some details on the finite-element formulation of the welding heat transfer problem are presented.

Governing equation—The governing incremental isoparametric finite-element equations for the nonlinear heat-transfer problem can be written in matrix form as follows [27,28]:

$$({}^{t}\underline{K}^{k} + {}^{t}\underline{K}^{c} + {}^{t}\underline{K}^{r})\Delta\underline{\theta}^{(i)} = {}^{t+\alpha\Delta t}\underline{Q} + {}^{t+\alpha\Delta t}\underline{Q}^{c(i-1)} + {}^{t+\alpha\Delta t}\underline{Q}^{r(i-1)} - {}^{t+\alpha\Delta t}\underline{\hat{Q}}^{(i-1)} \quad (10)$$

or

$${}^{t}\underline{\hat{K}}\Delta\underline{\theta}^{(i)} = {}^{t+\alpha\Delta t}\underline{\hat{Q}}^{(i-1)} \quad (10a)$$

where ${}^{t}\underline{\hat{K}}$ is the effective conductivity matrix at time t consisting of the conductivity, nonlinear convection, and radiation matrices, ${}^{t+\alpha\Delta t}\underline{Q}$ is the heat flow vector including the effects of surface heat flow inputs, internal heat generation and temperature-dependent heat capacity, ${}^{t+\alpha\Delta t}\underline{\hat{Q}}^{(i-1)}$ is the effective heat flow vector, and $\Delta\underline{\theta}^{(i)}$ is the increment in nodal-point temperatures in iteration i:

Table 2 Temperature dependence of heat convection coefficient

$\theta^s - \theta_e$[R]	h[Btu/sec in.^{2} R]		
	Case 1	Case 2	Case 3
0	0	0	0
100	0.2×10^{-5}	0.2×10^{-5}	0.1×10^{-4}
500	0.5×10^{-5}	0.1×10^{-4}	0.6×10^{-4}
1000	0.1×10^{-4}	0.2×10^{-4}	0.1×10^{-3}
5000	0.58×10^{-3}	0.58×10^{-4}	0.6×10^{-3}
50000	0.12×10^{-2}	0.12×10^{-2}	0.12×10^{-2}

NOTE: θ^s = surface temperature.
θ_e = environmental temperature.

$$t+\alpha\Delta t\underline{\theta}^{(i)} = t+\alpha\Delta t\underline{\theta}^{(i-1)} + \Delta\underline{\theta}^{(i)} \quad (11)$$

Equation (10) represents the heat flow equilibrium at time $t+\alpha\cdot\Delta t$, where $0\leq\alpha\leq 1$ and α is chosen to obtain optimum stability and accuracy in the solution. Furthermore, the solution using these equations corresponds to the modified Newton-Raphson iteration scheme.

Boundary conditions—Convection and radiation boundary conditions are taken into account by including the matrices ${}^{t}\underline{K}^{c}$ and ${}^{t}\underline{K}^{r}$ and the vectors ${}^{t+\alpha\Delta t}\underline{Q}^{c}$ and ${}^{t+\alpha\Delta t}\underline{Q}^{r}$ in equation (10). Additional external heat flow input on the boundary is specified in ${}^{t+\alpha\Delta t}\underline{Q}$ as surface heat flow input. Prescribed temperature conditions can also be specified.

With respect to the welding problem these boundary conditions can be stated in more detail as follows:

1. Convection heat losses from the plates' surfaces can be modeled according to Newton's linear law

$$q^s = h\cdot(\theta_e - \theta^s) \quad (12)$$

where h is the temperature-dependent convection coefficient, θ_e the environmental temperature, and θ^s the surface temperature at the point under consideration. There is some difficulty in estimating the temperature dependence of h. Although most previous investigators considered h to be constant, efforts were made at M.I.T. to rationally estimate it on the basis of past semi-empirical studies. Table 2 provides the three different sets of values tested. Discussion on the obtained results are made later.

2. Radiation heat losses are very significant in the vicinity of the weld metal because of the large difference between the surface and environmental temperatures. These losses are modeled according to the quartic Stefan-Boltzman law

$$q^s = \sigma\epsilon A(\theta_r^4 - \theta^{s4}) \quad (13)$$

where

σ = Stefan-Boltzman constant
ϵ = emissivity of surface
A = shape factor
θ_r = sink temperature
θ^s = surface temperature

In the M.I.T. studies the shape factor was taken to be unity and the emissivity coefficient 0.8.

3. Temperatures can be prescribed at any point and/or surface of a weldment. Such a case, however, seldom arises in welding analyses.

4. The heat input during welding is modeled using the concept of arc efficiency. For the space distribution of the heat input, a consistent formulation should be adopted assuming a uniform distribution over the top of each weld bead. Finally, the time distribution of the heat input is modeled in such a way that the passing of the arc over the cross section examined could be simulated (a linear increase as the arc approaches, uniform

as the arc travels over the cross section, followed by a linear decrease).

Time integration schemes—A family of one-step methods [34] is considered for the time integration using the parameter α. The scheme is found to be unconditionally stable for $\alpha \geq \frac{1}{2}$ and to generally give better solution accuracy when $\alpha = 1$ (Euler backward method). Finally the modified Newton iteration is guaranteed to converge provided the time step Δt is small enough.

Material properties—One of the significant features of the finite-element method is that it can take into account any nonlinear dependence of the material physical properties with temperature, something that is very important in the welding analysis. Furthermore, it can incorporate the latent heat of fusion or of any solid-state material transformation, which cannot be furnished by closed-form analytical solutions [13, 33].

Dimensionality of problem—At first glance even the simpler welding heat-transfer analysis looks as a three-dimensional one. If the assumptions are made, however, that the welding heat source (arc) is moving at a constant speed along a regular path (for example, a straight line in a planar weld), that the weld speed is sufficiently high relative to the material's characteristic diffusion rate, and that end effects resulting from either initiation or termination of the heat source can be neglected, the three-dimensional character of the heat-transfer problem can be simplified. This can be achieved by analyzing a cross section of the weldment of unit thickness and located in the midlength region of the weld [2,31].

Molten-pool modeling—The heat-transfer mechanism in the weld metal, when molten, is extremely complex and its physics are not well understood as of today. These complexities arise not only from the difficulty involved in modeling the welding arc heat flux correctly, but also from the behavior of the convective motion of the molten metal, the thermal properties of the molten metal (including the phase transformations that take place during melting and solidification), the electric heating due to the current flow in the base metal, the boundary conditions for heat losses, etc. Many investigators have recognized these difficulties and have tried to find ways to approximate the phenomena involved.

A look at the available literature reveals that there are generally three ways for handling the problem. The first one, still at its developing stages, tries to understand and subsequently mathematically model the physical phenomena involved, that is, the fluid flow, the convective heat transfer, etc. [35]. Since no conclusive general results are available yet, this approach cannot be generally used.

In the second way the problem is divided into two parts. First the shape of the molten pool is semi-empirically determined, then the heat flow equations are solved numerically in the solid metal only using the melting isotherm as a boundary condition [26]. This method cannot be used, however, because the temperature distribution in the weld metal has to be calculated too if a stress analysis is to follow (most plastic deformation that causes the formation of residual stresses takes place in this region).

The third and final approach tries to simulate the convective heat transfer mechanism in the molten metal by using a value for the thermal conductivity of the molten metal an order of magnitude higher than that of the material at the solidus temperature. This approach, although strictly not physically correct, was used in the M.I.T. investigation.

Finally, since the cases analyzed involved multipass welding, it is necessary to find a way to model the laying of the various beads during the welding cycle. This was made possible by the element birth and death capabilities of the code used. In other words, the program ADINAT is capable of giving birth to a predetermined number of elements at predetermined time instances, thus enabling one to model the laying of a bead by specifying the appearance of the elements representing it at the time it physically appears [27].

Analysis of transient strains and residual stresses due to welding

Using the temperature distributions predicted on the basis of the techniques described in the previous section, one can calculate the transient strains, transient stresses and residual stresses due to welding since the problem is assumed to be uncoupled. The calculation of strains and stresses, however, poses a much more formidable problem than the one encountered in the heat-transfer analysis, making the use of numerical techniques a necessity. These difficulties stem from the complicated thermal-elastic-plastic state developed in and around the weld metal during welding.

Two general techniques have been developed to solve the problem. One is a simple one-dimensional analysis and the other a more sophisticated one based on the finite-element method. Both will be considered here, although emphasis will be placed on the latter.

One-dimensional analysis

The one-dimensional model for calculating stresses parallel to the weld line only was first developed in 1964 by Tall [36]. Using this model, Masubuchi, Simons, and Monroe [37] developed a computer program which was later modified and improved both at M.I.T. and elsewhere [20–22,38,39].

The basic assumption inherent in the one-dimensional stress analysis is that the only stress present is the one parallel to the weld line, σ_x, and that this stress is a function of the transverse distance from the weld centerline only. As a consequence, the equilibrium conditions are not satisfied. Despite this, however, it appears that the obtained solutions correlate reasonably well with experimental data in certain cases, as will be further explored.

The analysis lends basically the procedure originally proposed by Tall [36]; the computer code implementing the solution with the latest modifications can be found in [22].

The algorithm for solving the problem is based on the method of successive elastic solutions as proposed by Mendelson [40]. The program can take into account the temperature dependence of all material properties, any type of strain hardening and can solve bead-on-plate, edge, and butt welds of flat plates with finite width. One of the input requirements, the temperature distribution, can also be calculated if desired by the same program using the line heat source solution. The output at each time step consists of the temperature, total strain, mechanical strain, plastic strain, and stress at each of the predetermined points located at various transverse distances from the weld centerline.

Previous applications of the program have shown that it gives good results in the case of thin plates. This happens because in thin plates all stresses, except σ_x, are very small, sometimes an order of magnitude smaller than σ_x. Further discussion is delayed until the next section when experimentally obtained results are compared with analytical solutions.

Finally, it should be mentioned that the one-dimensional analysis can be used with proper minor modifications for the analysis of simple structural forms other than plates. An example is the welding analysis of built-up T-beams [20,22].

Finite-element analysis

The complex behavior of a weldment, and in particular the highly nonlinear material response and the material loading and unloading that occur in the multidimensional stress space

can be handled more accurately using numerical techniques such as the finite-element method.

One of the first applications of FEM to weld problems was presented by Hibbitt and Marcal [13], who considered a thermo-mechanical model for the welding and subsequent loading of a fabricated structure. Their model simulates GMA welding processes and accounts for temperature-dependent material properties. Friedman [31–33] also developed finite-element analysis procedures for calculating stresses and distortions in longitudinal butt welds. These procedures are applicable to planar or axisymmetric welds. Rybicki and co-workers [41] have developed similar procedures. At M.I.T. a team headed by Masubuchi has also developed two-dimensional finite-element programs capable of performing plane-strain and plane-stress analyses [1,20,29,30].

Japanese investigators have also been very active in the field. Ueda and co-workers [14], Satoh et al [42], and more recently Fujita and Nomoto [43] have all developed models to calculate transient strains and residual stresses due to welding based primarily on the initial strain method.

A recent report [44] contains an annotated bibliography of research efforts in the area that have been published since 1977.

In this subsection some details on the finite-element formulation of the welding stress problem are presented. Although the discussion pertains to the multipurpose nonlinear stress finite-element program ADINA [45,46], it is felt that what is discussed can be equally well applied to any similar code.

Finite-element formulation—Some basic considerations regarding the thermo-elastic-plastic and creep constitutive model used in conjunction with ADINA are discussed in the following.

The governing incremental finite-element equations for the problem can be written as [45]

$$ {}^{\tau}\underline{K}\Delta\underline{U}^{(i)} = {}^{t+\Delta t}\underline{R} - {}^{t+\Delta t}\underline{F}^{(i-1)} \tag{14} $$

where ${}^{\tau}\underline{K}$ is the tangent stiffness matrix corresponding to time τ; ${}^{t+\Delta t}\underline{R}$ is the nodal-point external force vector at time $t+\Delta t$; ${}^{t+\Delta t}\underline{F}^{(i-1)}$ is a vector of nodal-point forces that are equivalent, in the virtual work sense, to the internal element stresses at time $t+\Delta t$ and iteration $i-1$

$$ {}^{t+\Delta t}\underline{F}^{(i-1)} = \int_V \underline{B}_l^T {}^{t+\Delta t}\underline{\sigma}^{(i-1)} dv \tag{15} $$

and $\Delta\underline{U}^{(i)}$ is the increment in nodal-point displacement in iteration i

$$ {}^{t+\Delta t}\underline{U}^{(i)} = {}^{t+\Delta t}\underline{U}^{(i-1)} + \Delta\underline{U}^{(i)} \tag{16} $$

The solution using equation (14) corresponds to the modified Newton-Raphson iteration procedure which is helpful in improving the solution accuracy and in many cases in preventing the development of numerical instabilities. The convergence of the iteration can be accelerated using the Aitken method or, in complex material nonlinear cases (like the welding problem), improved using the BFGS (Broyden-Fletcher-Goldfarb-Shanno) matrix updating method [46].

In the thermo-elastic-plastic and creep model, and assuming infinitesimal strains, the total strain at time τ, ${}^{\tau}e_{ij}$, is assumed to be given by

$$ {}^{\tau}e_{ij} = {}^{\tau}e_{ij}^{E} + {}^{\tau}e_{ij}^{P} + {}^{\tau}e_{ij}^{C} + {}^{\tau}e_{ij}^{TH} \tag{17} $$

where

${}^{\tau}e_{ij}^{E}$ = elastic strain
${}^{\tau}e_{ij}^{P}$ = plastic strain
${}^{\tau}e_{ij}^{C}$ = creep strain
${}^{\tau}e_{ij}^{TH}$ = thermal strain

so that at any time τ during the response the stress is given by the constitutive law for an isotropic thermo-elastic material

$$ {}^{\tau}\sigma_{ij} = {}^{\tau}C_{ijrs}^{E}({}^{\tau}e_{rs} - {}^{\tau}e_{rs}^{P} - {}^{\tau}e_{rs}^{C} - {}^{\tau}e_{rs}^{TH}) \tag{18} $$

with ${}^{\tau}C_{ijrs}^{E}$ denoting a component of the elastic constitutive tensor.

The thermal strains are

$$ {}^{\tau}e_{rs}^{TH} = {}^{\tau}\alpha_m({}^{\tau}\theta - \theta_R)\delta_{rs} \tag{19} $$

where ${}^{\tau}\alpha_m$ is the average thermal expansion coefficient, θ_R is the reference temperature, and δ_{rs} the Kronecker delta. This term can be modified to include, in addition to the thermal strain, the strains that are induced from the solid phase transformations occurring during the heating and cooling stages of the thermal history [2,47].

The creep strains can be determined by any of a number of different approaches proposed in the literature. Given that in the welding problem the time intervals at high temperature are short, however, creep can be neglected.

For the plastic strains, ${}^{\tau}e_{rs}^{P}$, the situation is more complicated. Although the classical theory of isothermal plasticity is a well-tested one, extension of the theory to nonisothermal cases is difficult to substantiate experimentally. Several investigators have proposed modifications but very few experiments have been performed. Relatively good agreement between theory and experiments has generally been reported but for temperatures up to about 538°C (1000°F) only. During welding, though, the temperatures rise to above the A_1 temperature [654°C (1210°F) for steel] inside the HAZ-base metal boundary and above the liquidus temperature in the weld metal. For lack of any alternative, however, the same nonisothermal theory of plasticity can be used throughout the temperature range encountered in welding problems.

The general form of the yield or loading function for multiaxial stress conditions is

$$ F({}^{\tau}\sigma_{ij}, {}^{\tau}\alpha_{ij}, {}^{\tau}\sigma_y) \tag{20} $$

where ${}^{\tau}\alpha_{ij}$ and ${}^{\tau}\sigma_y$ are functions of the history of plastic deformation and temperature. For elastic behavior, ${}^{\tau}F < 0$, and for plastic behavior ${}^{\tau}F = 0$. As a consequence of Drucker's postulate for stable plastic materials, ${}^{\tau}F$ defines a convex surface in the stress-temperature space. It is also assumed that the isothermal normality condition remains valid, so that

$$ {}^{\tau}\dot{e}_{rs}^{P} = {}^{\tau}\lambda\frac{\partial {}^{\tau}F}{\partial {}^{\tau}\sigma_{ij}} \tag{21} $$

where ${}^{\tau}\lambda$ is a positive scalar. The selection of a hardening rule is also required for the calculation of ${}^{\tau}\lambda$. In ADINA either isotropic or kinematic hardening can be assumed. Because cyclic plasticity is expected in the welding problem, the kinematic hardening mechanism, thought by many to better model the phenomena involved, should be chosen. The assumptions involved in this mechanism are that the size of the yield surface depends on the temperature only, whereas the translation rate of the yield surface in the stress space depends on the plastic strain rate.

Further details on the numerical aspects of the problem can be found in [46].

Geometry and boundary conditions—A cross section of the weldment in its midlength can be used to calculate the transient strains, transient stresses, and residual stresses due to welding. This is rationalized by the fact that for relatively long plates the maximum stresses are developed in this region. Furthermore, the plane-strain assumption can be used (that is, all plane sections normal to the weld line remain plane during the entire welding process).

The boundary conditions to be used in the analysis should be

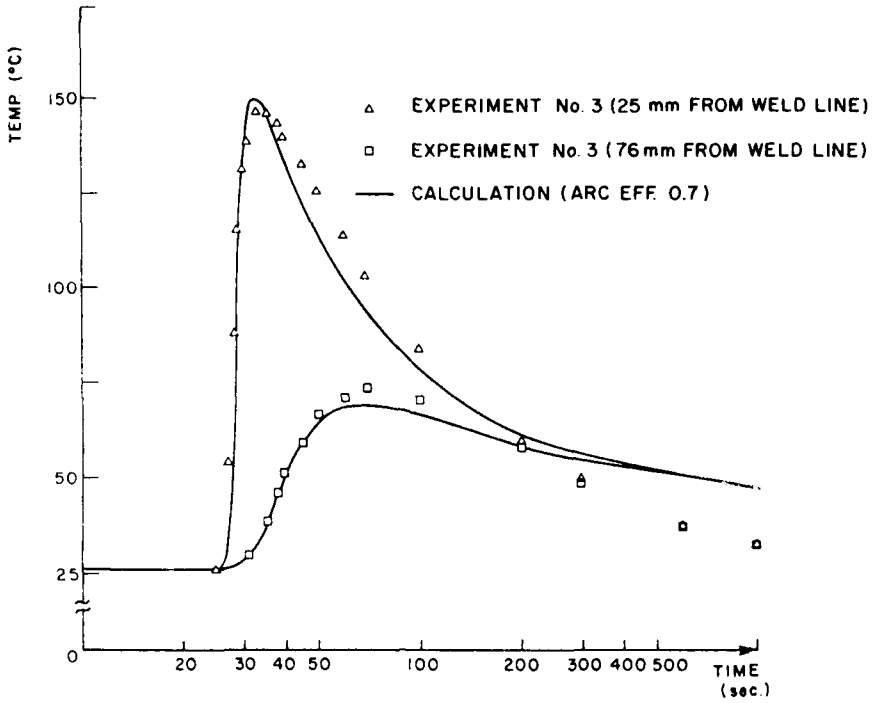

Fig. 6 Temperature distribution—analysis versus experiment (bead-on-plate weld; line heat source)

such so as to allow free expansion of the weldment in the transverse direction as well as bending. At the same time the structure should be properly restrained to eliminate all possible modes of rigid-body motion; otherwise the stiffness matrix will not be positive definite.

The foregoing holds for a relatively thick weldment. In the case of a thin plate, a plane-stress analysis can alternatively be performed over the top surface of the plate (assuming negligible through-thickness stress gradients).

Material properties—The temperature dependence of Young's modulus E, Poisson's ratio, ν, virgin yield stress, σ_{ty}, and strain hardening modulus, E_T, are all required input for the thermo-elastic-plastic model used.

A word of caution is appropriate at this point as far as the material properties above the liquidus temperature are concerned. The material does not have any strength when molten since all its mechanical properties are zero. But due to numerical considerations, zero properties cannot generally be entered as input to the program. Hence to avoid any instabilities (or even divisions by zero) very small values for E, σ_{ty}, and E_T should be used above the liquidus temperature.

Another point is the accumulation of plastic strains in the regions that become molten during the welding cycle. When the temperature reaches the liquidus these plastic strains are physically relieved, starting to accumulate again when the metal solidifies. The presence of nonzero material properties above the liquidus, however, would cause the plastic strains not only to continue accumulating but also to reach artificially high values owing to the very low magnitude of the mechanical properties. It was therefore necessary to modify ADINA by imposing a total relief of plastic strains when the material melts.

Solution strategy—One of the most important decisions an analyst has to make when performing a nonlinear incremental stress analysis is the solution strategy to be followed, because the accuracy and the convergence characteristics of the solution depend very much on it. This is especially true for complex situations involving highly nonlinear material behavior like the one encountered in the welding problem. It is therefore necessary to perform several numerical experiments prior to a full analysis of the problem.

Experimental verification of models

In the previous two sections various analytical and numerical methods for the prediction of temperature, transient strain, and residual stress distributions due to welding were described. It was suggested that these methods could be very useful to designers and fabricators for the prediction of residual stresses. Before the methods can be widely used, however, the level of confidence in their predictive capabilities should be well established. This can be done by comparing their predictions with results obtained from systematic series of experiments that cover different cases encountered in practice. Through these comparisons the analytical and numerical models can be tested and modified where necessary.

During the past ten or so years efforts towards this goal have been continuously made by several M.I.T. investigators. Their results have been published in a number of theses, reports, and papers [2,4,5,20–22,26,29,30,37,38,47]. In this section some of the most recent investigations will be reported. At the same time the capabilities and limitations of the several methodologies will be discussed.

Temperature distributions

Line heat source—To investigate the predictive capabilities of the line heat source solution, experiments performed on 6.35-mm thick (¼ in.) 6061-T6 aluminum alloy plates [48] were analyzed. Bead-on-plate welds using the GMAW process were performed with an arc voltage of 19 V, arc current of 240 A, and welding speed of 13.6 mm/sec (0.54 in./sec). The plates were 76.2 cm (30 in.) long and 45.7 cm (18 in.) wide. Figure 6 shows how the experimentally obtained data compare with the analytical predictions [22] at two points located 25 and 76

AD-A125 746 STUDY OF RESIDUAL STRESSES AND DISTORTION IN STRUCTURAL WELDMENTS IN HIGH..(U) MASSACHUSETTS INST OF TECH CAMBRIDGE DEPT OF OCEAN ENGINEERIN.. 2/2

UNCLASSIFIED J E AGAPAKIS ET AL. 30 NOV 82 F/G 11/6 NL

END

FILMED

DTIC

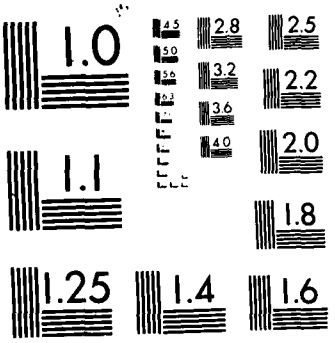

mm (1 and 3 in.) away from the weld centerline and on the midsection of the plate (quasi-stationary state). It can be seen that the correlation is very favorable. Note that this would not be the case if locations closer to the weld centerline were considered because of the singularity (heat source) present on this line.

Similar good predictions have been obtained when plates up to about 12.7 mm (½ in.) in thickness and bead-on-plate or butt welded using conventional processes were analyzed. In addition, analyses of plates up to 25.4 mm (1 in.) thick and welded using high-energy-density welding processes (electron beam and laser) seem to accurately predict temperature distributions [49].

A common characteristic of all the cases for which the line heat source solution gives reasonably accurate predictions at points some distance away from the weld centerline is the presence of negligible temperature gradients in the plate's thickness direction (two-dimensional heat transfer). This characteristic can therefore be used as a criterion for when such a solution can be utilized.

Finite heat source—As previously mentioned, the line heat source solution does not give accurate results at points close to the weld centerline, even for thin plates, the reason being that the heat source introduces a singularity which does not model the phenomena in this area properly. This difficulty, however, can be overcome by the three-dimensional point heat source model discussed in an earlier section.

To test this proposition, experimental results previously obtained [26] when welding a 3.2-mm-thick (⅛ in.) low-carbon steel plate were analyzed. The welding speed was 3.80 mm/sec (0.15 in./sec) and the arc power 5000 J/sec. Figure 7 shows the comparison between experiments and analysis at two points located 10.2 and 17.8 mm (0.4 and 0.7 in.) away from the weld centerline. As postulated, the finite heat source model gives good results in this thin-plate case.

Point heat source—The point heat source solution is more appropriate when relatively thick welded plates, say more than 12.7 mm (½ in.), are to be analyzed. This is the case because in these instances the heat-transfer problem is a three-dimensional one due to the presence of temperature gradients in the thickness direction too. When joining thicker plates, however, more than one welding pass is required, necessitating the use of the modifications described at an earlier section (that is, the positioning of the point source at the center of each pass). Moreover, one should note that as in the line heat source case the temperature predictions close to the weld centerline will not be very accurate due to the singularity induced by the presence of the point source. To remedy the situation somewhat one should limit the maximum temperature calculated to a fixed value, such as the liquidus temperature; otherwise, artificially high values will be obtained.

To demonstrate the aforementioned points the first pass of a multipass welding experiment on a 25.4-mm-thick (1 in.) HY-130 plate welded using the GMAW process was analyzed. Details of the experiments can be found in [2,4,49]. Figure 8 presents some of the results obtained. Shown are the cases of constant material properties with the point heat source located on the top surface of the plate (conventional solution) and at a distance 11.1 mm (0.4375 in.) from the top (simulating the first pass of the actual welding experiment) and the case of variable properties (iterative solution).

The results show clearly the overestimation of temperatures if the conventional point heat source is applied even if the temperature variation of material properties is considered. This overestimation is even more pronounced in the high-temperature region close to the weld centerline. Finally, comparison of the modified solutions predictions with experimentally obtained data revealed good correlation [2].

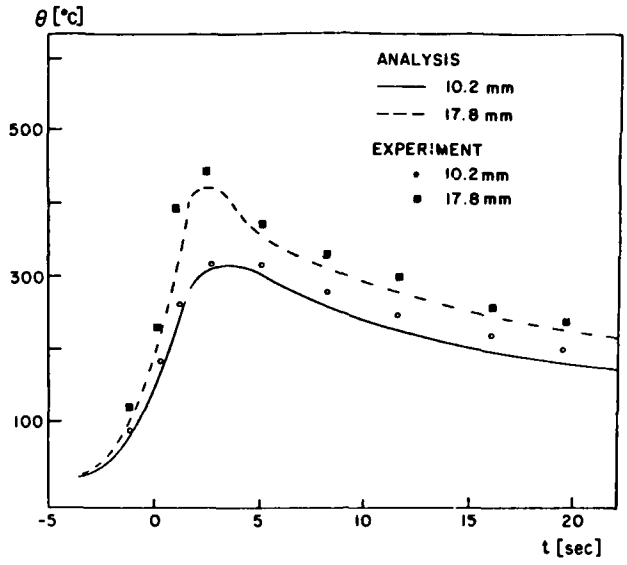

Fig. 7 Comparison of finite heat source solution with experimental data for a 3.2-mm-thick welded plate

Finite-element solution—To test the predictive capabilities of the more accurate nonlinear finite element heat-transfer program ADINAT, a series of experiments involving the multipass GMA welding of 25.4-mm-thick (1 in.) HY-130 plates was analyzed.

Figure 9 shows the test plate arrangement for these experiments. The weld joint consisted of a double-V groove with a

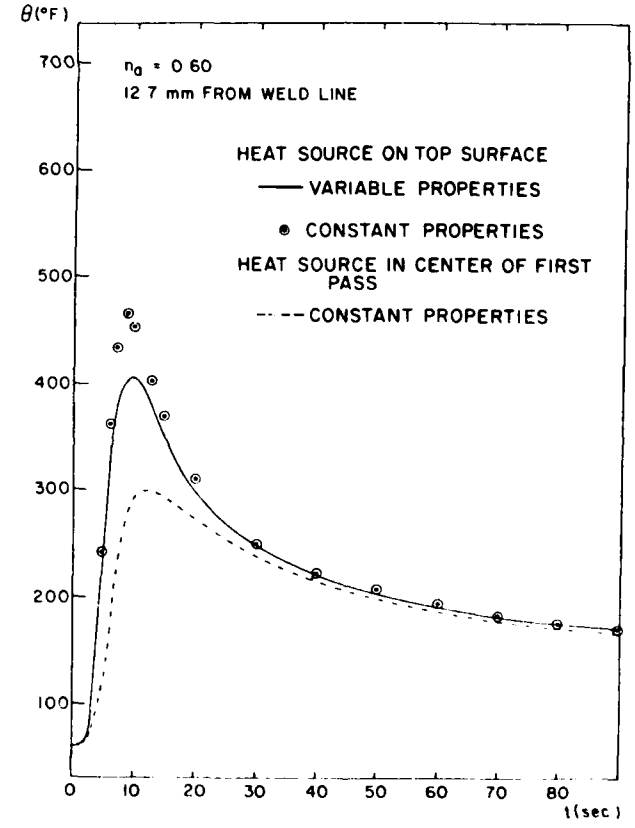

Fig. 8 Investigation of point heat source solutions (12.7 mm away from weld centerline)

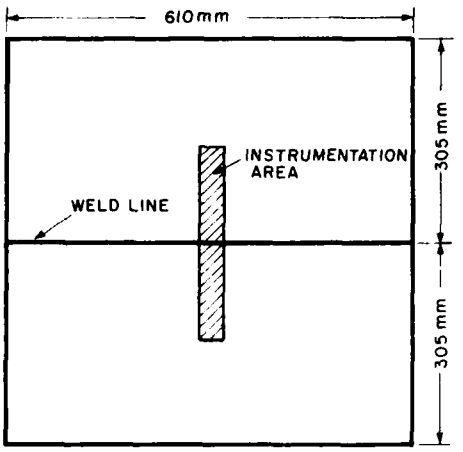

Fig. 9 Test plate arrangement

60-deg included angle in accordance with U.S. Navy specifications. The test plate support arrangement consisted of knife-edge supports located through the whole specimen length at 127 and 203 mm (5 and 8 in.) from the weld centerline on either side; this way the experiments were performed with the specimens completely unrestrained. Twelve passes were needed to complete the welding with an arc voltage of 25 V, a travel speed of 5.1 mm/sec (0.2 in./sec) and a heat input of 14.6 kJ/cm (37 kJ/in.). Temperatures and transient strains were measured throughout the welding operation using Chromel/Alumel adhesive bonded thermocouples and 90-deg Rosette electric resistance strain gages, respectively, located at preselected distances from the weld centerline (the instrumentation area is shown in Fig. 9).

A cross section of the plate at its midlength was analyzed. Figure 10 shows the finite-element mesh used for the analysis. Four- to six-node isoparametric elements were used; special care was taken not to include any triangular elements in the mesh. A total of 77 nodes and 47 elements was utilized.

Table 3 summarizes the four analyses performed. Two parameters were varied, the arc efficiency, η_a, and the temperature variation of the convection coefficient, h, given the fact that some uncertainty exists regarding their true values. All other variables were kept constant in the four cases.

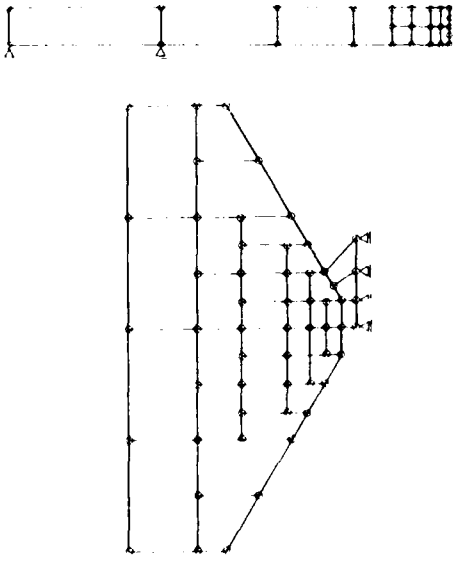

Fig. 10 Finite-element mesh used in the analysis of the welding problem

Cases A2, A3, and A4 are compared with experimentally obtained results in Fig. 11 for a point on the plate's top surface 12.7 mm (0.5 in.) away from the weld centerline and for the first welding pass. Considering the same heat input (η_a = 0.60), little difference is found between Cases A2 and A3. This is due to the fact that although higher values for the convection coefficient were chosen in Analysis A3, these values were not high enough to significantly alter the heat losses from the top and bottom surfaces of the plate and consequently the temperature distribution. A substantial increase in the convection coefficient was therefore chosen for Case A4; at the same time, however, an increase in the arc efficiency was made to partially compensate for the higher h and thus to obtain a good estimate of the maximum temperature reached. As seen in Fig. 11, the combination of values used in this latter analysis succeeded in bringing the cooling rate much closer to the experimental one. At the same time a 4 percent overprediction of the maximum temperature is observed. The difference, however, was very small so that any further analysis was not felt necessary.

Similar results were found at other points of the plate and for the consecutive welding passes. Case A4 always came closest at matching the experimentally obtained results.

Transient strain and residual stress distributions

One-dimensional analysis—The same experiments as the ones mentioned in the line heat source solution were analyzed to test the predictive capabilities of the one-dimensional computer program. Figure 12 shows the longitudinal strain history at a point 25.4 mm (1 in.) away from the weld centerline. Presented are experimental data and predictions based on the old [21] and new [22] versions of the program (the most important modification is a change in the numerical integration scheme). It can be seen that the analytical results have a good correlation with the experimentally obtained ones. Similar conclusions can also be drawn with regard to the residual stress distribution [22].

To investigate the limits of the predictive capabilities of the one-dimensional model, experiments on 25.4-mm-thick (1 in.) plates welded using the electron beam (EB) and the GMAW processes were analyzed. The EB specimens had the same geometric configuration as the GMA welded ones (described previously when the finite-element heat-transfer analysis was discussed), the only difference being the joint shape which was square butt in the case of EB welding.

Figure 13 shows the comparison between experiment and analysis of the longitudinal transient strain history, ϵ_x, in the EB specimen at two points 17 and 25.4 mm (0.67 and 1 in.) away from the weld centerline. Despite the thickness of the specimens [25.4 mm (1 in.)] the results show a remarkably good correlation of analysis and experiment. This can be attributed to the physics of the EB welding process which result in a relatively uniform through-thickness temperature distribution and a narrow heat-affected zone. As a consequence, stresses σ_y, σ_{xy}, and σ_z are small compared with σ_x, a fact substantiated

Table 3 Summary of analyses performed

Analysis	η_a[a]	h Case[b]
A1	0.65	1
A2	0.60	1
A3	0.60	2
A4	0.70	3

[a] η_a is the arc efficiency utilized.
[b] Refers to the cases presented in Table 2.

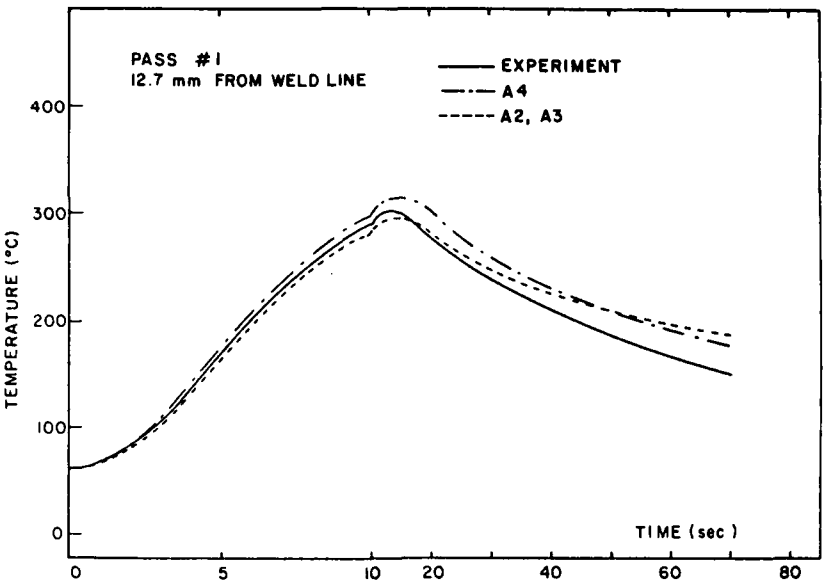

Fig. 11 Comparison of finite-element analysis results with experimental data (weld pass No. 1)

by the experimental data. The assumption of the one-dimensional theory that σ_x is the only stress present is, therefore, approximately valid. It should be emphasized once more, however, that these results apply for the midlength of a relatively long plate [longer than 457.2 mm (18 in.)], where the maximum possible stresses have been developed and where the end effects can be neglected.

The comparison between experimental data and analytical results for the longitudinal transient strain history in the GMA welded specimens at two points 25.4 and 57.2 mm (1.0 and 2.25 in.) away from the weld centerline is shown in Fig. 14. Here the story is completely different. The correlation is not good, especially for the closest point; at around 45 sec from the commencement of welding, for example, the experimental data show a maximum positive longitudinal strain of about 0.9, whereas the analysis predicts a negative longitudinal strain 0.4 in magnitude. It is thus apparent that the assumptions involved in the one-dimensional analysis break down in the case of multipass GMA welds of thick plates. Experimental data actually confirm this by showing that the transverse strains are of the same order of magnitude as the longitudinal ones.

In conclusion, then, the one-dimensional program seems to be appropriate for analyzing thin plates welded by conventional processes or medium-thickness plates welded by one of the high-energy-density processes.

Finite-element analysis—The same experiments as the ones

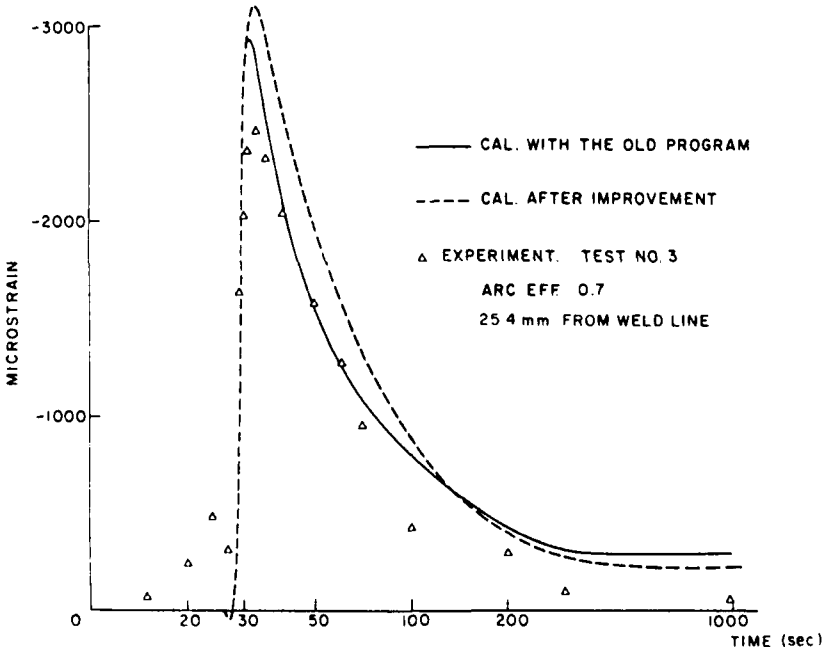

Fig. 12 Longitudinal strain history—analysis versus experiment (bead-on-plate weld; one-dimensional program)

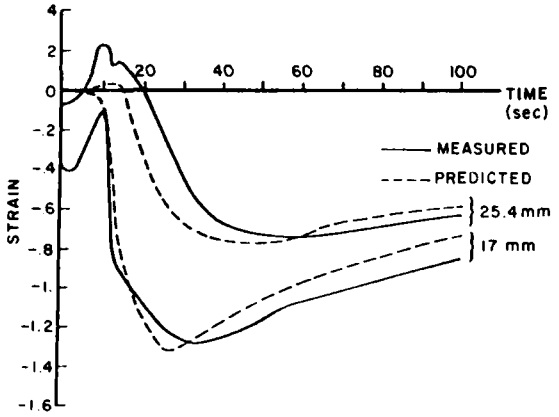

Fig. 13 Longitudinal transient strain histories for EB welded specimen (experiment and analysis)

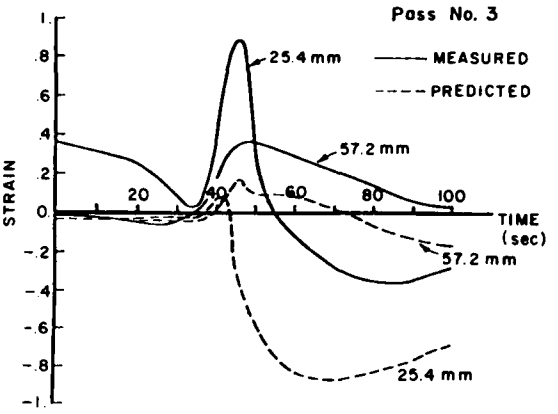

Fig. 14 Longitudinal transient strain histories for GMA welded specimens (experiment and analysis)

analyzed for the finite-element heat-transfer problem were also used in the stress analysis. The finite-element mesh used was also the same (see Fig. 10); now the appropriate nodal restraints were also imposed.

Comparison of the experimentally measured transverse transient strain history at a point located at the top surface of the plate is made with the numerically obtained results in Fig. 15. The correlation is relatively good if one takes into account the various assumptions involved in modeling the complex welding problem. A delay in the transition from tensile to compressive and again from compressive to tensile strains is observed in the analysis. The same delay as far as the occurrence of the maximum strain is also exhibited. It is believed that this phenomenon is primarily due to the relative coarseness of the finite-element mesh, and the complex loading history present in the welding problem.

Figure 16 shows calculated transient longitudinal stress distributions. Compressive stresses exist in the weld metal prior to melting. When the metal is in its molten stage, negligible compressive or tensile stresses were calculated. As cooling commences, tensile stresses start appearing in the weld metal. These stresses then build up to the residual stress pattern when ambient temperature is reached. For self-equilibrating purposes, compressive stresses exist in areas removed from the weld centerline. Note in Fig. 16 the effect of phase transformation, causing a sudden decrease in the tensile stresses.

Summarizing, it can be said that the finite-element model developed based on ADINA modified for phase transformation effects captures most of the important aspects of the welding stress analysis. Although some discrepancies have been observed between the obtained results and experimental data, considerations of cost and the assumptions made do not allow much more sophisticated analyses at present. It is expected, however, that the dramatically decreasing computer costs, together with developments in the areas of coupled thermoplasticity, will enable investigators to perform more accurate analyses in the future.

Part 2

Analysis of consequences of residual stresses

This part of the paper addresses the problem of analyzing the consequences of residual stresses on the service behavior of welded structures. A brief introduction on the subject is first given, mostly qualitative in nature, followed by a discussion on how the various problems in the area can be analyzed. Because of the vastness of the field, however, and due to length limitations, one particular case only has been singled out and analyzed in some detail. It consists of an investigation on the fracture characteristics of weldments made of high-strength quenched-and-tempered steels.

Finally, and in accordance with the general philosophy of always testing the predictive capabilities of any analysis, the analytical results are compared with data obtained during a series of experiments.

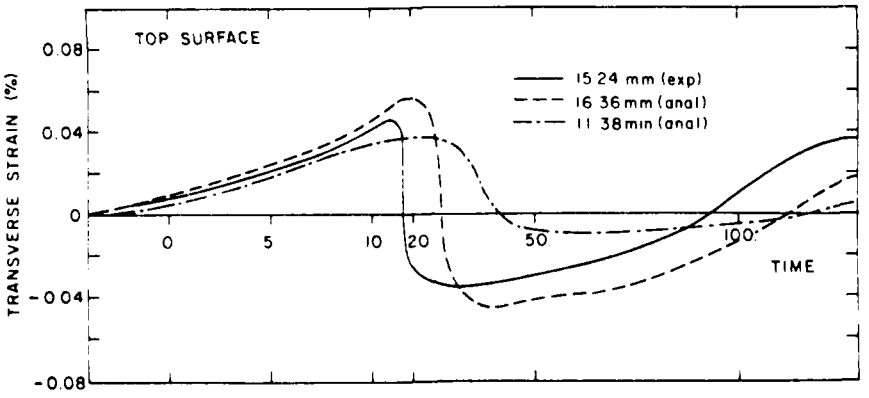

Fig. 15 Transverse transient strains on plate's top surface (experiment and analysis; first welding pass)

Effects of residual stresses

Besides the basic issues of structural and material strength, several additional factors have to be taken into account when one wishes to analyze the service behavior of a welded structure. One of the most important of these factors is the presence of residual stresses due to welding.

Unfortunately, there are no general rules that can guide the designer of a welded structure in the determination of the effects these residual stresses will have on the reliability of the structure. This is mainly due to the fact that these effects can be very complex in nature. Furthermore, and depending on the nature of the structural or material characteristic one is interested in, controversial opinions might be found in the available literature regarding the true effect the residual stresses have.

In this section an effort will be made to briefly discuss some aspects of the consequences of residual stresses on the service behavior of welded structures in a more or less quaiitative manner. This discussion will thus lead to the more specific analysis of the fracture characterization of weldments.

Brittle fracture

It is widely known that to avoid brittle fracture in a welded structure, the material must have adequate notch toughness. Differently stated, and using concepts from the fracture mechanics theory [1], unstable fracture occurs when stresses are applied to a structure containing a crack longer than a given value (critical crack length). For low-carbon steel this critical crack is several inches long at the yield stress. Brittle fractures in welded structures have been observed to originate, however, from relatively short cracks and under an overall stress equal to about one-third of the material yield strength.

These catastrophic failures of welded structures from subcritical cracks, called low applied-stress fractures, are due to presence of high tensile residual stresses in areas where the cracks are located. The crack can thus grow uncontrollably even though the level of applied stress is low [1].

Fatigue fracture

Only limited studies have been made on the analysis of the effects of residual stresses on the fatigue strength of welded structures. This stems from the major difficulties that come from the change in stress distributions around a crack as it grows due to the repeated loading.

Because of these and several other reasons [1], our knowledge of the relationship between residual stress and fatigue strength is confused. An observation that has been reported by several investigators, although not conclusive, is that the fatigue strength of welded specimens seems to increase when compressive residual stresses exist in regions near the surface of a plate. It should be pointed out, however, that the fatigue strength depends greatly on the condition of the surface; the effect of residual stress is thus secondary and is overshadowed by such major factors as weld geometry and surface irregularities [1].

Stress-corrosion cracking and hydrogen embrittlement

As previously mentioned, residual stresses significantly affect those phenomena that occur under a low applied stress. Since stress-corrosion cracking and hydrogen-induced cracking of a weldment has been observed to occur without any external loading, it can be concluded that residual stresses, especially the high tensile residual stresses, do significantly affect these phenomena, leading to catastrophic failures [1].

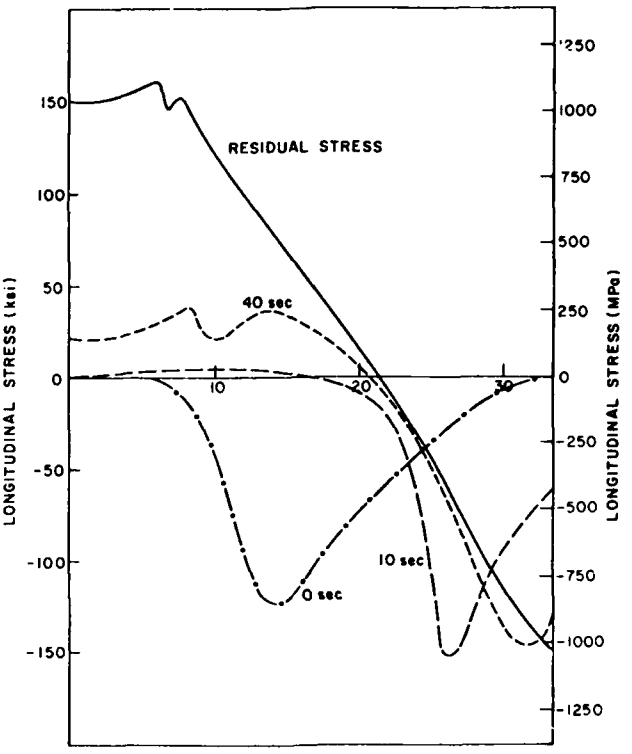

Fig. 16 Longitudinal stress distribution at several time instances (first welding pass)

Buckling strength

It is generally known that residual compressive stresses decrease the buckling strength of a welded structure, as measured for example by the externally applied critical stress. This is true for columns, plates, stiffened plate structures, spherical and cylindrical shells [1,20,38].

Methodologies for analyzing residual stress effects

In Part 1 of this paper, and in particular when discussing methods for predicting residual stresses, it was pointed out that, due to the complex nature of the problem and before the wide use of the electronic digital computer, most investigations in the area were done experimentally. This statement is even more true in the case of analyzing the effects of residual stresses on the service behavior of welded structures.

Very few analytical studies have actually been performed in the area. Moreover, these studies appear to be rather isolated attempts at addressing the various problems. A more systematic effort has been followed by M.I.T. investigators aimed at providing designers of ships and other welded structures with tools capable of aiding in the reliability assessment of these structures.

The methods used by M.I.T. investigators are both analytical and numerical. The former ones can be used whenever a rougher estimate of the residual stress effects is desirable, whereas numerical techniques, such as the finite-element method, should be used when more detailed and accurate estimates are required or when the problem is too complex to analyze otherwise.

Examples of cases that have already been studied using analytical techniques include the corrugation damage of ship bottom plating [20], the effect of residual stresses on the buck-

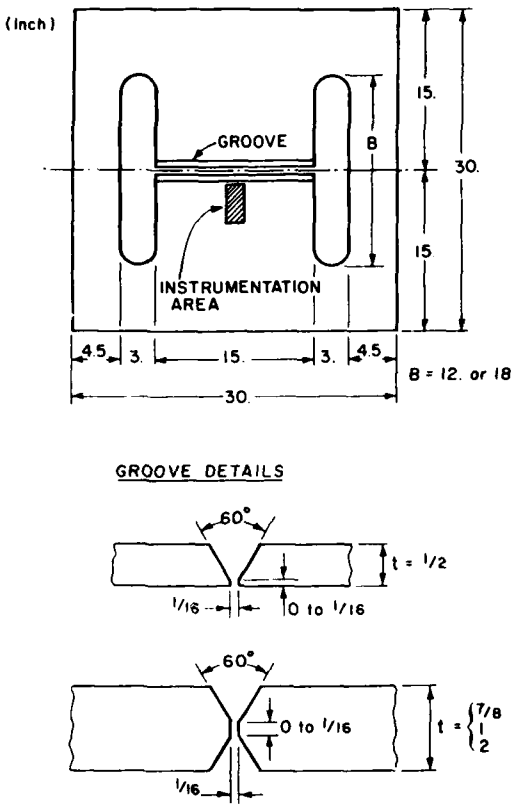

Fig. 17 Configuration of simple restrained specimens

ling strength of welded plates [38], the systems analysis approach to the fatigue crack growth of surface and embedded transverse cracks in a butt weld in the pressure hull of a deep submersible [1], and others.

On the other hand, the more sophisticated numerical techniques have been used, for example, in the fracture analysis on weldments. This analysis will be the topic of the next section.

Fracture analysis of weldments: a case study

The pursuit of improved technology for designing high-performance marine vessels has led to the use of new materials having high strength-to-weight ratios, as is the case with the HY-80 steel used in present day U.S. Navy applications or the even more advanced HY-130 steel.

Unfortunately, however, these high-strength steels can be susceptible to catastrophic failures in the presence of small flaws, making the initiation and propagation of cracks in the presence of residual stress fields of the utmost concern. Presently the U.S. Navy evaluates the cracking sensitivity of the base metal and welding electrodes through tests on various restrained welded specimens. The results of these tests are used on a "go" or "no go" basis, which means that when the restrained joint can be welded successfully without cracking, then the material and the welding procedures used in the test can also be used successfully during actual construction. Very little effort has been done to obtain quantitative information on the fracture potential of such weldments.

A study was thus undertaken at M.I.T. to investigate the effects of residual stresses on some of the fracture characteristics of welded structures, especially those made of high-strength quenched-and-tempered steels [3]. The methodology used and some results obtained in this study are reported next, serving as a case study of how one can analyze the effects of residual stresses on the service behavior of a welded structure.

Table 4 Parameters of specimens for fracture experiments

Specimen Number	Type of Steel	Thickness mm (in.)	B mm (in.)	K_s (MPa/mm)
1	SAE 1020	12.7 (1/2)	305 (12)	32.5
2	SAE 1020	25.4 (1)	457 (18)	34.6
3	SAE 1020	25.4 (1)	305 (12)	65.1
4	SAE 1020	50.8 (2)	457 (18)	68.0
5	SAE 1020	50.8 (2)	305 (12)	130.2
6	HY-130	22.2 (7/8)	457 (18)	29.8
7	HY-130	22.2 (7/8)	305 (12)	56.9
8	HY-130	50.8 (2)	305 (12)	130.2

Fracture experiments

As previously mentioned, one's confidence in the predictive capabilities of any analysis can grow only if the analytical results correlate with experimentally obtained data in a satisfactory manner. For this reason a series of experiments was performed and later analyzed as discussed in the next subsection.

Figure 17 shows the typical configuration of the simple restrained specimens used in the experimental program. A total of eight similar specimens was used as detailed in Table 4. Welding was performed using the GMAW process according to U.S. Navy specifications.

Both temperature changes and transient strains were measured during the welding operation using thermocouples and electric resistance strain gages, respectively, at preselected locations. The joint transverse shrinkage was also measured after each welding pass using a clip gage. Results of these measurements, which are not of interest in the present discussion, can be found in [3,4,49].

After the completion of welding, the crack-opening displacement (COD) was measured in all specimens. It should be noted that the COD concept can be used instead of the stress-intensity factor since both can provide similar information regarding the fracture characteristics of a weldment.

The COD was recorded while a notch, inserted in a direction parallel to the weld (x-direction) and located on the weld centerline, was continuously propagating in the specimen's thickness direction. No external stresses were applied during this process; the only stresses present were the residual stresses due to welding. Under such conditions the crack would propagate through zones of relatively constant fracture toughness (that of the weld metal) under the influence of high values of transverse residual stresses, σ_y, which can be considered to be independent of x in the central portion of the specimen.

Notches were made with 0.8-mm-thick (1/32 in.), 15.25-cm-diameter (6 in.) circular blade saws. The saw tips were ground to a 90-deg angle so that a sharp notch tip could be obtained. The COD was measured using a specially designed clip gage with four Type SP-133-20-35 semiconductor strain gages bonded on its spring steel arms. To improve accuracy and sensitivity of measurements, all four strain gages were active in the Wheatstone bridge arrangement.

Results—Curves of COD versus notch depth were obtained for all specimens tested. The relevant curves for two HY-130 specimens (Nos. 6 and 7 in Table 4) are reproduced here in Fig. 18.

It is interesting to mention that the relatively high values of COD shown were obtained with no applied external stresses. Furthermore, the nonlinear character of the curves signifies the presence of a complex through-thickness residual stress distribution.

Numerical analysis

Joint degree of constraint—As a first step towards analyzing the fracture experiments on the simple restrained specimens, the joint degree of constraint has to be calculated. This is defined by

$$K_s = \sigma_0/\delta$$

where σ_0 is a tensile stress uniformly distributed along the joint and δ is the joint transverse dispacement (for complex joints an average value is used). K_s is a kind of spring constant of the structure. Its value can thus be assigned to a number of linear springs which model the restraint imposed on the central part of the structure by the surrounding material.

The degrees of constraint for all the specimens were calculated using a simple linear elastic finite-element analysis [3]. The results are given in Table 4.

Estimation of residual stress field—The fracture experiments were performed in the absence of any externally applied stresses; the only stresses present were the residual stresses due to welding. To successfully analyze these experiments using linear elastic fracture mechanics (LEFM), therefore, it is necessary to know the residual stress field, and in particular the residual stresses perpendicular to the crack surfaces, σ_y.

One way of calculating these residual stresses is through the thermal-elastic-plastic finite-element analysis outlined in Part 1 of this paper. Such an analysis, however, of all eight specimens would be prohibitively expensive. Instead, a simplified approximate approach was used for determining the surface and through-thickness distribution of transverse residual stresses.

This approximate method is based on the fact that the COD measured during the fracture experiment was due to the elastic release of the residual stresses present around the notch. Thus by applying the superposition principle the distribution of the transverse residual stresses can be obtained by finding the stress which if applied on the notch surface would result in the same COD values as the experimental ones [3].

A finite-element code, utilizing several subroutines of the finite-element program FEABL [50], was developed to implement the method.

Figure 19 shows the finite-element mesh used, where only triangular and quadrilateral assumed displacement elements were used. From symmetry considerations only one-half of each specimen was considered; the restraint was simulated by equivalent elastic springs.

The notch depth increase was simulated by 16 incremental steps, each equal to $^1/_{16}$ of the plate's thickness. Steps 1 and 10 are shown in Fig. 19. In each step the nodal force distribution that would give the same COD as the experimentally obtained one was calculated iteratively using the method of false position

Figure 20 shows the calculated through-thickness residual stress distribution, σ_y, for two HY-130 specimens (Nos. 6 and 7).

Calculation of stress-intensity factor—To calculate the stress-intensity factor for the specimens used in the fracture experiments a linear elastic finite-element analysis was performed. Instead of using standard finite elements, however, something that would require up to 1500 degrees of freedom to obtain reasonable accuracy, a hybrid crack element was developed enabling one to simulate the crack growth in a much more inexpensive way. The element developed is an extension of the one proposed by Tong et al [51]. It introduces stresses on the crack surface to simulate the residual stress field, whereas the original element assumed stress-free crack surfaces. Details on the development of this element are not included here. The interested reader is referred to [3,4].

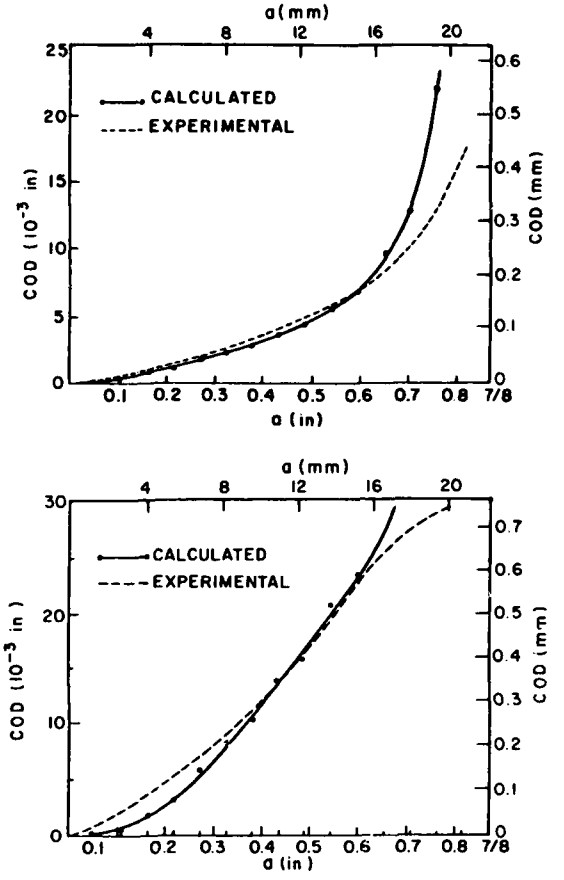

Fig. 18 FEM and experimental COD versus *a* results (Specimens 6 and 7)

The hybrid crack element was used in conjunction with FEABL to perform a linear finite-element fracture analysis of the experiments described earlier.

Figure 21 shows the finite-element mesh used in the analysis. Only the central part of a specimen is represented in the mesh; a series of springs applied on both sides of the mesh simulates the restraint the rest of the specimen exhibits on this central portion of the plate.

The crack growth was simulated by two ways: first, by increasing the size of the crack in the hybrid crack element without changing the rest of the mesh; and second, by moving the hybrid crack element deep into the mesh, something that required changes in the position of some of the other elements, increases in the number of nodes, and a renumbering of approximately half of the nodes in the mesh. The crack growth was done automatically by the program in increments of $^1/_{16}$ of the plate thickness, t, from $^1/_{16}t$ to $^{14}/_{16}t$. Figure 22 presents schematically several of these crack growth steps.

Equivalent nodal forces and distributed stresses on the crack surface were determined and prescribed automatically by the program at each step.

Numerical results of the Mode I stress-intensity factor, K_I, obtained by the finite-element analysis, are presented in Fig. 23 for Specimens 6 and 7, where K_I is plotted versus the crack depth, a.

It is interesting to note the nonlinear character of the curves, which usually show high values of K_I for cracks with depths equal to about one quarter of the plate's thickness; some of the curves even show negative values for K_I.

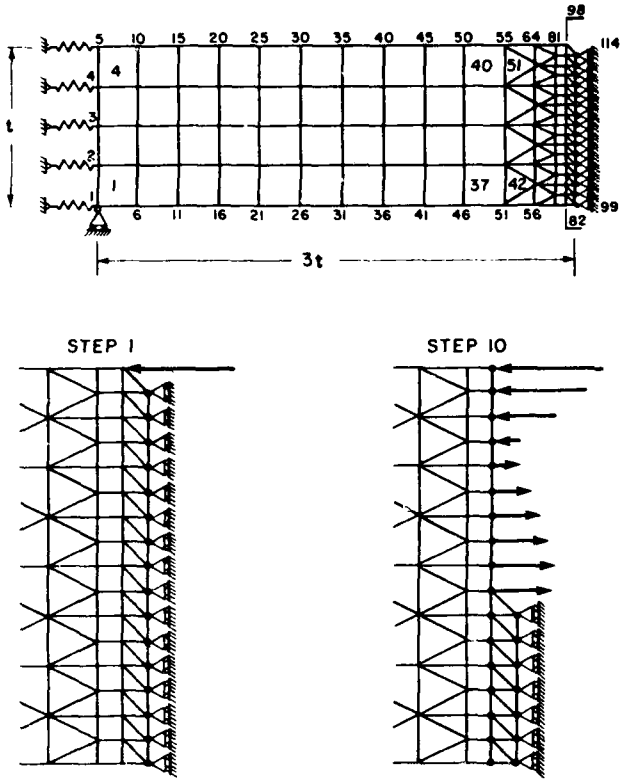

Fig. 19 Finite-element mesh used for the approximate calculation of the through-thickness residual stress distribution

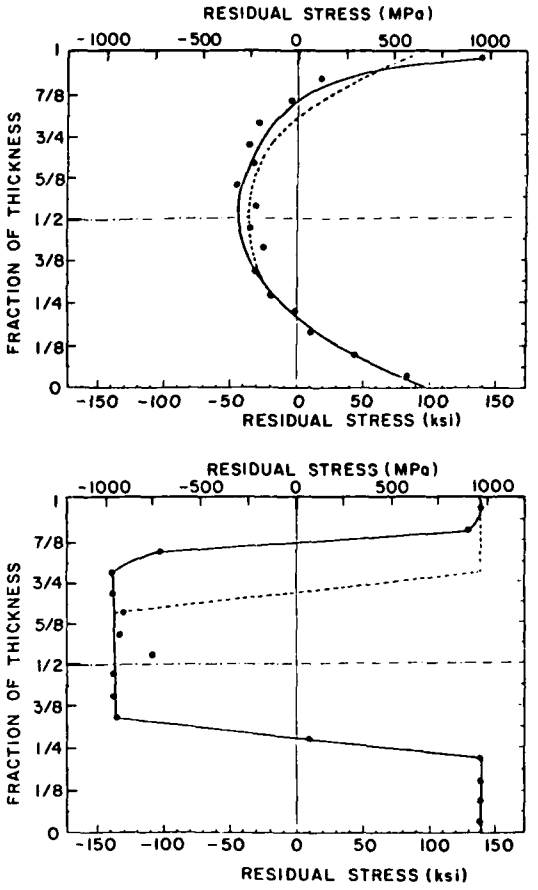

Fig. 20 *Through-thickness* distribution of transverse residual stress, σ_y (Specimens 6 and 7)

The calculated values of the crack-opening displacement at a distance 6.35 mm (0.25 in.) from the crack centerline are compared with the experimentally obtained ones in Fig. 18 for the same specimens. Close agreement between the two is observed for the case of small cracks. The divergence between the numerical and experimental curves observed for longer cracks is probably due to three-dimensional effects as the crack grows deeper.

Summary, conclusions and future possibilities

This paper presents computer-aided methodologies for solving the problems of predicting residual stresses due to welding and of analyzing their consequences on the service behavior of welded structures. These methodologies represent

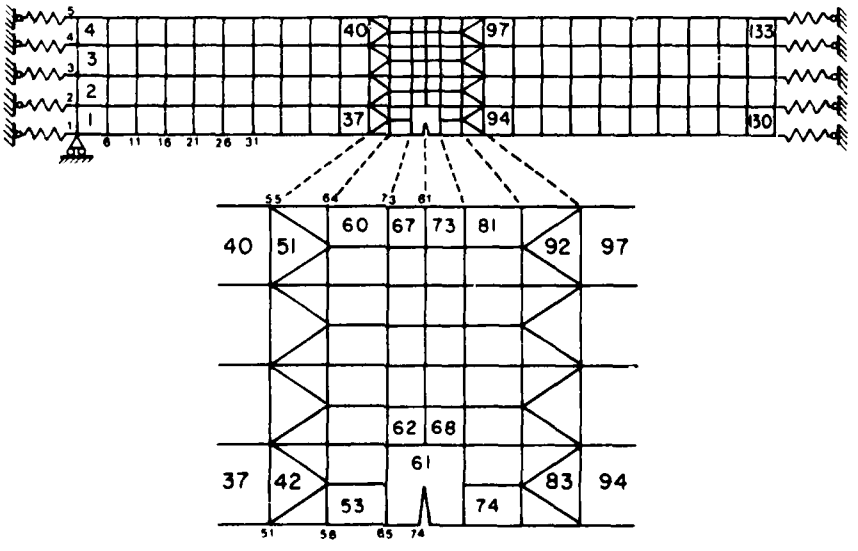

Fig. 21 Finite-element mesh used for analysis of fracture experiments

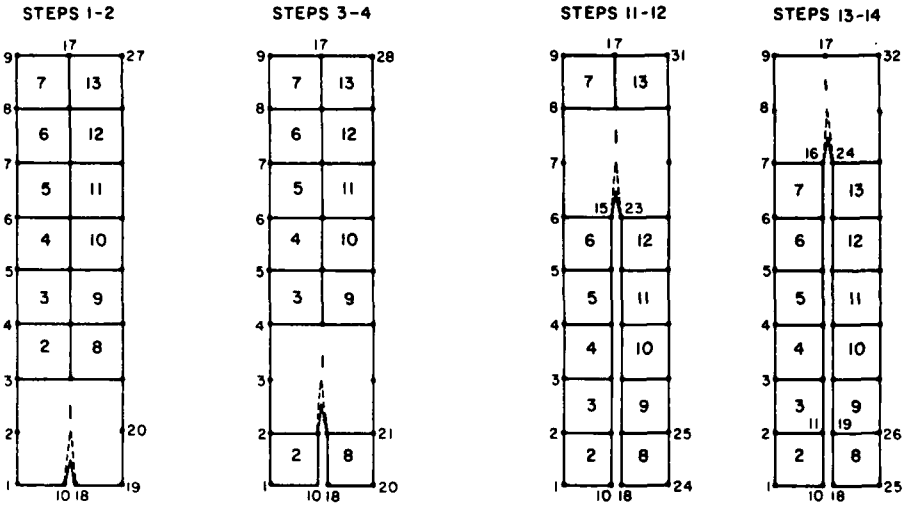

Fig. 22 Schematic representation of crack growth process

the efforts of M.I.T. investigators over a period of more than ten years in this area and can be thought of as the state of the art on a subject that is very complex but at the same time very important for the naval architectural community.

Part 1 of the paper discusses the subject of residual stress prediction. General information is first presented, including how residual stresses can be classified, how they are formed during the welding operation, and which are the physical mechanisms that should be accounted for in any accurate analysis capable of predicting them. This is followed by a historical overview of the different methodologies developed for their analysis. It is concluded that the most accurate analysis is the one based on the simulation of the whole welding operation using a computer.

The welding simulation consists of first calculating the temporal and spatial temperature distributions resulting from the application of the intense welding heat source, and subsequently of using this information as one of the inputs in a thermal-elastic-plastic stress analysis. Both analytical and numerical methods for performing each of these two steps are presented. These are then investigated with respect to their predictive capabilities and their limitations by comparing results from sample analyses with experimentally obtained data.

It is concluded that closed-form analytical solutions and simple numerical ones (that is, the one-dimensional computer program) can be used with reasonable degree of confidence in the analysis of thin plates welded by conventional processes (for example, GMAW, GTAW) and in the analysis of medium-thickness plates welded by high-energy-density processes (for example, electron beam and laser). On the other hand, if high accuracy is required (that is, when fabricating critical structures such as deep-sea submersibles) or when analysis of thick structures is desired, the only currently available technique that can be used is a numerical one based on the finite-element method.

Following completed discussion of the problem of residual stress prediction, Part 2 of the paper concentrates on the consequences residual stresses have on the service behavior of welded structures. This is a very important problem since it is well known that residual stresses adversely affect, among others, the brittle fracture, fatigue life, buckling, stress corrosion cracking, and hydrogen embrittlement characteristics of weldments.

The vastness of this subject area does not allow for a detailed description of all the methods that can be used for analyzing the various problems encountered. For this reason, after a brief qualitative general discussion, the emphasis of Part 2 is placed on a particular subject, that of the quantitative characterization of the fracture of welded high-strength quenched-and-tempered steels. A linear elastic fracture mechanics analysis using the finite-element method is first developed. Its predictions

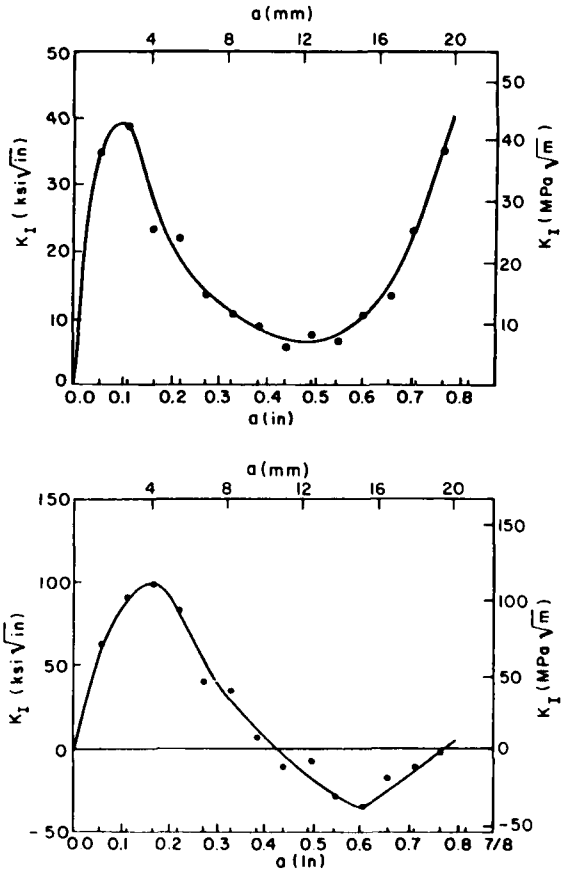

Fig. 23 Stress intensity factor versus crack depth (Specimens 6 and 7)

are then compared with experimentally obtained data.

A major conclusion can be drawn from the discussion presented in this paper. Among the various disciplines in naval architecture, including hydrodynamics, structural mechanics, and dynamics, the technology of welding fabrication has long been primarily empirical. One of the major reasons for this may be the complex, transient phenomena involved during welding. In the authors' opinion, however, computer-aided analyses like the ones presented in this paper prove that it is possible for the designers and fabricators to start incorporating manufacturing-related parameters in their analyses. It is hoped that such practice can start soon because it makes a lot of sense economically.

Future research efforts

The question that one might ask is, Where do we go from here? Although there is no single answer, it is the authors' belief that very exciting opportunities lie ahead.

For one, the fact that an analysis of such a complex phenomenon as welding has been proven to be feasible leads to the possibility of analyzing several other welding-related or more general fabrication processes. The flame heating and flame bending operations, the thermal stress relieving process, and the problem of weld metal overmatching or undermatching are just a few that come to mind. In addition, it will be well worth analyzing several of the quality acceptance tests currently used and which are mostly empirical in nature; some of them do not even provide any quantitative information but are rather performed on a "go" or "no go" basis, such as the explosion bulge test or the restrained cracking window test. There is a high probability that these analyses will aid in the rationalization of the tests or even in the development of new, more scientifically meaningful ones. We believe that the ever-increasing power and speed of the large digital computers that is spurred by such developments as parallel processing will enable analyses of this type to become more economical and hence more widespread.

On the other hand, the tremendous increase in the power of microprocessors and microcomputers, referred to by many as the second industrial revolution, will soon enable a single, inexpensive chip to perform calculations based on some of the simple models described in this paper. If one couples this with appropriate sensors, it could be possible to develop welding machines with fully adaptive automatic control that can always perform perfect welds in the presence of any external disturbances. Such machines, the dream of all fabricators, will be possible some time in the future if enough effort is applied in this direction.

Acknowledgment

This study was done as part of a 4½-year contract with the Office of Naval Research (Contract No. N00014-75-C-0469) entitled "Study of Residual Stresses and Distortion in Structural Weldments in High-Strength Steels." The authors greatfully acknowledge the financial support provided by ONR.

We would also like to thank Mrs. Muriel B. Morey for her painstaking and highly professional efforts in drawing the figures for this paper.

References

1 Masubuchi, K., *Analysis of Welded Structures. Residual Stresses, Distortion, and their Consequences*, Pergamon Press, Oxford New York, 1980.

2 Papazoglou, V. J., "Analytical Techniques for Determining Temperatures, Thermal Strains, and Residual Stresses During Welding," Ph.D. Thesis, Department of Ocean Engineering, M.I.T., Cambridge, Mass., May 1981.

3 Gonçalves, E., "Fracture Analysis of Welded Structures," Ph.D. Thesis, Department of Ocean Engineering, M.I.T., Cambridge, Mass., May 1981.

4 Papazoglou, V. J. and Masubuchi, K., "Study of Residual Stresses and Distortion in Structural Weldments in High-Strength Steels," 3rd Technical Progress Report to ONR under Contract N00014-75-C-0469, M.I.T., Cambridge, Mass., Nov. 1981.

5 Gonçalves, E., "Investigation of Welding Heat Flow and Thermal Strain in Restraint Steel Plates," M.S. Thesis, Department of Ocean Engineering, M.I.T., Cambridge, Mass., May 1980.

6 Macherauch, E. and Wohlfahrt, H., "Different Sources of Residual Stress as a Result of Welding," *Proceedings*, International Conference on Residual Stresses in Welded Construction and Their Effects, The Welding Institute, London, 1977, pp. 267–282.

7 Masubuchi, K., "New Approach to the Problems of Residual Stresses and Distortion Due to Welding," *Monthly Reports of Transportation Technical Research Institute*, Vol. 8, No. 12, Tokyo, Japan, March 1959 (in Japanese).

8 Masubuchi, K., "Analytical Investigation of Residual Stresses and Distortions Due to Welding," *Welding Journal*, Vol. 39, No. 12, Dec. 1960, pp. 525s–537s.

9 Moriguchi, S., "Fundamental Theory of Dislocation in an Elastic Body," *Applied Mathematics and Mechanics*, Vol. 1, 1948, pp. 29–36, 87–90 (in Japanese).

10 Kihara, H., Watanabe, M., Masubuchi, K., and Satoh, K., "Researches on Welding Stress and Shrinkage Distortion in Japan," *60th Anniversary Series of the Society of Naval Architects of Japan*," Vol. 4, 1959.

11 Mróz, Z. and Raniecki, B., "On the Uniqueness Problem in Coupled Thermoplasticity," *International Journal of Engineering Sciences*, Vol. 14, 1976, pp. 211–221.

12 Mróz, Z. and Raniecki, B., "A Derivation of the Uniqueness Condition in Coupled Thermoplasticity," *International Journal of Engineering Sciences*, Vol. 14, 1976, pp. 395–401.

13 Hibbitt, H. D. and Marcal, P. V., "A Numerical, Thermomechanical Model for the Welding and Subsequent Loading of a Fabricated Structure," *Computers and Structures*, Vol. 3, 1973, pp. 1145–1174.

14 Ueda, Y., Fukuda, K., and Nakacho, K., "Basic Procedures in Analysis and Measurement of Welding Residual Stresses by the Finite Element Method," *Proceedings*, International Conference on Residual Stresses in Welded Construction and Their Effects, The Welding Institute, London, 1977, pp. 27–37.

15 Rosenthal, D., "Étude théorique du régime thermique pendant la soudure de l'arc," *2-me Congrès National des Sciences*, Brussels, 1935, pp. 1277–1292.

16 Rosenthal, D., "Mathematical Theory of Heat Distribution During Welding and Cutting," *Welding Journal*, Vol. 20, No. 5, 1941, pp. 220s–234s.

17 Rosenthal, D., "The Theory of Moving Sources of Heat and Its Application to Metal Treatment," *Transactions*, ASME, Nov. 1946, pp. 849–866.

18 Boulton, N. S. and Lance-Martin, H. E., "Residual Stresses in Arc-Welding Plates," *Proceedings*, Institute of Mechanical Engineers (London), Vol. 133, 1936, pp. 295–347.

19 Myers, P. S., Uyehara, O. A., and Borman, G. L., "Fundamentals of Heat Flow in Welding," Welding Research Council Bulletin No. 123, July 1967.

20 Masubuchi, K. et al., "Analysis of Thermal Stresses and Metal Movements of Weldments—A Basic Study Towards Computer-Aided Analysis and Control of Welded Structures," TRANS. SNAME, Vol. 83, 1975.

21 Papazoglou, V. J., "Computer Programs for the One-Dimensional Analysis of Thermal Stresses and Metal Movement During Welding," Manual No. 2 of Report to ONR under Contract No. N00014-75-C-0469, M.I.T., Cambridge, Mass., 1977.

22 Imakita, A., Papazoglou, V. J., and Masubuchi, K., "One-Dimensional Computer Programs for Analyzing Heat Flow, Transient Thermal Strains, Residual Stresses, and Distortion in Weldments," Report to ONR from M.I.T. prepared under Contract No. N00014-75-C-0469 (M.I.T. OSP No. 82558), Cambridge, Mass., Dec. 1981.

23 Christensen, N., Davies, V., and Gjermundsen, K., "The Distribution of Temperature in Arc Welding," *British Welding Journal*, Feb. 1965, pp. 161–167.

24 Rykalin, N. N., "Calculation of Heat Processes in Welding," Lecture presented before the American Welding Society, April 1961.

25 Rykalin, N. N. and Nikolaev, A. V., "Welding Arc Heat Flow," *Welding in the World*, Vol. 9, Nos. 3/4, 1971, pp. 112–132.

26 Tsai, C. L., "Parametric Study on Cooling Phenomena in Un-

derwater Welding," Ph.D. Thesis, Department of Ocean Engineering, M.I.T., Cambridge, Mass., Sept. 1977.

27 Bathe, K. J., "ADINAT—A Finite Element Program for Automatic Dynamic Incremental Nonlinear Analysis of Temperature," AVL Report 82448-5, Department of Mechanical Engineering, M.I.T., Cambridge, Mass., May 1977 (revised, Dec. 1978).

28 Bathe, K. J. and Khoshgoftaar, M. R., "Finite Element Formulation and Solution of Nonlinear Heat Transfer," *Journal of Nuclear Engineering and Design*, Vol. 51, 1979, pp. 389–401.

29 Muraki, T., Bryan, J. J., and Masubuchi, K., "Analysis of Thermal Stresses and Metal Movement During Welding, Part I: Analytical Study, and Part II: Comparison of Experimental Data and Analytical Results," *Journal of Engineering Materials and Technology*, ASME, Jan. 1975, pp. 81–84 and 85–91.

30 Masubuchi, K., "Applications of Numerical Analysis in Welding—Present State-of-the-Art and Future Possibilities," Colloquium on Application of Numerical Analysis in Welding, I.I.W. Annual Assembly, Dublin, Ireland, 1978.

31 Friedman, E., "Thermomechanical Analysis of the Welding Process Using the Finite Element Method," *Journal of Pressure Vessel Technology*, ASME, Aug. 1975, pp. 206–213.

32 Friedman, E. and Glickstein, S. S., "An Investigation of the Thermal Response of Stationary Gas Tungsten Arc Welds," *Welding Journal*, Vol. 55, No. 12, 1976, pp. 408s–420s.

33 Friedman, E., "Numerical Simulation of the Gas Tungsten Arc Welding Process," *Proceedings*, Numerical Modeling of Manufacturing Processes, ASME Winter Annual Meeting, Atlanta, Ga., 1977, pp. 35–47.

34 Hughes, T., "Unconditionally Stable Algorithms for Nonlinear Heat Conduction," *Computer Methods in Applied Mechanics and Engineering*, Vol. 10, 1977, pp. 135–139.

35 Dilawari, A. H., Szekely, J., and Eagar, T. W., "Electromagnetically and Thermally Driven Flow Phenomena in Electroslag Welding," *Metallurgical Transactions B*, Vol. 9B, 1978, pp. 371–381.

36 Tall, L., "Residual Stresses in Welded Plates—A Theoretical Study," *Welding Journal*, Vol. 43, No. 1, 1964, pp. 10s–23s.

37 Masubuchi, K., Simons, F. B., and Monroe, R. E., "Analysis of Thermal Stresses and Metal Movement During Welding," Battelle Memorial Institute, BSIC-820, Redstone Scientific Information Center, NAGA-TM-X-613000, N68-37857, July 1968.

38 Masubuchi, K. and Papazoglou, V. J., "Analysis and Control of Distortion in Welded Aluminum Structures," TRANS. SNAME, Vol. 86, 1978, pp. 77–100.

39 De Young, R. M. and Chiu, S. S., "Some Applications of Numerical Methods to Practical Welding Problems," *Proceedings*, Numerical Modeling of Manufacturing Processes, ASME Annual Winter Meeting, Atlanta, Ga., 1977, pp. 143–156.

40 Mendelson, A., *Plasticity: Theory and Application*, MacMillan, New York, 1968.

41 Rybicki, E. F. et al., "Residual Stresses at Girth-Butt Welds in Pipes and Pressure Vessels," Battelle Columbus Laboratory Report to U.S. Nuclear Regulatory Commission, NUREG-0376, 1977.

42 Satoh, K. et al., "Thermal Elasto-Plastic Analysis of Stress and Strain in Weld Metal During Multipass Welding," International Institute of Welding Document X-706-73, May 1973.

43 Fujita, Y., Nomoto, T., and Hagesawa, H., "Thermal Stress Analysis Based on Initial Strain Method," International Institute of Welding Document X-926-79, April 1979.

44 Imakita, A., Papazoglou, V. J., and Masubuchi, K., "Annotated Bibliography on Numerical Analysis of Stresses, Strains, and Other Effects due to Welding," International Institute of Welding Document X-906-81, July 1981.

45 Bathe, K. J., "ADINA—A Finite Element Program for Automatic Dynamic Incremental Nonlinear Analysis," AVL Report 82448-1, Department of Mechanical Engineering, M.I.T., Cambridge, Mass., Sept. 1975, revised, Dec. 1978.

46 Snyder, M. D., "An Effective Solution Algorithm for Finite Element Thermo-Elastic-Plastic and Creep Analysis," Ph.D. Thesis, Department of Mechanical Engineering, M.I.T., Cambridge, Mass., Oct. 1980.

47 Papazoglou, V. J. and Masubuchi, K., "Numerical Analysis of Thermal Stresses During Welding Including Phase Transformation Effects," *Journal of Pressure Vessel Technology*, ASME, Vol. 104, No. 3, Aug. 1982, pp. 198–203.

48 Andrews, J. B., Arita, M., and Masubuchi, K., "Analysis of Thermal Stresses and Metal Movement During Welding," NASA Contract Report NASA CR-61351, prepared for the G.C. Marshall Space Flight Center, Dec. 1970.

49 Papazoglou, V. J. and Masubuchi, K., "Study of Residual Stresses and Distortion in Structural Weldments in High-Strength Steels," First and Second Technical Progress Reports to ONR under Contract No. N00014-75-C-0469 (M.I.T. OSP No. 82558), M.I.T., Cambridge, Mass., Nov. 30, 1979 and Nov. 30, 1980.

50 Orringer, O., French, S. E., and Weinreich, M., "User's Guide for the Finite Element Analysis (FEABL 2, 4 and 5) and the Element Generation Library (EGL), Aeroelastic and Structure Research Laboratory, Department of Aeronautics and Astronautics, M.I.T., Cambridge, Mass., Jan. 1978.

51 Tong, P., Pian, T. H. H., and Lasry, S. J., "A Hybrid Element Approach to Crack Problems in Plane Elasticity," *International Journal of Numerical Methods in Engineering*, Vol. 7, 1973, 297–308.

Appendix 1

Closed-form solution of three-dimensional fin heat source model

The solution to the governing partial differential equa of heat transfer during welding under the assumptions discussed in the main text was found using the method of separation of variables, the appropriate boundary conditions, and by dividing the plate into two regions, inside and outside the heat input circle of radius r_h [2]. The obtained solution can be written as

$$\theta = \theta_0 + \frac{1}{\gamma} \cdot (\sqrt{1 + 2\gamma \cdot e^{-\lambda v \xi} \cdot \phi(r,z)} - 1)$$

where

$$\phi(r,z) = \phi^1(r,z) \cdot [u_{-1}(r) - u_{-1}(r - r_h)] + \phi^0(r,z) \cdot u_{-1}(r - r_h)$$

with $u_{-1}(r-a)$ being the unit step function and

$$\phi^0(r,z) = \sum_{n=1}^{\infty} C_n \cdot K_0(\zeta_n r) \cdot \left[\frac{h_2}{k_0 \cdot \omega_n} \cdot \sin(\omega_n z) + \cos(\omega_n z)\right]$$

$$\phi^1(r,z) = \sum_{n=1}^{\infty} \left\{ \frac{2 \cdot q_0 \cdot K_n \cdot J_0(\delta_n r) \cdot [h_2 \cdot \sinh(\chi_n z) + k_0 \cdot \chi_n \cdot \cosh(\chi_n z)]}{J_1^2(\delta_n r_h) \cdot [k_0 \chi_n (h_1 + h_2) \cdot \cosh(\chi_n H) + (k_0^2 \chi_n^2 + h_1 h_2) \cdot \sinh(\chi_n H)} + C_n \cdot K_0(\zeta_n r_h) \cdot \frac{I_0(\zeta_n r)}{I_0(\zeta_n r_h)} \cdot \left[\frac{h_2}{\omega_n \cdot k_0} \cdot \sin(\omega_n z) + \cos(\omega_n z)\right] \right\}$$

$$C_n = \frac{1}{a_n} \cdot \sum_{m=1}^{\infty} \frac{2 \cdot q_0 \cdot K_m \cdot \delta_m \cdot [r_{mn} \cdot \tanh(\chi_m H) + s_{mn}]}{(\chi_m^2 + \omega_n^2) \cdot (J_1(\delta_m r_h)) \cdot [d_m + e_m \cdot \tanh(\chi_m H)]}, \quad n = 1,2,3,\ldots$$

$$a_n = b_n \cdot c_n$$

$$b_n = \zeta_n \cdot \left[K_1(\zeta_n r_h) + K_0(\zeta_n r_h) \cdot \frac{I_1(\zeta_n r_h)}{I_0(\zeta_n r_h)}\right]$$

$$c_n = \frac{H}{2} \cdot \left(1 + \frac{h_2^2}{\omega_n^2 \cdot k_0^2}\right) + \frac{1}{4\omega_n} \cdot \left(1 - \frac{h_2}{\omega_n^2 \cdot k_0^2}\right) \cdot \sin(2\omega_n H) + \frac{h_2}{\omega_n^2 \cdot k_0} \cdot \sin^2(\omega_n H)$$

$$d_m = k_0 \cdot \chi_m \cdot (h_1 + h_2)$$

$$e_m = k_0^2 \cdot \chi_m^2 + h_1 \cdot h_2$$

$$r_{mn} = h_2 \cdot \left(\omega_n + \frac{\chi_m^2}{\omega_n}\right) \cdot \sin(\omega_n H) + \left(k_0 \chi_m^2 - \frac{h_2^2}{k_0}\right) \cdot \cos(\omega_n H)$$

$$s_{mn} = \chi_m \cdot \left(k_0 \cdot \omega_n + \frac{h_2^2}{k_0 \cdot \omega_n}\right) \cdot \sin(\omega_n H)$$

$$\zeta_n^2 = \omega_n^2 + (\lambda v)^2$$

$$(k_0^2 \cdot \omega_n^2 - h_1 \cdot h_2) \cdot \tan(\omega_n H) = k_0 \cdot \omega_n \cdot (h_1 + h_2)$$

$$J_0(\delta_n \cdot r_h) = 0, n = 1,2,3, \ldots$$

$$\delta_n^2 = \chi_n^2 - (\lambda v)^2$$

$$K_n = \int_0^1 x \cdot e^{-C \cdot r_h^2 \cdot x^2} \cdot J_0(\delta_n \cdot r_h \cdot x) \cdot dx$$

h_1 and h_2 the heat-transfer coefficients at the top and bottom surfaces of the plate, respectively; H the plate thickness; $J_0(x)$ and $J_1(x)$ the Bessel functions of first kind and of zero and first order, respectively; $I_0(x)$ and $I_1(x)$ the modified Bessel functions of first kind and of zero and first order, respectively; and $K_0(x)$ and $K_1(x)$ the modified Bessel functions of second kind and of zero and first order, respectively. All other variables have been previously defined.

A computer program has been written in the FORTRAN IV language to perform the necessary calculations.

END

FILMED

4-83

DTIC